UNIVERSITY OF CALIFORNIA, SAN DIEGO

An *In Vivo* Biosensor for Neurotransmitter Release and *In Situ* Receptor Activity: Acetylcholine and the M1 Muscarinic Receptor

A dissertation submitted in partial satisfaction of the requirements for the degree

Doctor of Philosophy

in

Neurosciences

by

Lee Frederick Schroeder

Committee in charge:

Professor David Kleinfeld, Chair
Professor Palmer Taylor, Co-Chair
Professor Tamas Bartfai
Professor Darwin Berg
Professor Paul Slesinger
Professor Roger Tsien

2009

The dissertation of Lee Frederick Schroeder is approved, and it is acceptable in quality and form for publication on microfilm:

_____

_____

_____

_____

_____

Co-Chair

_____

Chair

University of California, San Diego

2009

Dedication

For Laurel

Table of Contents

List of Figures

List of Tables

List of Abbreviations

ACh:	acetylcholine
ACSF:	artificial cerebral spinal fluid
AFP:	*Aequorea* fluorescent proteins
asp/gly:	aspartate/glycine
Citrine:	third-generation yellow fluorescent protein, Citrine cp174
CNiFERs:	Cell-based Neurotransmitter Fluorescent Engineered Reporters
CNS:	central nervous system
CRAC:	Ca2+-release-activated Ca2+ channel
eCFP:	enhanced cyan fluorescent protein
EC_{50}:	half maximal effective concentration (50%)
ECoG:	electrocorticogram
FRET:	fluorescence resonance energy transfer
GABA:	gamma-Aminobutyric acid
GDP, GTP:	Guanosine-5'-diphosphate, Guanosine-5'-triphosphate
GFAP:	glial acidic fibrillary protein
GFP:	green fluorescent protein
GPCR:	G protein-coupled receptors
GRIN:	gradient index (lens)
GRK:	G protein-coupled receptor kinase
GRP:	glial restricted precursor (cell line)
[^{3}H]QNB	tritium 3-quinuclidinyl benzilate
[^{3}H]NMS	tritium scopolamine methyl chloride
HEK293:	Human Embryonic Kidney (cell line)
IP_3:	inositol triphosphate
M1:	muscarinic M1 acetylcholine receptor
mCherry:	mCherry fluorescent protein
NBM:	Nucleus Basalis Magnocellularis
NMDA:	N-methyl-D-aspartic acid
Norepi:	norepinephrine
PBS:	phosphate buffered saline
$PH_{PLC\delta}$:	pleckstrin homology domain of PLCδ1
PLC:	phospholipase C
TN-XXL:	Troponin C FRET-based calcium reporter
VIP:	vasoactive intestinal peptide

Acknowledgements

I'd first like to thank my advisor, David Kleinfeld, who has taught me to appreciate both the forest *and* the trees—he showed me the importance of a careful measurement, the value of a good laugh, and that the two need not be far separated.

None of this work would have transpired without Quoc-Thang Nguyen, who not only conceived of the sensor design but with whom I worked side by side for over two years.

I'd also like to thank Palmer Taylor, in whose lab I worked for one year but who has always since provided advice and an open door for my continued research.

I am grateful to Tamas Bartfai, Darwin Berg, Jean-Pierre Changeux, Jim Conner, Harvey Karten, Zoran Radic, Paul Slesinger, Todd Talley, Roger Tsien, and Mark Tuszinsky for critical discussion and sometimes tireless humoring of my questions. Within our lab, I'd like to thank everyone, including those from the early days and those more recent—for too many things to possibly list. I thank Atsushi Miyanohara for producing the lentiviruses and Rodolfo Figueroa for running the cell culture room and doing the other 50 things that he does each day.

Work can be neither endured nor enjoyed without a deep support from loved ones. In my case, this is overwhelmingly true. My wife Laurel and her parents know exactly what they did to make the writing of this dissertation possible. I also

thank my parents for their unconditional, ongoing support, encouragement and inspiration. And, of course, for their patience. Finally, there are the two little ones in my life, who are waiting for me to stop writing already…

Parts of this dissertation will be prepared for submission for publication. The dissertation author will be a primary co-investigator and co-author of this paper along with Quoc-Thang Nguyen, who conceived of the biosensor design. The methods for the data published in this dissertation were largely developed together with Quoc-Thang Nguyen. All figures in this dissertation were created by the dissertation author except Figure 22, which was created by Quoc-Thang Nguyen, and Figure 12, which was adapted from Lohse et al., 2008[1]. All data for this dissertation was collected by the dissertation author except for that in Figure 15 and Figure 23, which was collected or processed by the dissertation author and Quoc-Thang Nguyen, Figure 22, which was collected by Quoc-Thang Nguyen, and Figure 8, which was collected by the dissertation author and Arnaud Muller.

Vita

2009	Doctor of Philosophy in Neurosciences, University of California, San Diego
2003-2009	Graduate Student University of California, San Diego *Laboratory of Professor David Kleinfeld, PhD*
2001-present	Medical Scientist Training Program, University of California, San Diego
1996	Bachelor of Arts in Physics, University of Pennsylvania

ABSTRACT OF THE DISSERTATION

An *In Vivo* Biosensor for Neurotransmitter Release and *In Situ* Receptor Activity: Acetylcholine and the M1 Muscarinic Receptor

by

Lee Frederick Schroeder

Doctor of Philosophy in Neurosciences

University of California San Diego, 2009

Professor David Kleinfeld, Chair
Professor Palmer Taylor, Co-Chair

From moment to moment, dynamic patterns of neurotransmitter release and surface receptor activity determine the function of the central nervous system. Fundamental to neuroscience is the ability to measure these patterns. However, the tools to make these measurements at a physiologically relevant temporal and spatial resolution are largely unavailable. Recent advances in genetically encoded optical biosensors have begun to allow direct visualization of molecular events previously only indirectly inferable. The aim of the work presented in this dissertation is to develop and characterize a novel *in vivo* cellular biosensor that

takes advantage of current optical biosensor technology as well as standard cell-based assays used in high-throughput screening by the pharmaceutical industry.

The biosensors are named Cell-based Neurotransmitter Fluorescent Engineered Reporters (CNiFERs). In this initial realization, we express the M1 muscarinic acetylcholine receptor and the fluorescent Ca^{2+} indicator TN-XXL in cultured HEK293 cells. Activation of the M1 receptor by acetylcholine leads to an increase in HEK293 cytosolic Ca^{2+} then reported by TN-XXL. *In vivo*, M1-CNiFERs are implanted with control-CNiFERs: HEK293 cells expressing TN-XXL and the non-functional fluorescent protein mCherry, but not M1. M1- but not control-CNiFERs respond robustly, up to 40% signal change, to endogenous acetylcholine release evoked via electrical stimulation of Nucleus Basalis Magnocellularis (NBM). The response is a single peak initiated within 2 s with a half-maximal rise time as short as ~1 s and a full width at half maximal amplitude of < 10 s. As expected for NBM stimulation, we observe an inverse correlation between M1-CNiFER response and electrocorticogram delta band power. The cholinergic nature of this response is further verified by enhancement with the acetylcholinesterase inhibitor physostigmine and suppression with the muscarinic antagonist atropine.

The pharmaceutical industry has made such extensive use of the cell-based assay in part because of its modularity. By simply expressing a different receptor, CNiFERs can be built to detect the release of a large number of endogenous neurotransmitters and signaling molecules implicated in a wide variety of central nervous system functions.

Chapter I: Introduction

Measuring Released Neurotransmitters and Receptor Activity

The central nervous system (CNS) is awash with a continuously varying set of neurotransmitters. These neurotransmitters in turn activate a continuously varying set of surface receptors expressed on CNS neurons. Activity at these receptors determine phenomenon as reduced as synaptic plasticity[2] and as emergent as cognitive states (*e.g.*, sleep, wakefulness, or arousal)[3,4]. As an example, widespread activation of acetylcholine receptors by acetylcholine is part of the state switch from Non-Rapid Eye Movement sleep (NREM) to Rapid Eye Movement sleep (REM)[5]. Historically, the actions of neurotransmitters have been deduced primarily from gain-of-function or loss-of-function experiments in which the neurotransmitter or associated receptor is in some way expressed or suppressed, *e.g.*, by stimulation, by pharmacology, or with genetics. These are very effective strategies, especially for determining if the purported role of the molecule is necessary and/or sufficient for function, but they do have drawbacks. For example, loss-of-function experiments can be misleading when the role played by the molecule is only conditional or indirect[6]. A third approach is direct physiological observation of the varying levels of neurotransmitters using tools like microdialysis or electrochemistry. However, these tools have significant limitations, either in spatial and temporal resolution, or in the set of neurotransmitters detectable. Current advances in genetically-encoded optical biosensors have created the potential for directly visualizing signaling molecules and activity of CNS receptors both *in vivo* and in (near) real time[7-10]. Our goal has

been to create an optical biosensor for the release of neurotransmitters and activity of surface receptors that offers a physiologically relevant spatial and temporal resolution and is furthermore modular in nature and thus easily adapted to a diversity of research aims.

Volume Transmission

Neurotransmitters can act via two primary modes: wired transmission and volume transmission. Wired transmission occurs in synapses, where neurotransmitter is released from the presynaptic terminal and activates receptors located immediately opposed in the post-synaptic density. The prototypic wired transmission synapse is found in the neuromuscular junction, where 10,000 receptors per square micrometer are found in the synapse while outside the synapse that number drops to 10. Also, high concentrations of acetylcholinesterase line the basal lamina, ready to breakdown released acetylcholine and prevent synaptic spillover[11].

Less well-described is volume transmission, which occurs with release of neurotransmitter that travels via the extracellular space over distances larger than the synaptic cleft to activate various receptors distributed within its sphere of influence. In addition to spillover from the synapse, neurotransmitter can be released from non-synaptic regions of the nerve terminal. Large dense-cored vesicles are often found near and release their neurotransmitters from these non-synaptic regions. Furthermore, many nerve terminals or varicosities found in the brain are not opposed to post-synaptic densities[11,12]. Neurotransmitter release

from these sites necessarily transmits by volume. Also, many examples of neurotransmitter-receptor mismatches are known. These are defined as synaptic receptors that are not activated by the neurotransmitter released in that synapse. Examples include the M1 and M2 muscarinic acetylcholine receptors found in asymmetric (non-cholinergic) synapses in monkey[13] as well as presynaptic neuronal nicotinic acetylcholine receptors found on non-cholinergic terminals[14]. Such receptors could only be activated by volume-transmitted acetylcholine. The large family of G protein-coupled receptors (GPCRs), with which 60% of modern pharmaceuticals are thought to interact[15], offers strong candidates for stimulation by volume transmission. Many have been found extrasynaptically, where they could only be activated by volume transmission[11,16,17]. Many GPCRs also exhibit very high affinity for their endogenous neurotransmitter, a requirement for volume transmission where released neurotransmitter is diluted into the vast extrasynaptic environment[11].

An example of volume transmission in the intact brain is co-release of the opioid neuropeptide dynorphin by mossy fibers in the hippocampus. Its release was shown to depress synaptic activity in neighboring unstimulated fiber pathways. Furthermore, this activity persisted for up to an hour and was reversible by naloxone, an opioid antagonist. These findings suggests dynorphin had diffused throughout the hippocampal tissue by volume transmission[11,18].

Detection of released neurotransmitter is conventionally performed by sampling the extracellular space. Such detection is necessarily extrasynaptic and thus indicative of volume transmission, or at least non-functional spillover from

synaptic clefts. Our reporter too will sample from the extracellular space and thus we will focus on a neurotransmitter and receptor that are thought to interact at least in part via volume transmission.

Acetylcholine and the Muscarinic Receptor

In the initial realization of our reporter, we focus on the neurotransmitter acetylcholine and its muscarinic receptor. Acetylcholine was the first neurotransmitter discovered and its receptors among the first studied. As stated above, it likely targets the muscarinic receptor at least in part by volume transmission as non-synaptic varicosities are common on cholinergic fibers[12]. Also, muscarinic receptors can be found both in non-cholinergic synapses[13] and outside of synapses altogether[17]. Finally, muscarinic action throughout the CNS is multiplicative and robust and serves as a suitable test bed.

Functions of Acetylcholine

Acetylcholine is found in all neuromuscular junctions and is widely distributed throughout the autonomic nervous system. In the central nervous system, acetylcholine is a key component of the ascending reticular activating system that activates brainstem and forebrain during waking states and is the primary neurotransmitter to activate forebrain during rapid eye movement sleep[19,20]. Pharmacologically, cholinergic activation of nicotinic and muscarinic receptors modulates release of neurotransmitter[21-26] as well as increases the excitability of cells by altering several currents, including suppression of the M-current and small conductance Ca^{2+} dependent current[24-26]. On a neuronal level, it modulates

the signal-to-noise ratio[27-39] and facilitates long-term potentiation and map reorganization in numerous sensory and motor cortices[40-50]. Cognitively, acetylcholine has been shown to be necessary for normal attentional function[28,51-61] and some forms of learning[49,62-69]. Several disease states are linked to cholinergic dysfunction including Alzheimer's disease and several studies point to dysfunctions of the cholinergic system in brains subjected to abused substances, such as metamphetamine, cocaine and morphine[70-73].

Current Technology

Microdialysis and Chromatography

Microdialysis coupled to high-performance liquid chromatography is the current standard for detecting neurotransmitter levels in the brain. It has a spatial resolution on the order of the diameter of the probe (240 μm x 1000 μm) and a typical temporal resolution of 5 minutes[74](Table 1). Theoretically, the temporal resolution of this technique is limited by mass detection[75]. In typical systems, ~50 femtomoles of acetylcholine is necessary for detection[74]. The microdialysate can be pumped at ~2 μl/min. Baseline acetylcholine levels measured in the rodent brain during urethane anesthesia is 4 nM[74]. Assuming a 50 femtomole sensitivity, a first-order estimate suggests that ~5 minutes acquisition time is the minimum time required to detect ~4 nM acetylcholine in the dialysate and stands as the practical temporal resolution for standard microdialysis of acetylcholine[74]. Estimates of acetylcholine levels in the brain using microdialysis are on the order of 10 to 100 nM[74,76-78], though these measures are confounded by missing phasic

peaks due to temporal averaging over 5-15 minutes, reduced effective surface area in the brain in comparison to *in vitro* calibration dishes, and finally, the use of acetylcholinesterase inhibitors in the dialysate to prevent breakdown of acetylcholine and therefore amplify small signals[79].

If the microdialysate is analyzed via capillary electrophoresis combined with Laser-Induced Fluorescence (CE-LIF), detection of very small quantities is possible and thus nanoliter samples can be collected, bringing temporal resolution down to ~20s[80]. However, LIF requires a method of conjugating a fluorophore to the analyte, and CE-LIF for acetylcholine and most other neurotransmitters has not been published to date. Another possibility is to combine capillary electrophoresis with electrochemistry, which has lower sensitivity and an associated temporal resolution on the order of minutes[81].

Electrochemical Detection

Amperometry

Amperometric methods offer 100 ms temporal resolution for changes in a molecular concentration and typically 1 s for cyclic voltammetry, which helps to identify the molecule[82]. The spatial resolution is the diffusion zone of the electrode, typically 100 μm, and multiple spatial points require arrays. Amperometric technology has been most successfully used in the detection of dopamine and serotonin, although it is sometimes difficult to distinguish neurotransmitters. For example, dopamine is indistinguishable from norepinephrine, and serotonin is indistinguishable from its metabolite even using cyclic voltammetry[83].

Enzyme-Assisted Amperometry

Though detection of choline, a surrogate marker for acetylcholine, looks promising[84], electrochemical detection of acetylcholine has proven more difficult[85]. Current designs have a sensitivity of 200 nM[86] *in vitro* whereas estimates of basal levels of acetylcholine using microdialysis are on the order of 10 to 100 nM (see above). The temporal resolution of these systems is on the order of 1 second and the size of the probes are approximately 60 x 750 μm[84](Table 1). Also, mechanical instability of the enzyme layer leads to gradual reductions in signal, although this may be reduced with covalent linking[87]. Past attempts to differentiate acetylcholine from choline have been confounded by the fast activity of endogenous acetylcholinesterase [88]. Finally, enzyme-assisted amperometry is limited to those neurotransmitters susceptible to enzymes that would convert them into an oxidizable or reducible form by the amperometric probe. This list currently includes glutamate and acetylcholine.

Genetic Optical Techniques

In comparison to the above-mentioned technologies, optical methods hold the potential to provide superior temporal and spatial resolution. In particular, the *Aequorea* Fluorescent Proteins (AFPs) have been used in many ways as fluorescent probes in biological systems including analyte-sensitive AFPs (e.g. the synaptophluorin pH sensor for vesicular release) and as fusion proteins in conformation-sensitive molecules(e.g. TN-XXL for calcium detection)[89]. A very successful method of creating a conformation-sensitive genetically-encoded fluorescent biosensor utilizes fluorescence resonance energy transfer (FRET), a

non-radiative energy transfer between the donor and acceptor fluorophores. FRET biosensors are built typically by fusing two AFPs, (e.g., Yellow Fluorescent Protein and Cyan Fluorescent Protein) to a binding protein scaffold, chosen for its affinity to a signaling molecule of interest. When the protein scaffold binds its ligand, a conformational change moves the fused AFPs either closer or further apart. The FRET efficiency between the AFPs is highly dependent on distance and therefore large changes in FRET can occur with slight conformational changes in the scaffold protein[90]. A change in FRET efficiency results in an enhanced fluorescence of one of the AFPs and diminished fluorescence in the other, and this change is detected as the signal.

Relevant to detection of neurotransmitters, a FRET biosensor has been developed from the bacterial periplasmic binding protein for glutamate[9,10]. This has provided a de facto optical sensor for glutamate. Similarly, a small number of G protein-coupled receptors have been used as a scaffold for FRET-based sensors, including the parathyroid hormone receptor, adrenergic α_{2A} and β_1-receptors, and adenosine A_{2A} receptor[8,91]

These are promising approaches with several great advantages. First, the biosensor is genetically encoded and as such can be delivered via viral transduction or genetic animal models[7]. This would avoid damage to the parenchyma as is necessary for microdialysis or electrochemistry. One drawback to genetic delivery however is that the expressed protein may interfere with cellular processes[92]. Genetic delivery also holds the potential for selective expression of the biosensor to particular cell types or even locations in cells, like

synapses[7]. Microdialysis and electrochemical methods can only measure extrasynaptic levels of neurotransmitter-that which is either spillover from synaptic transmission or released directly into the extrasynaptic space during volume transmission[11]. To date, however, the detection of either neurotransmitters or surface receptor activity by these optical biosensors is limited to only a couple molecules and has yet to be employed *in vivo*.

Proposal of Biosensor

It is in the context of the current technology for measuring neurotransmitters and surface receptor activity that we propose a complementary methodology: Cellular Neurotransmitter Fluorescent Engineered Reporters (CNiFERs). CNiFERs are cultured cells genetically engineered to express a cloned surface receptor as well as a fluorescent indicator that responds to activity of the receptor. CNiFERs are implanted in the brain and their optical signal detected by fluorescence microscopy. When the receptor-specific neurotransmitter is released locally, the CNiFERs respond with a fluorescence change, reporting both the presence of the neurotransmitter as well as activity of the expressed receptor.

In this initial realization, we chose to express the M1 muscarinic acetylcholine receptor in human embryonic kidney (HEK293) cells. We chose HEK293 cells as they are a hardy cell line that strongly expresses transgenes[93]. We chose the muscarinic M1 as it is a G_q protein-coupled receptor and therefore when activated by acetylcholine induces a robust increase in cytosolic calcium by the

IP_3 pathway in the CNiFERs[94]. Calcium is a ligand for which many genetically encoded FRET based sensors are available[95]. We have expressed the troponin based TN-XXL indicator, which provides both fast kinetics and a large signal change[89]. TN-XXL is a recombinant fusion protein between troponin C and the fluorescent proteins eCFP and Citrine. These cells are implanted in rat cerebral cortex and imaged using two photon microscopy.

CNiFERs harness technology that was initially developed for drug discovery[96-100]. We thus take advantage of an enormous existing resource and extend the use of cell-based indicators from *in vitro* ligand screening to the *in vivo* detection of *in situ* surface receptor activity and neurotransmitter release.

History of the Cell-Based Assay in Drug Discovery

Drug discovery that makes use of recombinant expression of receptors in fluorescent cell-based assays required several technologies. These include recombinant DNA methodology[101] and fluorescent-based reporters, such as cell-permeant Ca^{2+}-indicators[102].

The first realization of high-throughput screening that used a fluorescent cell-based assay was the fluorescent imaging plate reader (FLIPR)[98]. This technology screens plates with multiple wells seeded with cultured cells expressing a surface receptor of interest and typically loaded with an organic dye that is sensitive to a molecule modulated by the surface receptor, for example, calcium. Each of a library of drugs is robotically delivered to individual wells and fluorescence measurements are made. If the surface receptor is activated by a drug, this is

reported by a fluorescence change of the dye and marks the drug for further characterization. Of relevance to the current work, high-throughput screening has driven the development of cell-based assays expressing receptors that are coupled to a change in intracellular calcium[103]. As an example, non-G_q G protein-coupled receptors may be linked to the G_q protein Ca^{2+}-signaling cascade with chimeric G protein α-subunits[104]. This instantly provides access to all G protein-coupled receptors, which roughly equal 1000 in the human genome and are specifically activated by ~60 endogenous neurotransmitters[105]. CNiFERs are thus modular in nature and development of a CNiFER for another neurotransmitter/receptor pair is achieved by simply changing the surface receptor expressed.

Grafted Cells

Instead of being used in *in vitro* assays as in drug discovery, CNiFERs are implanted in the brain. Implantation of genetically-modified cells is the essence of *ex vivo* gene therapy, where an implantable cell line is genetically modified to express a secreted protein of interest. In one body of work, this involved expression of Nerve Growth Factor, a protein that has been shown to be regenerative to cholinergic cell bodies in the basal forebrain and supportive of CNS function[106]. This has led to a large body of work describing various donor cells, methods of gene transfer and subsequent tests of persistent gene expression and histological effects of chronic implantation[107]. A number of cell types have been used, including Schwann cells, endothelial cells, astrocytes, and

skin fibroblasts [107-109]. Recently, promising results were obtained in a phase I clinical trial in which autologous fibroblast cells expressing NGF were implanted in humans with Alzheimer's disease in hopes of restoring CNS cholinergic function[110].

Taking from *ex vivo* gene therapy, we have chosen to use a retroviral gene transfer into our CNiFERs. While many methods exist for expression of recombinant dna in cell lines, retroviral transfer of genetic material (e.g., lentivirus) has been generally accepted as the preferred method for stable expression in cell lines exhibiting consistent growth and replication as do HEK293 cells[107,108].

Ex vivo gene therapy studies have also established that implanted cells will normally be rejected by the host immune system unless they are autologous or isogeneic lines. Alternatively, cyclosporine can be used to suppress this rejection over a period of several months[111]. As we use HEK293 cells, which are non-autologous and non-isogeneic, cyclosporine was injected for chronic implantation studies.

Histological findings have shown that a glial scar is formed around grafted cells[107]. This scar may inhibit the free diffusion of released neurotransmitters to the implanted CNiFERs and is an unknown with regard to long term (>2 days) chronic experiments.

While cell lines that do exhibit contact inhibition (such as primary skin fibroblasts) will not form a tumor in the brain, immortalized lines such as HEK293s that do not exhibit contact inhibition will eventually form a tumor[107]

(Figure 1). This places a potential temporal limitation for chronic experiments with CNiFERs using lines that persistently replicate.

Finally, it has been shown that implanted cells will continue to express protein up to 24 months after implantation[109], which is a prerequisite for long term implantations. Expression levels however were much lower that measured *in vitro* and whether this decrement will preclude use of CNiFERs over a long time scale remains to be seen.

Previous Biosensors

Previous studies using biosensors have motivated this work. Prolactin-secreting pituitary cells were transplanted into rat striatum as a means to detect striatal dopamine release[112]. The spread of prolactin immunoreactivity from the transplanted cells inversely related to dopamine levels measured by microdialysis. Since dopamine inhibits prolactin secretion by the pituitary cells, increased (obtained by injecting amphetamine) or decreased (obtained by lesioning dopamine terminals with 6-hydroxydopamine) dopamine concentration in the extracellular fluid decreased or increased the halo of prolactin immunoreactivity, respectively. These experiments showed that dopamine concentration present in the extracellular fluid under basal conditions is capable of inhibiting prolactin secretion in transplanted pituitary cells. Hence, dopamine released from striatal nerve terminals into the extracellular space, a form of volume transmission, achieves functionally relevant concentrations and activates D2 dopamine receptors expressed in these transplanted cells. In another

example, *Xenopus* myocytes that strongly express nicotinic cholinergic receptors were recorded with whole cell electrophysiological techniques and used *in vitro* as reporters for acetylcholine release from *Torpedo* electric organ synaptosomes. The finding was that the machinery necessary for a quantal and pulsatile release of neurotransmitter remained functional in the synaptosome preparation and resembled that of normal nerve-muscle contact during synaptogenesis in *Xenopus* cultures[113]. Finally, *in vivo*, neuroblastoma cells filled with organic calcium dye were implanted in rat brain as a test bed for a fiber-optic imaging system[114]. The same work proposed transfection of specific receptors in the neuroblastoma cells for detection of signaling molecules of interest in the brain. This, in essence, is the basis for CNiFER cells.

Figures and Tables

Table 1 Current Technology for Measuring Released Neurotransmitters.

Method	ACh Sensitivity	Temporal Response	Size of Sensor	Neurotransmitter Diversity
Microdialysis	1 to10 nM[b]	~ 100 seconds[b]	~1 millimeter[c]	High[b]
Enzyme Assisted Amperometry	~100 nM[a]	~1 second[a]	~1 millimeter[a]	Limited[d]
CNiFER Cells	~10 nM[e]	~10 second[e]	~.1 millimeter[e]	High[e]

References: a[86]; b[74]; c[115]; d[85]; e - see Chapter II: Design and *In Vitro* Characterization of CNiFER Cells.

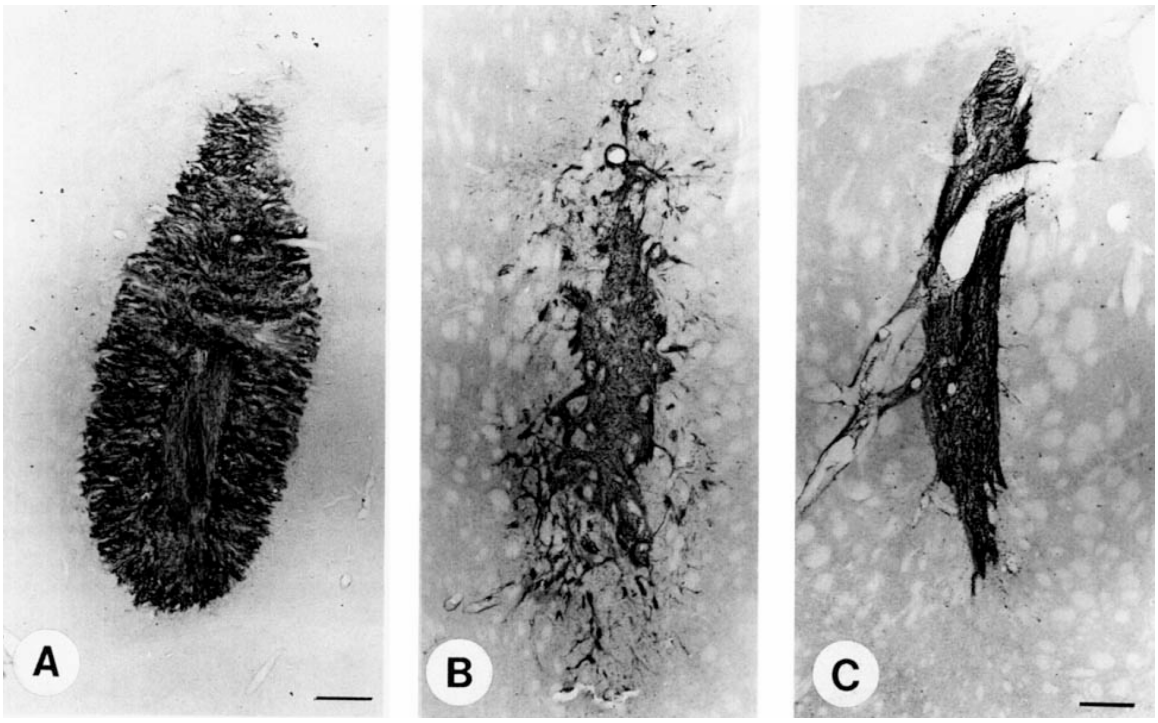

Figure 1 Implants, *Ex Vivo Gene Therapy*

Fibronectin immunoreactivity. Cells implanted in rodent striatum. A: immortalized Rat1 fibroblasts at 3 weeks B: isogeneic primary fibroblasts at 3 weeks C: isogeneic primary fibroblasts at 4 months. Rat1 cells appear to give rise to intracerebral tumors, whereas grafts of primary cells do not differ in size between 3 weeks and 4 months. Bar, A: 400 μm; B,C: 200 μm[107]

Chapter II: Design and *In Vitro* Characterization of CNiFER Cells

Introduction

As discussed above, detection of *in vivo* neurotransmitter levels is traditionally achieved via microdialysis or electrochemistry, both of which are hindered with significant drawbacks in either sensitivity, temporal and spatial resolution, or applicability to only a small number of signaling molecules. To address these drawbacks, genetic optical techniques are becoming well-recognized for detection of signaling molecules and receptor activity[1,9,10]. Acknowledging the current and future gains promised by *de novo* development of single-protein neurotransmitter or receptor optical sensors [7], a difficulty to this approach is that each sensor generally requires extensive development. Idiosyncracies of fusing the AFPs to each binding protein and optimization of such insertions to make the most of often modest conformational changes must be addressed[9,10]. Furthermore, genetically encoded single molecule reporters for neurotransmitters or receptor activity have yet to be used effectively *in vivo*. In contrast, by exploiting the modular design of cell-based CNiFERs, extending function to include another receptor requires only the transduction of different cDNA.

Design of CNiFER Cells

Although many variations of M1-CNiFERs can be imagined, those used in this dissertation are HEK293 cells stably expressing the M1 muscarinic acetylcholine receptor as well as the troponin based TN-XXL calcium inidicator[89]. control-CNiFERs, cells controlling for any endogenous HEK293 response, stably express the mCherry fluorescent protein in place of the M1 receptor (Figure 2).

Proteins are delivered into the HEK293 cells by lentivirus as described in Chapter V: Methods. Mechanisms for cytosolic calcium increase due to muscarinic activation include IP_3-mediated release of intracellular stores as well as calcium influx from membrane channels[94,116,117].

M1 Muscarinic Acetylcholine Receptor

Detection of acetylcholine by CNiFERs can be achieved using either nicotinic or muscarinic receptors. Although nicotinic receptors, being ligand-activated ion channels, may have enhanced temporal kinetics with respect to cytosolic calcium dynamics, we chose the muscarinic receptor. Either M1,M3, or M5 could reasonably be used, since each is G_q coupled to the IP_3 system and as such are known to robustly increase cytosolic calcium levels[118]. We chose to use M1. M2 and M4 are both G_i coupled, affecting primarily the cAMP pathway via inhibition. These could potentially be paired with a reporter for cAMP, *e.g.*, AKAR[119] or co-expressed with chimeric G proteins[120] that would couple them to the G_q system (see Chapter IV: Discussion-Expanding CNiFERs).

TN-XXL, Genetically Encoded Calcium Indicator

There are numerous calcium indicators appropriate for use with CNiFERs. Pilot versions of CNiFERs used organic, cell-permeable Ca^{2+}-indicators of the AM (acetoxymethyl ester) type[121]. These indicators, e.g., Oregon Green BAPTA AM, provide large signal changes in response to calcium increase[102]. However, long-term experiments (> 1 day) with these dyes are not be possible due to their eventual sequestration into intracellular organelles and/or degradation[122]. On the other hand, many genetically encoded calcium indicators (*e.g.*, TN-XXL) are now

available[123-125]. Each is a fusion of a calcium binding protein along with one or more *Aequorea* fluorescent proteins (AFPs) (see Chapter IV: Discussion-Genetically Encoded Calcium Indicators).

TN-XXL is the latest member of the troponin C-based family of Ca^{2+}-indicators[89,126,127], consisting of a troponin C Ca^{2+} binding site flanked by enhanced cyan fluorescent protein (eCFP) and the yellow fluorescent protein Citrine cp174. Upon calcium binding, troponin C undergoes a conformational change that triggers fluorescence resonance energy transfer (FRET) between the two fluorophores. An increase in cytosolic [Ca^{2+}] leads to a characteristic decrease in eCFP fluorescence and an increase in Citrine fluorescence. FRET-based sensors allow one to distinguish motion artifact (where fluorescence of the AFPs fluctuate together) and *bona fide* signals (where fluorescence of the AFPs move in opposite directions). TN-XXL was chosen as it offers large maximal signal change (400%), fast kinetics (<500ms on/off rates) and functions well in HEK293 cells[89].

Two Photon Laser Scanning Microscopy

Many different approaches are available to image the fluorescence of TN-XXL and other calcium indicators, especially *in vitro*. *In vivo*, however, imaging is more complicated (see Chapter IV: Discussion-In Vivo Imaging). Briefly, epifluorescence techniques are easily employed, but optical sectioning is very poor and therefore resolving CNiFERs deep in tissue is not possible. Fiber optic epifluorescence techniques however, allow cells to be implanted arbitrarily deep inside the brain and are also compatible with freely-behaving animals[128,129]. The

drawback is that only a single point in space is imaged and so, for instance, control- and M1-CNiFERs would not be resolved.

Two Photon Laser Scanning Microscopy, on the other hand, allows for optical sectioning at depths of several hundred micrometers routinely[130]. Therefore, control- and M1-CNiFERs are easily resolved. Furthermore, two-photon excitation of FRET-based signals is possible, and in fact, can result in similar FRET efficiency changes as in epifluorescence excitation [131]. Finally, two photon microscopy is compatible with various endoscopic techniques to allow arbitrarily deep imaging, or with head mounted systems to allow for experiments with freely-behaving animals[132,133].

Results

Creation of CNiFERs

M1-CNiFERs are HEK293 cells stably expressing the human M1 muscarinic receptor and genetically encoded TN-XXL calcium indicator[134] (Figure 2). Stimulation of M1 increases cytosolic calcium via activation of the G_q/IP_3 second messenger pathway. Cytosolic TN-XXL binds the incoming calcium, inducing a conformational change that enhances FRET between its eCFP and Citrine domains. Activation of M1 therefore decreases cyan but increases yellow fluorescence in M1-CNiFERs. In addition, we create control-CNiFERs expressing mCherry fluorescent protein[135] instead of the M1 receptor.

For all *in vitro* experiments, the entire field of view was averaged for each time point. Typically, this included ~100 cells.

Fast Perfusion of CNiFER Cells

To determine M1-CNiFER kinetics and temporal resolution, responses are studied under two photon microscopy (TPLSM)[136] using a fast perfusion system(SF-77B, Warner Instruments, CT). Robust FRET signals are elicited by 2.5 s pulses of 100 nM or 60 nM acetylcholine (Figure 3). M1-CNiFERs initiate response within 2 s, have a half-maximal rise-time ~2 s, and a full width at half maximal amplitude of ~7 s. Peak response ($\Delta R/R$) to the presentation of 100 nM or 60 nM acetylcholine is ~90% and ~30% respectively. M1-CNiFERs can resolve 2.5 s pulses of 100 nM acetylcholine with an interstimulus interval ≥ 6s (Figure 4). To assess response profile to repetitive stimulations, short pulses of 300 nM acetylcholine are presented with a 30 s interstimulus interval. M1-CNiFERs do adapt to roughly 50% response but stabilization occurs at ~5 presentation (Figure 5).

Bath Application of Acetylcholine

Bath application of acetylcholine (1 nM – 300 nM for 8 minutes), to determine M1-CNiFER sensitivity to extended agonist presentation, features a single peak (phasic response) observed ~20-40 s after the onset followed by a plateau (tonic response) remaining until termination of acetylcholine (Figure 6). For phasic responses, EC_{10}, EC_{50}, EC_{90}, and Hill coefficient equal 3nM, 11nM, 34 nM, and 1.9 respectively, and the maximum $\Delta R/R$ = 110%. The corresponding tonic responses are 5nM, 9nM, 14nM, 4.4, and the maximum $\Delta R/R$ = 18% (Figure 7). Importantly, the M1-CNiFER dynamic range is suited to acetylcholine levels measured in the rat brain with microdialysis (~1-100nM) [74,76-78]. Considering the

K_i of acetylcholine to the M1 muscarinic receptor is ~10 μM[105], such a low EC_{50} for M1-CNiFERs suggests a large receptor reserve.

Calcium-Free Media

To explore the nature of the calcium signal during acetylcholine evoked M1-CNiFER activation, experiments with calcium-free media were performed. These demonstrated that the M1-CNiFER tonic, but not phasic, response is dependent upon calcium in the media (Figure 8). In Figure 8a M1-CNiFERs respond to 30 nM acetylcholine in calcium media with typical phasic and tonic components. Figure 8b shows M1-CNiFERs respond in calcium-free media with the phasic, but not the tonic, component. When calcium is returned to the media in the continued presence of 30 nM acetylcholine, M1-CNiFERs respond with a phasic and tonic component, though possibly with a slower phasic onset. Finally, in Figure 8c calcium withdrawal from media during the M1-CNiFER tonic response abolishes the response completely.

High-Throughput Screening using Flexstation™ 3

Since HEK293 cells can express endogenous surface receptors, M1-CNiFER response specificity is a concern. Acetylcholine as well as potentially confounding neurotransmitters present *in vivo* are screened on a high-throughput Flexstation™ 3 (Figure 9; Figure 11). All responses are normalized to the M1-CNiFER response to saturating acetylcholine (100 nM) and expressed as S/S_{M1}. Acetylcholine at 100 nM strongly activates M1- but not control-CNiFERs (S/S_{M1} = 1 vs. S/S_{M1} = 0, respectively). In addition, M1-CNiFERs are far more sensitive

than control-CNiFERs to acetylcholine (EC_{50} = 7.5 nM vs. EC_{50} > 10 μM, respectively). Finally, 100 nM atropine sulfate abolishes the M1-CNiFER response to 100 nM acetylcholine, verifying that the mechanism of activation is muscarinic (Figure 10). In this last experiment, ΔR/R (%) is reported.

Potentially confounding neurotransmitters are typically found to have EC_{50}s > 1-10 μM and S/S_{M1} < .05 (Figure 9; Figure 11). Notable exceptions include norepinephrine (S/S_{M1} = .21 at 3.3 μM), adenosine (S/S_{M1} = .19 at 10 μM) and vasoactive intestinal peptide (S/S_{M1} = .33 at 100nM). In the case of vasoactive intestinal peptide, M1- and control-CNiFERs respond slightly differently. However, this occurs only at the highest concentrations and the magnitude of the difference is less than 15% of the M1-CNiFER response to 100 nM acetylcholine. Still, *in vivo*, pharmacological controls are necessary to verify that an M1-CNiFER response is due to cholinergic action at muscarinic receptors.

Conclusion

In vitro, M1-CNiFERs respond with a ~30% ΔR/R within 2 s to a 2.5 s pulse of 100nM acetylcholine. The half-maximal rise-time is ~2 s, and full width at half maximal amplitude is ~7 s. M1-CNiFERs are capable of resolving pulses of acetylcholine that are delivered at least 6 seconds apart. Bath application of acetylcholine (1 nM - 1 μM for 8 minutes), results in a dose-dependent signal change up to 110% with a phasic peak followed by a decreased but stable plateau. Finally, control-CNiFERs not responsive in these ranges of acetylcholine.

Nature of the M1-CNiFER Signal

M1-CNiFERs respond to prolonged acetylcholine with an initial phasic peak followed by a reduced but stable tonic plateau (Figure 6). The tonic plateau is dependent on external calcium and thus likely represents calcium influx through membrane channels (Figure 8). This may have been expected as wildtype HEK293 cells (which express the M3 muscarinic receptor, albeit at a low concentration) respond with a qualitatively similar phasic/tonic response to prolonged exposure of the muscarinic agonist methylcholine[137]. And, similarly, exposure to methylcholine in calcium-free media resulted in a sharp phasic response but no tonic response and the tonic response was recovered by the readdition of calcium in the media[137,138]. However, what is the likely mechanism of this effect?

Activated G proteins from muscarinic M1 activity cause phospholipase C (PLC) to enzymatically process membrane bound phosphatidylinositol biphosphate (PIP_2) into inositol triphosphate (IP_3) and diacylglyercol, which stays in the membrane. IP_3, on the other hand, diffuses into the cytoplasm and activates IP_3 receptors expressed on the surface of the endoplasmic reticulum. IP_3 receptor activation releases endoplasmic reticulum calcium stores into the cytoplasm at which point the calcium is either pumped back into the endoplasmic reticulum by Sarco/Endoplasmic Reticulum Ca^{2+}-ATPase (SERCA) or out of the cell by the faster plasma membrane Ca^{2+} ATPase (PMCA)[94]. In the face of prolonged agonism of a G_q coupled receptor, at least in non-excitable cells like HEK293s, cellular calcium is gradually lost via PMCA activity leaving endoplasmic reticulum

stores empty. This emptiness triggers an influx of external calcium through store operated channels of which the Ca^{2+}-release-activated Ca^{2+} (CRAC) channel is prototypical[94].

The phasic response of M1-CNiFERs to prolonged acetylcholine is likely due to release from intracellular stores, while the tonic response is dependent on external calcium influx. As see in Figure 8, the phasic response persists whether or not in the presence of external calcium. Also, the phasic response is larger, consistent with the observation that release from intracellular stores is typically larger than influx from external calcium[94,139]. Finally, the Hill coefficient for the tonic response is 4.4 (Figure 7), suggesting a very high cooperativity. It has recently been found that CRAC channels open in response to depleted internal calcium stores with a Hill coefficient of 4. The very high cooperativity of CRAC channel activation is thought to be due to its dependence on oligimerization of stromal interaction molecule 1 (STIM1)[140]. Our data is therefore consistent with the tonic component of the CNiFER response being due to external calcium influx through CRAC channels.

Kinetics

The individual elements of a G protein-coupled receptor (GPCR) signaling cascade of the type relevant to the M1 muscarinic receptor are very well characterized[118]. The most important steps are agonist binding and receptor activation, receptor–G protein interaction, G protein conformational changes including GDP release and GTP binding, G protein–effector (phospholipase C) interaction, change in effector activity and the resulting second messenger

concentration changes (Ca^{2+})[91]. FRET-based molecular probes have been used extensively in measuring the temporal dynamics of the above steps and are summarized in the following paragraphs (Figure 12).

Activation of the receptor by its ligand, and subsequent conformational change, has been measured using FRET methods but in GPCRs other than the muscarinic receptor. The adrenergic α_{2A} and β_1 receptors, and A_{2A} adenosine receptors activate in 30-50 ms, but the parathyroid hormone receptor requires ~1s[91]. It is not yet known if this reflects a difference between small molecule and peptide receptors or is simply a matter of receptor diversity. Furthermore, different ligands of different classes (partial agonist, inverse agonist) seem to have different activation constants[91].

Interactions between GPCR and G proteins have been studied using FRET and found to have a rate constant of 30-50 ms after ligand presentation, providing the G proteins are expressed at sufficiently high levels[91,141]. This suggests that interaction with the G protein occurs almost immediately upon receptor activation.

The activation of G proteins by unbinding of GDP and binding of GTP occurs at a longer time scale. FRET measurements have shown that G_i and G_s type G protein complexes activate with a timescale of 500-1000 ms after ligand presentation[142,143], thus making this a rate-limiting step.

The temporal profile of PLC/IP_3 dynamics has been measured in experiments using a GFP fusion protein with the pleckstrin homology domain of PLCδ1 ($PH_{PLC\delta}$), which binds to IP_3, allowing visualization of IP_3 translocation from the

membrane (in the form of PIP2) to the cytosol[144-146]. However, the experiments have focused on the order of minutes, where IP_3 levels roughly follow Ca^{2+} levels. As for calcium, fast-perfusion experiments with M1-CNiFERs (Figure 3) measure Ca^{2+} changes to occur in roughly 5 seconds, the slowest step in the receptor-activated cascade.

The final step in M1-CNiFER signaling is binding of the calcium indicator TN-XXL to calcium. On and off rates are less than 500 ms and are likely only minor contributors to the kinetics of CNiFERs[127].

In summary of CNiFER temporal kinetics, it is likely that signaling steps after G protein activation are rate limiting (e.g., IP_3 generation and IP_3 receptor activated calcium release) and occurs at ~5 s (Figure 3), analogous to studies using G_s receptors where cAMP production is rate limiting[1].

Adaptation

M1-CNiFERs adapt to repetitive presentations of short acetylcholine pulses (Figure 5). M1-CNiFERs also adapt to sustained acetylcholine from a large initial phasic peak to a reduced but stable tonic plateau (Figure 6). These effects may reflect a shift of calcium dynamics from internal to external stores (see above), or a desensitization of the GPCR-mediated signaling cascade.

Sustained activation of GPCRs is followed eventually by G protein-coupled receptor kinase (GRK) mediated phosphorylation. Although phosphorylated GPCRs are still active, it leads to binding of β-arrestin that sterically inhibits further activation of the receptor (desensitization)[147 148]. FRET measurements of GRK-mediated phosphorylation suggest a time scale of ~20s in HEK293 cells but

β-arrestin binding occurs within seconds thereafter[1,149]. β-arrestin binding and receptor desensitization depends on continued agonist presence, as removal of agonist causes a dissociation of β-arrestin from the GPCR, though phosphorylation remains and rechallenge with agonist causes β-arrestin binding within seconds[148,149].

β-arrestin binding to receptor can occur quickly, but β-arrestin conformational change takes roughly 5 minutes and leads to association with clathrin coated pits and eventual internalization of the receptor for dephosphorylation and resensitization[1,150]. Resensitization of GPCRs is generally considered to occur in endocytic compartments in the presence of phosphatases. However, in the case of the M3 muscarinic receptor, this was shown only in neuroblastoma cells while in Chinese hamster ovary (CHO) cells, resensitization occurred in the cell membrane, with a half life of 7.5 minutes[147,151]. So, it seems that internalization speeds resensitization in some cell types, but may slow it in others. In another study of M1 receptors in HEK293 cells, after about 10 minutes of 1 mM carbachol, 40% of receptors were sequestered from surface, this increased to 50% by 1 hour. At 10 μM carbachol, there is 20% sequestration and at 100 nM carbachol there is only ~7% sequestration[152]. Dynamin dominant negative mutants suppressed this sequestration almost completely, suggesting a possible genetic approach to reduce internalization. Considering the likely large receptor reserve found in M1-CNiFERs (due to the very low EC_{50} to acetylcholine), sequestration of M1 receptors to physiological levels of acetylcholine seems unlikely to have a significant effect, though this remains to be seen.

Downstream of the receptor, PLC desensitizes rather slowly[147]. However, in experiments using $PH_{PLC\delta}$ to visualize IP_3 dynamics in neuroblastoma cells expressing an endogenous M3 muscarinic receptor, it was shown that prolonged agonism by carbachol led to an initial phasic peak followed by a sustained though reduced tonic level of IP_3, mirroring calcium levels as measured by fura-2 in the same cells[144-146]. Qualitatively, this response is very similar to the TN-XXL response of M1-CNiFERs in the face of prolonged acetylcholine presentation and suggests that the reduced tonic component may be driven at least in part by reduced IP_3 levels, perhaps due to muscarinic receptor desensitization or internalization[146]. Further experiments would be necessary to test this possibility.

Interferents

Ideally, CNiFER cells would not respond to any agonist except that which activates the chosen expressed receptor, in our case the M1 muscarinic receptor. Clearly, this is not the case as HEK293 cells express many endogenous receptors[138,153,154], even if only at minimal concentrations. For this reason, there will be a response to many neurotransmitters other than the neurotransmitter of interest, albeit often only at very high concentrations. But this is why control-CNiFERs are employed. Assuming M1- and control-CNiFERs are expressing similar endogenous receptors as they come from the same HEK293 line, then any interfering neurotransmitters that happen to activate one of these endogenous receptors should activate both M1- and control-CNiFERs equally. These responses can then be discarded.

However, one neurotransmitter was identified where the response of M1-CNiFERs was appreciably larger than the response of control-CNiFERs: vasoactive intestinal peptide (VIP). Fortunately, the response of M1-CNiFERs only diverged from the control-CNiFER response at roughly 30 nM, and control-CNiFERs did still respond quite robustly. Nevertheless, this presents a potential confound but the significance may be small. First, tissue stores of peptides are 50-1000 times less than classical neurotransmitters[155]. Second, microdialysis measurements of neuropeptides can to be 2-3 orders of magnitude lower than for acetylcholine and the monoamines[74,156]. Considering that phasic increases in monoamines as measured by amperometry are ~1 μM[82], it is quite possible that 30-100 nM VIP will not be reached even transiently *in vivo* and the potential interference with acetylcholine detection will be minimal. Furthermore, blockade of the M1-CNiFER response by local perfusion of atropine can be used to substantiate a cholinergic nature of the signal.

Figures

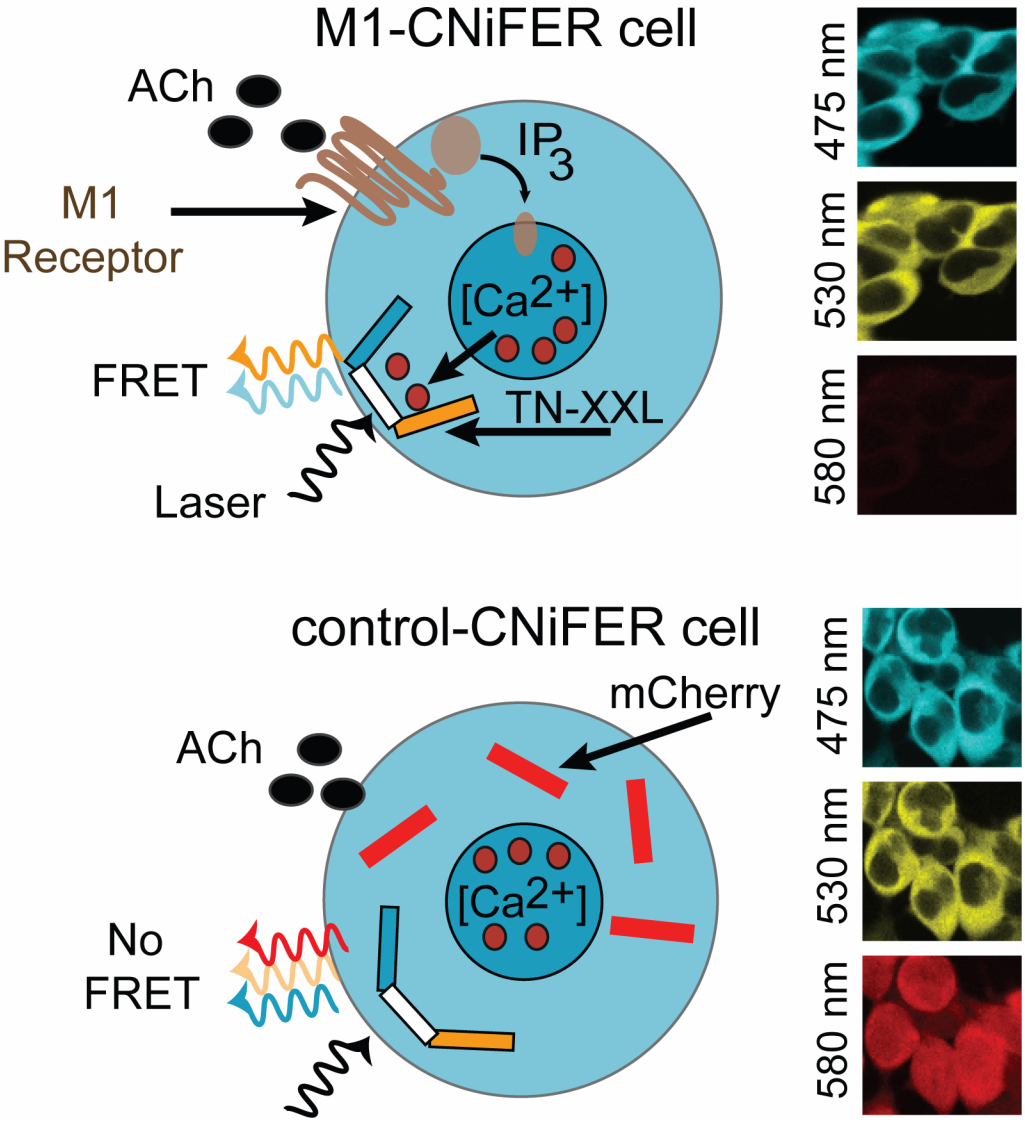

Figure 2 CNiFER Design

CNiFER cells are HEK293 cells stably expressing the genetically encoded calcium indicator TN-XXL. M1-CNiFERs are also stably expressing the M1 muscarinic acetylcholine receptor and control-CNiFERs are stably expressing the fluorescent protein mCherry. Images to the right are taken by two photon microscopy. In M1-CNiFERs, acetylcholine is depicted as activating M1 to induce IP_3-mediated Ca^{2+} cytoplasmic influx detected by TN-XXL. TN-XXL fluorescence (eCFP and Citrine) is collected for the FRET-based signal.

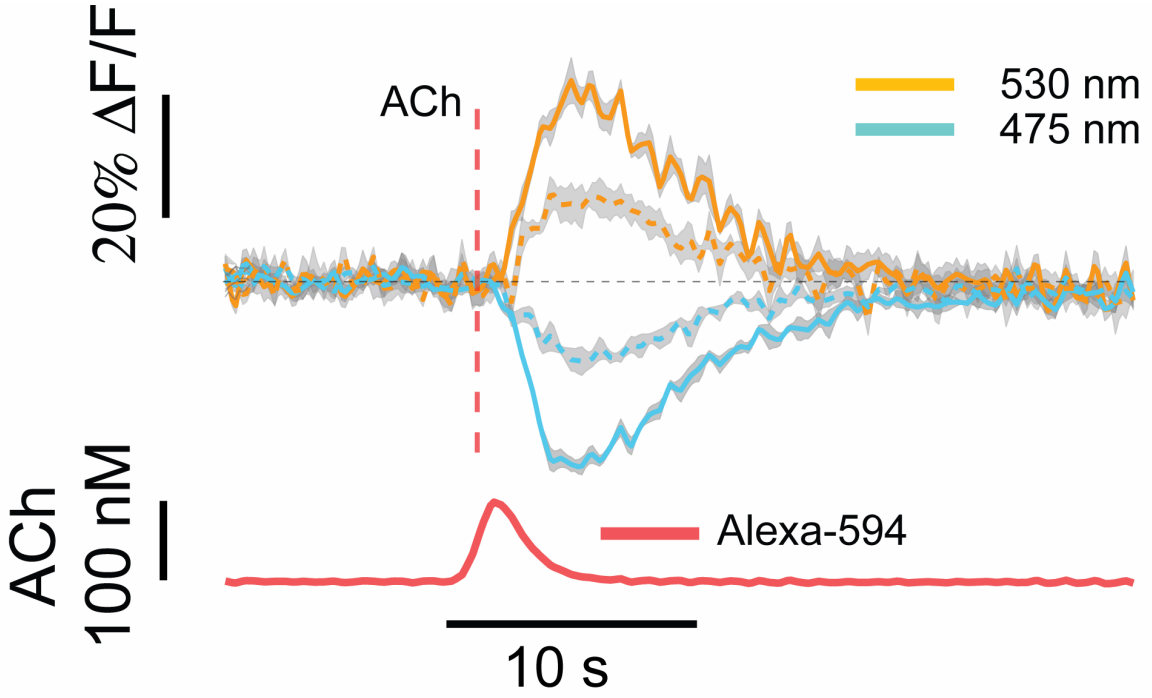

Figure 3 M1-CNiFER Response to Short Acetylcholine Presentations

M1-CNiFER cells in a bath culture chamber respond to acetylcholine (ACh) presented by an actuated perfusion stepper device. The FRET-based response is an increase in the Citrine channel (530 nm) and decrease in the eCFP channel (475 nm). Time to peak response is ~5 seconds and full width at half maximal response is ~7 seconds. Length of acetylcholine presentation (2.5 s) measured as full width at half maximal fluorescence in alexa-594 channel. Standard errors represented by shaded area, n = 5 runs per trace.

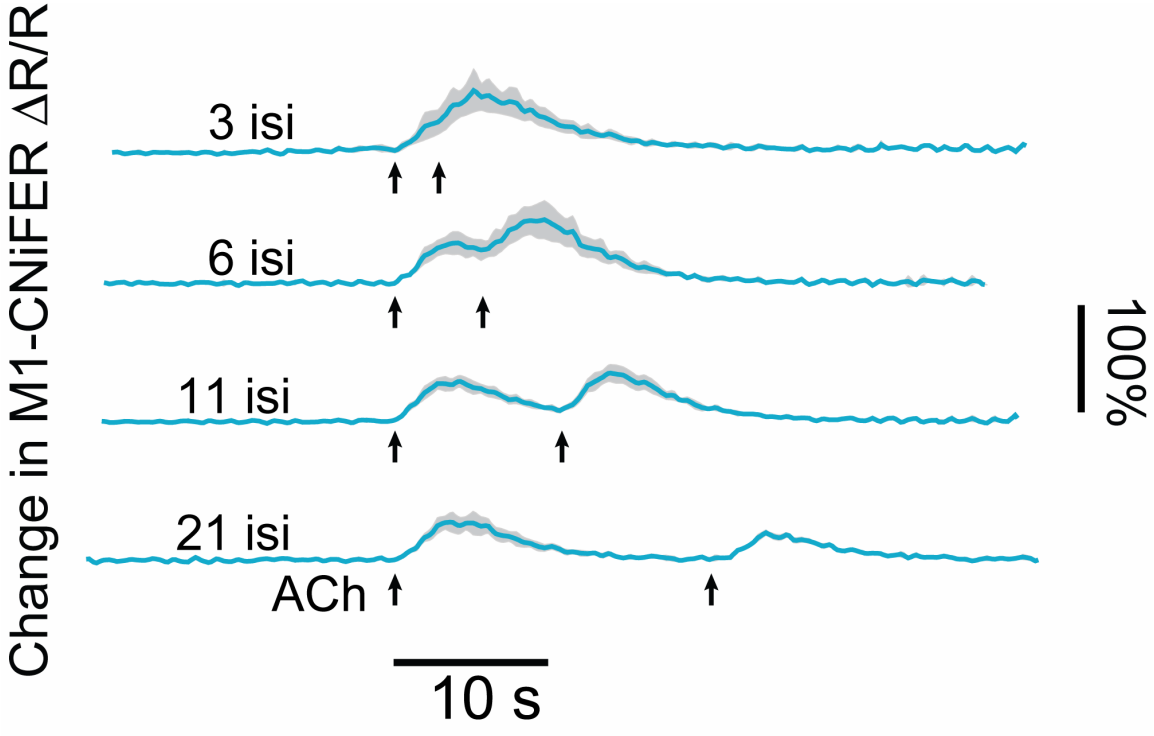

Figure 4 Temporal Resolution of M1-CNiFERs *In Vitro*

M1-CNiFERs are capable of resolving two 2.5 s presentations of 100nM acetylcholine when they are separated by at least 6 seconds. Standard errors represented by shaded area, n = 3 runs per trace.

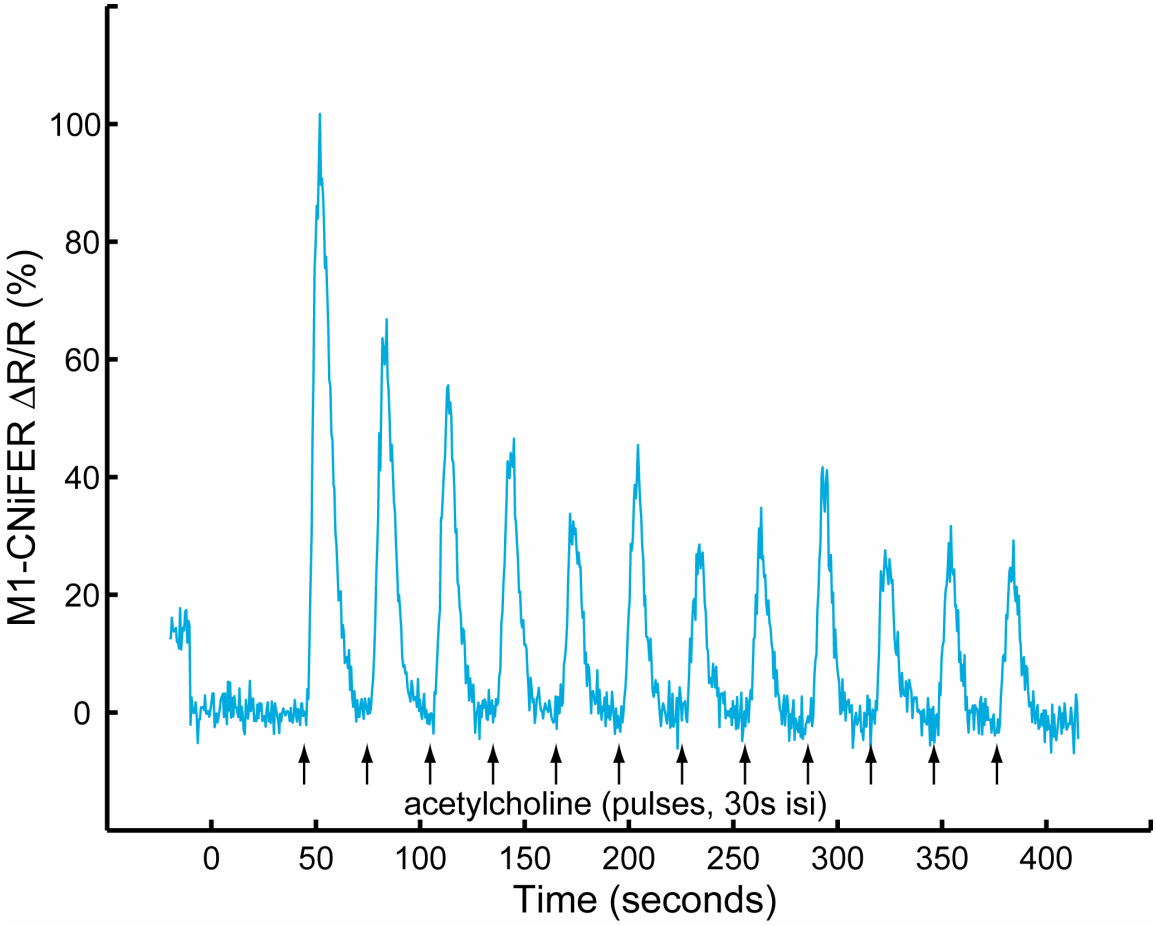

Figure 5 Repetitive Stimulation of M1-CNiFERs

M1-CNiFERs adapt to repetitive presentation of short 300 nM acetylcholine pulses with a 30 second interstimulus interval. Stabilization occurs at ~5th presentation.

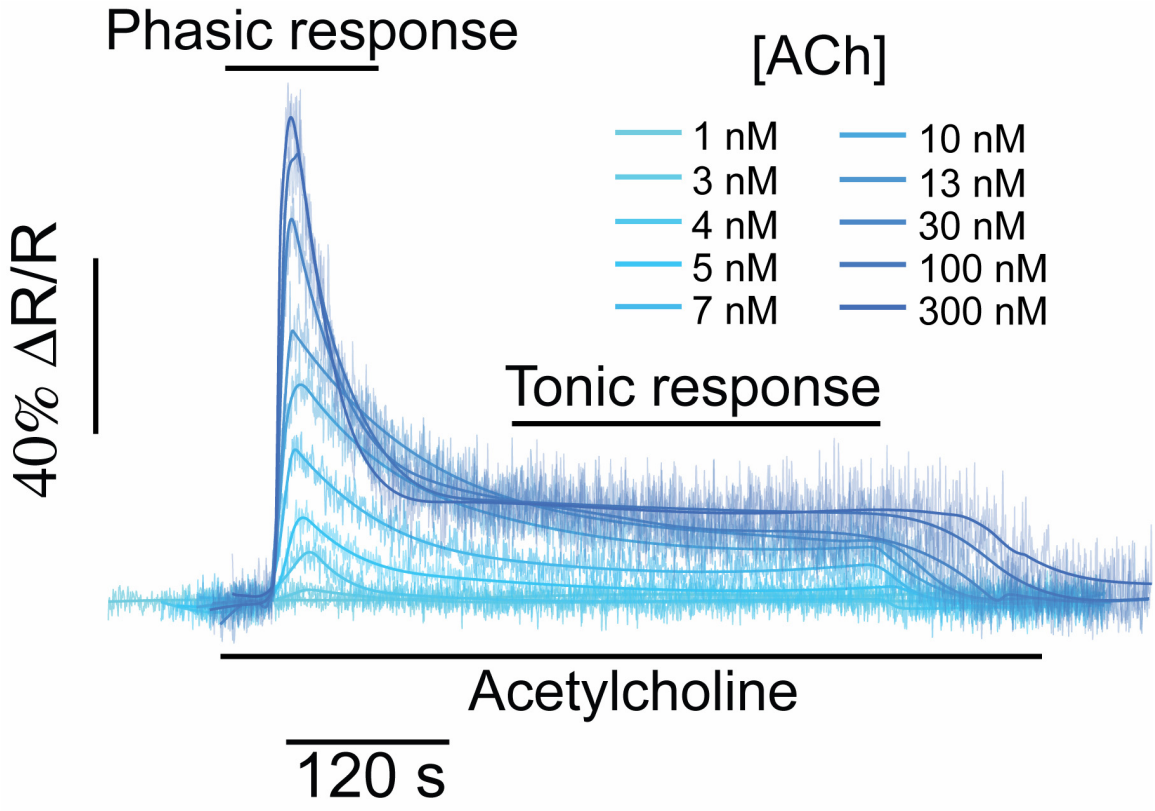

Figure 6 M1-CNiFER Response to 8 minute Applications of Acetylcholine.

M1-CNiFERs respond initially with a large phasic response followed by an attenuated, but stable, tonic response. control-CNiFERs do not respond in this concentration range (data not shown). Smooth lines are fitted curves to raw data.

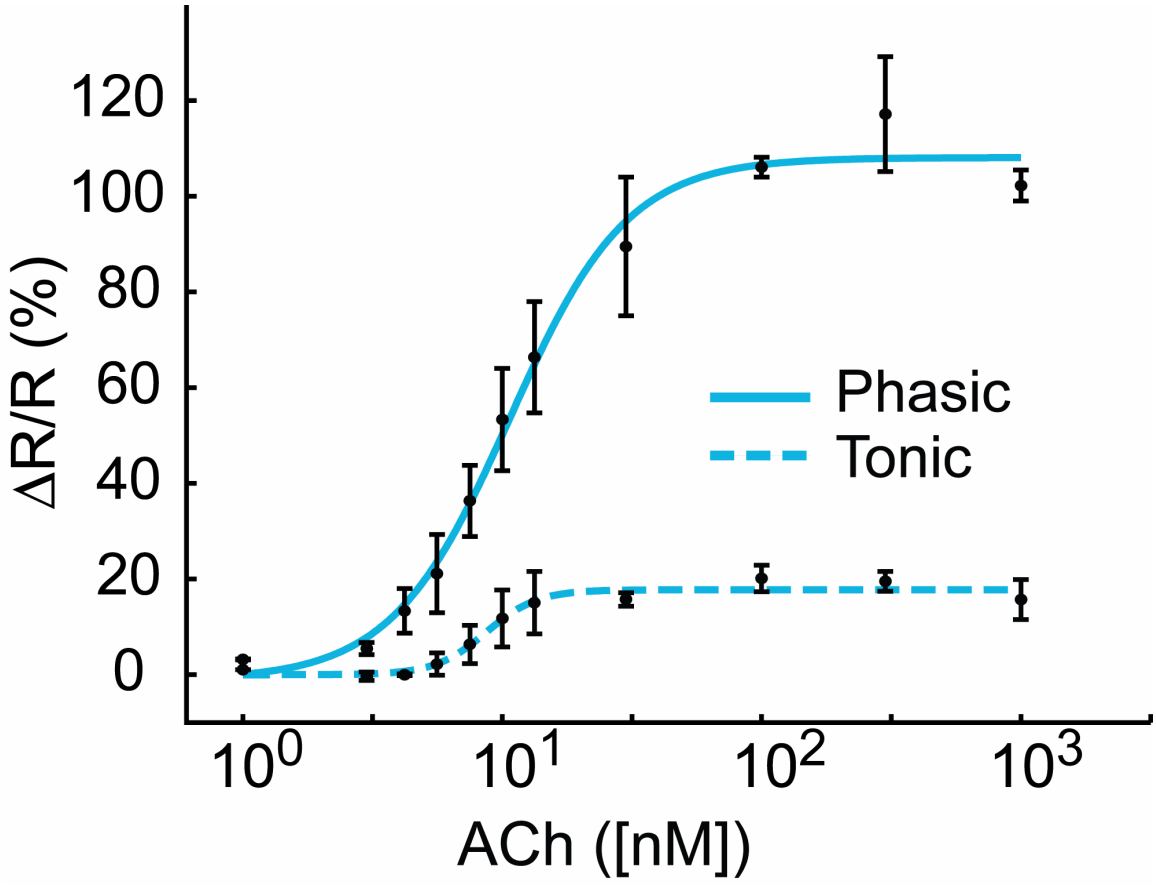

Figure 7 Dose Response Curve of M1-CNiFER Response to Acetylcholine

M1-CNiFERs respond to acetylcholine with a phasic (solid) followed by tonic (hashed) response. The phasic EC_{50} = 11 nM and tonic EC_{50} = 9 nM. Maximum phasic ΔR/R = 110% and maximum tonic ΔR/R = 18%. Error bars represent standard errors, n = 3 for each data point, using different passages separated by 1 week each.

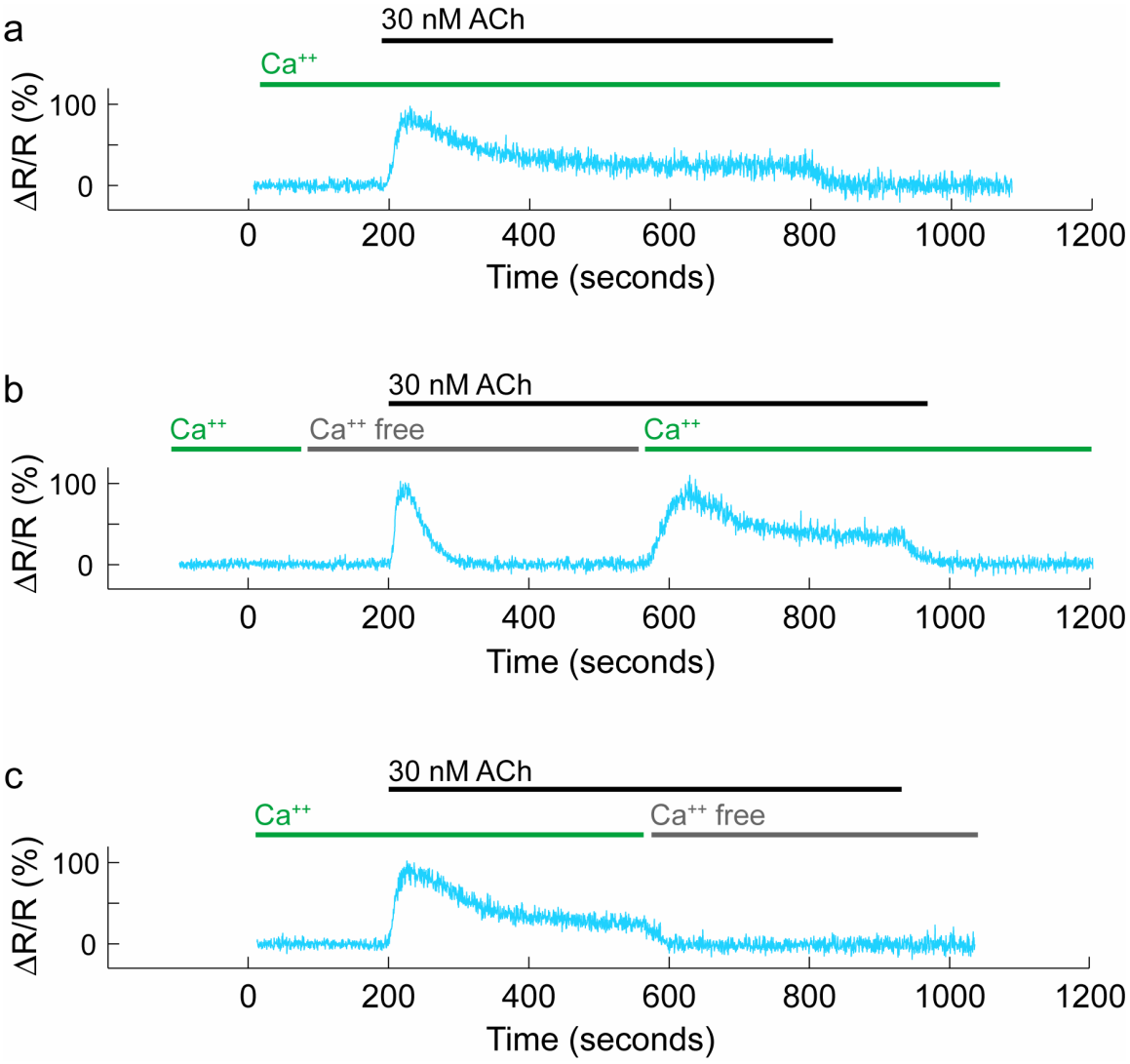

Figure 8 M1-CNiFER Dynamics in Calcium-Free media

Experiments with calcium-free media demonstrate that the tonic M1-CNiFER response is dependent upon calcium in the media. **a)** M1-CNiFERs respond with typical phasic and tonic components to 30 nM acetylcholine in the constant presence of calcium. **b)** M1-CNiFERs respond with the phasic component only in calcium free media. Calcium returned to the media in the continued presence of 30 nM ACh results in a response with phasic and tonic components, though possibly a slower phasic onset. **c)** Calcium withdrawal from media during the M1-CNiFER tonic response abolishes the response.

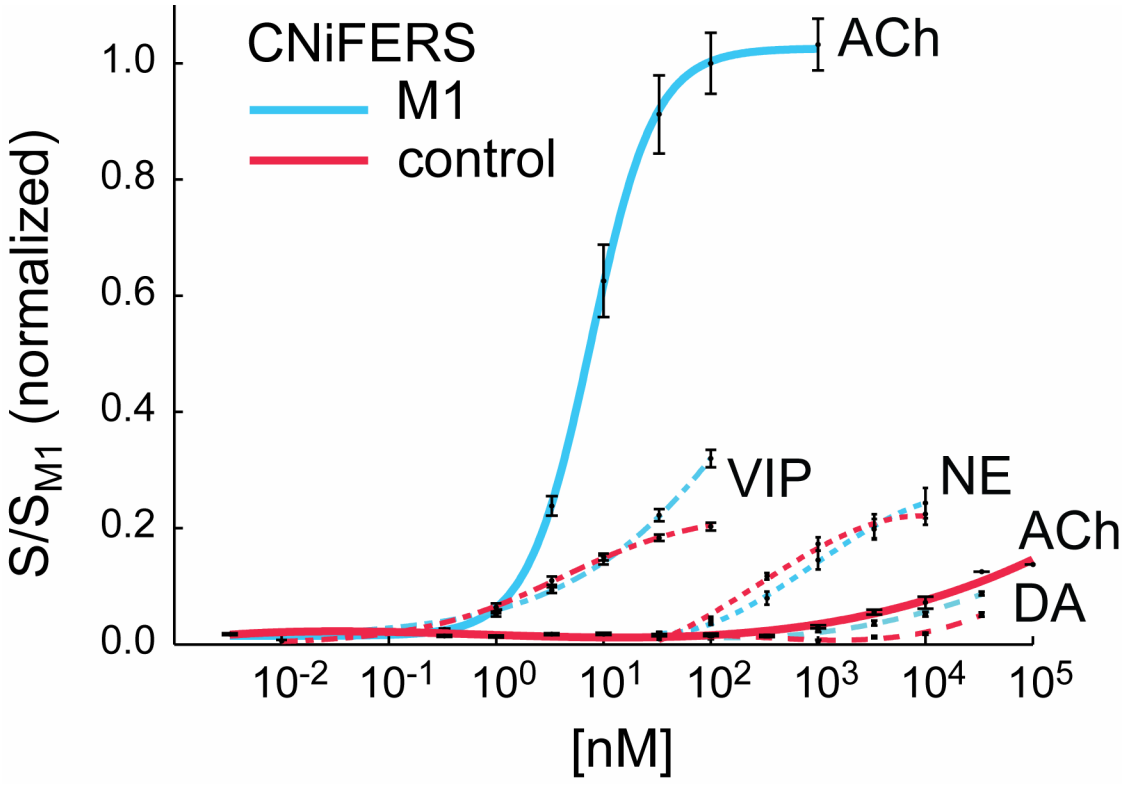

Figure 9 Dose-Response of CNiFERs to a Sampling of Potential Interferents

A collection of dose-response curves of M1-CNiFERS (cyan) and control-CNiFERs (red) to acetylcholine (ACh), vasoactive intestinal peptide (VIP), norepinephrine (NE) and dopamine (DA). Bars represent standard errors, n = 3 for ACh, n = 5 for rest; taken from different passages separated by 2 weeks.

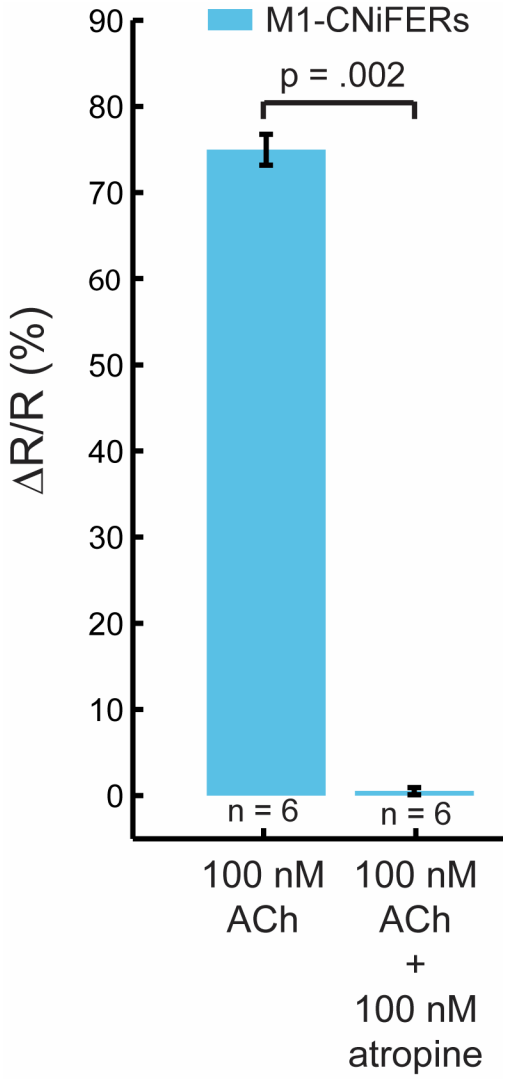

Figure 10 Atropine Abolishes M1-CNiFER Response to Acetylcholine

Using Flexstation™, M1-CNiFERs were pre-incubated with either 100 nM atropine sulfate or ACSF and then presented with 100 nM acetylcholine (ACh). Atropine abolishes the M1-CNiFER response. Effect significance assessed using the non-parametric Wilcoxon rank sum test. Error bars represent standard errors, n = 6 trials each.

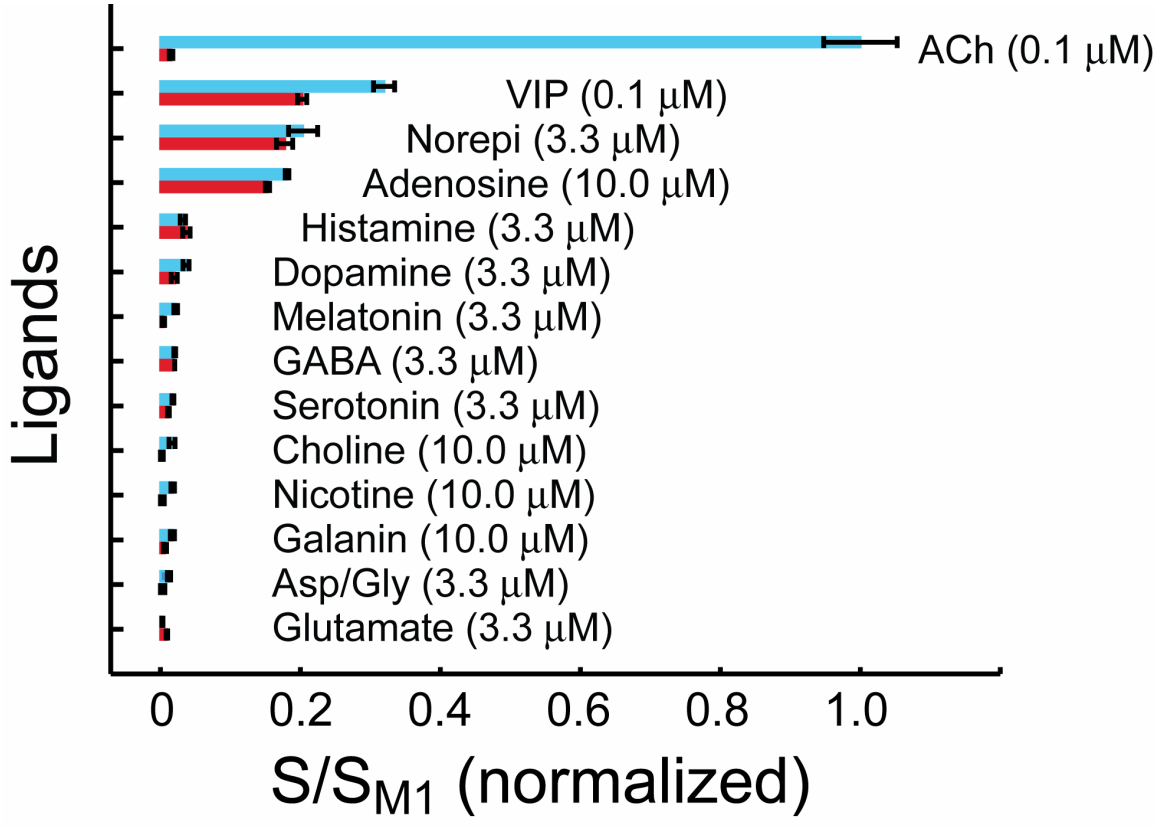

Figure 11 Response of CNiFERs to Acetylcholine and Interferents

M1- and control-CNiFER respond similarly in high-throughput screening to a large number of potential interferents found *in vivo*, see discussion on VIP in text. These data collected with Flexstation™ 3. Bars represent standard errors, n = 3-5; data taken from passages separated by 2 weeks each. M1-CNiFERs (cyan), control-CNiFERs (red).

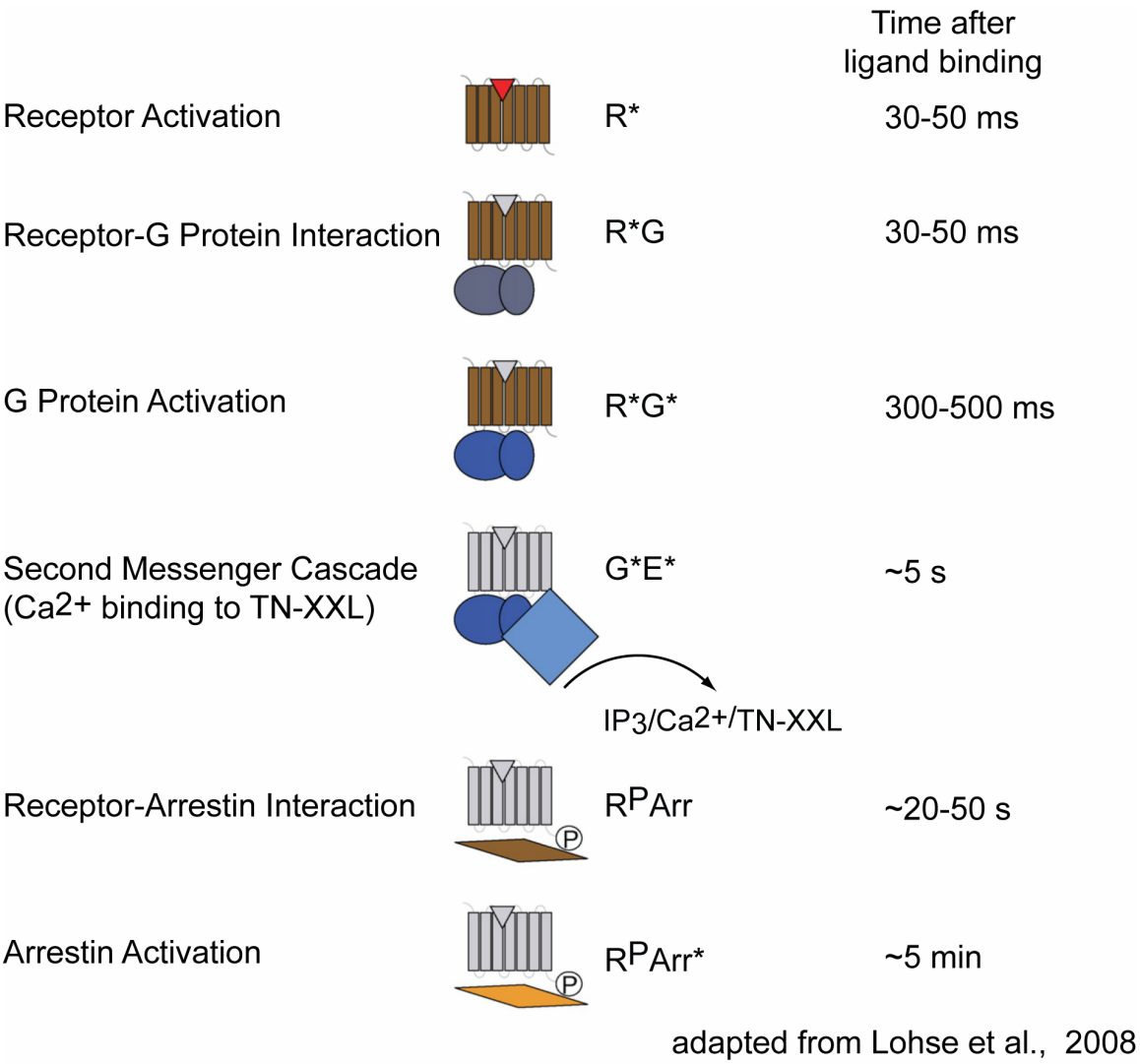

Figure 12 Kinetics of GPCR Activation

Depiction and kinetics of the stages of GPCR activation, the second messenger cascade, and receptor desensitization. Receptor, R; G protein, G; Effector, E; Phosporylated, P; Arrestin, Arr; Activation, *. Adapted from Lohse et al., 2008[1].

Chapter III: *In Vivo* Characterization of CNiFER Cells

Introduction

Although CNiFERs offer favorable *in vitro* characteristics as biosensors with relatively fast kinetics (~6 s temporal resolution) and large response amplitude (110% ΔR/R), their function *in vivo* may be hampered by many factors. First, CNiFERs may act differently *in vivo* than they do *in vitro*. This may be because of a host of reasons regarding exposure to the numerous signaling molecules diffusing throughout the central nervous system. For example, calcium influx into CNiFERs may be induced by an endogenous neurochemical (perhaps even high ambient acetylcholine, or some other molecule) and thus become saturated so as further activation would not be possible.

Second, given a functional CNiFER *in vivo*, the biosensor works on the assumption that released acetylcholine will diffuse the distance from the cholinergic terminal to the implanted CNiFERs. Importantly, *ex vivo* gene therapy studies have shown that a glial scar forms around brain implants of HEK293 cells[107] and this scar may impede the volume transmission of acetylcholine from the parenchyma to the CNiFERs. Furthermore, it is also possible that even in the absence of a glial scar endogenous acetylcholinesterase will metabolize acetylcholine too rapidly for the molecule to diffuse into the implantation site to activate the CNiFERs. Acetylcholinesterase is one of the fastest known enzymes, each molecule turning over ~20000 molecules of acetylcholine per second[157,158]. However, measurements of the diffusion distance of acetylcholine in the brain have not yet been made. Finally, assuming diffusion of acetylcholine to CNiFERs

does occur, it is possible that a long diffusion time will confound apparent acetylcholine release patterns and possibly be a limiting factor for CNiFER temporal resolution. The best studied diffusion kinetics *in vivo* have been with striatal dopamine using carbon fiber electrochemistry. These measurements scale diffusion distances of dopamine in the striatum to be ~10 micrometers with the half-life of striatal dopamine to be ~50 ms[159,160]. However, the half-life of dopamine in prefrontal cortex is much longer (~2s) due to reduced uptake sites and thus the diffusion distance there is ~30-40 micrometers[160]. If these estimates were to apply to acetylcholine, then diffusion of distances beyond 100 micrometers would take ~8 seconds and begin to dominate kinetics of the CNiFER response. Likely, implanted CNiFERs, at least on the outside of the column, will be in closer proximity than this, but cells on the interior of larger columns might be predicted to respond with an increased latency.

Nucleus Basalis Magnocellularis, Acetylcholine and Cortical Activation

Electrical activation of the cholinergic input to cerebral cortex provides a method for the *in vivo* characterization of CNiFER cells, to address the above-mentioned concerns. The rodent cerebral cortex is massively innervated by cholinergic fibers originating in the Nucleus Basalis Magnocellularis (NBM)[161,162]. In rats anesthetized with urethane, electrical stimulation of the NBM results in a release of acetylcholine into cerebral cortex[76]. At the same time, NBM stimulation induces a characteristic transition of the electrocorticogram (ECoG) from large amplitude, slow wave potentials to low amplitude, higher frequency potentials

[163,164]. This provides a valuable feedback signal, as efficacy of NBM stimulation (and thus acetylcholine release) can be monitored in ECoG leads and correlated with M1-CNiFER responses[165].

Results

Acute CNiFER Implantation

Isoflurane anesthetized rats are used for implantation. CNiFERs are harvested from flasks, triturated, concentrated, front-loaded into a capillary pipette connected to a syringe pump and implanted into neocortex with a stereotaxic apparatus (Figure 13). The capillary pipette is pulled to an internal diameter of ~40 μm. Roughly 1000 cells in 10-100 nl are injected into each site, which are chosen so as to avoid large surface blood vessels. Electrodes are implanted in Nucleus Basalis Magnocellularis and electrocorticogram electrodes placed across the implant and across hemispheres (see Chapter V: Methods).

Imaging is performed with two photon microscopy. Several hours after implantation, CNiFERs show normal morphology and no sign of degradation. In Figure 14 CNiFERs fill a column approximately 25-50 μm in diameter and are imaged at a depth of 40-60 μm in the brain. Implanted cells do not drift from the field of view, which indicates brain tissue provides adequate support. Periodic cell motions that result from heart beat and respiration were limited to 2 to 3 μm displacements.

For all *in vivo* experiments, a region of interest is drawn around the M1- and control-CNiFERs and averaged for each time point. Depending on the size of the implantation column, 10-150 cells were included in such regions.

Acetylcholine Injection

To determine if implanted M1-CNiFERs are still responsive to acetylcholine, 27 nl puffs of 1 mM acetylcholine are delivered intracortically via oocyte injector near the cells. M1-CNiFERs respond within seconds to the puff and reach maximum response ($\Delta R/R$ = 1.32, 1.33 and 1.42 for 3 animals, 3 trials each) within ~10 seconds (Figure 15). Return to baseline was incomplete, probably due to persisting levels of local acetylcholine after injection. M1-CNiFERs did not respond to equivalent puffs of phosphate buffered saline (PBS).

NBM Stimulation

A more physiologically relevant presentation of acetylcholine *in vivo* is achieved by electrical stimulation of Nucleus Basalis Magnocellularis, the basal forebrain structure projecting cholinergic fibers into cerebral cortex. Bipolar electrodes deliver 600-1000 μA of current in 200 μs pulses at 100 Hz for 200-500 ms (Figure 16). NBM stimulation induces a transient shift in electrocorticogram rhythm from high amplitude-low frequency waves to low amplitude-high frequency waves lasting several seconds (Figure 16 and Figure 17). This cortical activation is the hallmark of NBM stimulation[163-165]. M1-CNiFERs respond monotonically with current injection, and the edge of response begins within 2 seconds with a half-maximal rise time as short as ~1 s. Full width at half maximal

amplitude of the response is approximately 10 seconds, consistent with *in vitro* data (Figure 4). Control-CNiFERs display no detectable response.

As expected, we observe a strong correlation between electrocorticogram activation measured as the z transform within animals of δ-band inverse power from 1-6 Hz (ECoG Index, see Chapter V: Methods) and response amplitude in M1-CNiFERs (Figure 18; rho = .8, $p < .001$, n = 4 animals, 55 trials). Interpreting electrocorticogram activation as a surrogate for cholinergic release[163-165], this further verifies that M1-CNiFERs are detecting released acetylcholine.

To test the temporal limits of our reporters, we stimulate NBM consecutively with different interstimulus intervals (Figure 19, n=5 trials at each interstimulus interval). Consistent with the temporal resolution found *in vitro* (Figure 4), M1-CNiFERs are capable of discriminating NBM stimulations approximately 5-10 seconds apart.

The cholinergic nature of the NBM-evoked transient M1-CNiFER response is further verified by subcutaneous injection of the acetylcholinesterase inhibitor physostigmine. Physostigmine salicylate (200 μg/kg) enhances amplitude and duration of the NBM-evoked M1-CNiFER response for ~100 minutes after injection, consistent with pharmacokinetics of physostigmine (Figure 20**;** n = 3 rats)[166].

To test the ability of M1-CNiFERs to detect longer scale (tonic) fluctuations of background acetylcholine *in vivo*, a higher dose of physostigmine (300 μg/kg) is administered. As expected, physostigmine enhances the baseline M1- but not control-CNiFER signal (no NBM stimulation) over the ~100 minute period (Figure

21; n = 4 rats). As expected, there is a concurrent reduction of electrocorticogram power in the δ-band (increase in ECoG Index). These results are consistent with physostigmine pharmacokinetics and its enhancement of acetylcholine levels as measured by microdialysis techniques[166].

Chronic CNiFER Implantation

HEK293 cells are not isogeneic in rats and will eventually be rejected by the host immune system. Therefore, we use daily cyclosporine injection for chronic studies. Also, *ex vivo* gene therapy implants of immortalized cells lines such as HEK293s overgrow into tumors by 3 weeks[107]. For chronic CNiFER studies, overgrowth is a concern. We find chronically implanted CNiFERs can be imaged up to at least 2 days after injection without drastic growth within the intracerebral sites (see Histology).

Modulation by Atropine

NBM electrical stimulation releases acetylcholine into cortex, but it also releases other neurotransmitters, including GABA, glutamate and galanin[167,168]. In addition, NBM stimulation can evoke thalamic activity[169], indirectly driving cortical networks and likely altering extrasynaptic concentrations of many molecules other than acetylcholine. As a final confirmation that M1-CNiFERs are responding to cholinergic muscarinic activation and not some other signaling molecule, atropine is injected intracerebrally near the implant. The NBM-evoked M1-CNiFER response is reversibly suppressed by low dose atropine (1-5 μM, n =

4 rats) but completely abolished by high dose atropine (100 μM, n = 3 rats) (Figure 22).

Histology

Histology is performed on CNiFERs implanted chronically for 2 days. It can be seen that the implantation columns measure ~100x500 μm and that CNiFER cells have maintained normal morphology with TN-XXL excluded from the nuclei but mCherry distributed throughout the cells (Figure 23). Astrocyte staining is performed to assess the state of a glial scar that is seen in *ex vivo* gene therapy studies[107]. Immunostaining for glial acidic fibrillary protein (GFAP) is performed to visualize astrocytes. Astrocytes are apparent at the surface of the brain in the glial limitans and also in deeper layers at ~ 1 mm. However, there is no obvious astrocyte concentration (glial scar) surrounding the implantation site. Functional data is typically acquired at 100-200 μm in depth, where it can be seen that there is minimal astrocytic staining.

Conclusion

In both acute and chronic studies (~2 days) CNiFERs are brightly fluorescent and responsive to injected acetylcholine (only studied in acute preparation) and NBM stimulation. M1- but not control-CNiFERs respond robustly, up to 40% ΔR/R, to endogenous acetylcholine release evoked via electrical stimulation of Nucleus Basalis Magnocellularis (NBM). The response is a single peak initiated within 2 s with a half-maximal rise time as short as ~1 s and a full width at half maximal amplitude of < 10 s. We observe a strong inverse correlation between

M1-CNiFER response and electrocorticogram (ECoG) delta band power after NBM stimulation (rho = .8). Furthermore, CNiFER responses are enhanced with the acetylcholinesterase inhibitor physostigmine and suppressed by the muscarinic antagonist atropine. This demonstrates that implanted CNiFERs maintain functionality in the *in vivo* milieu. Specifically, the M1 muscarinic receptor and TN-XXL indicator continue to be expressed and baseline cytosolic calcium levels have not changed so much as to saturate the CNiFERs, *i.e.*, cytosolic calcium levels can still be modulated by muscarinic activity.

Temporal Resolution

Consistent with *in vitro* experiments, CNiFERs have a ~6 s temporal resolution *in vivo*, a ~100 times improvement over standard microdialysis. This is also competitive with electrochemistry, with which physiological *in vivo* measurements have only been made for choline and not acetylcholine[84,85] but see[86].

Spatial Resolution

Two factors determine the spatial resolution of a probe. One is the size of the probe, and the other is how closely two probes can be used in an array. Microdialysis probes have a membrane region with a 240 μm diameter and 1000 μm length (CMA 11, CMA Germany) but the remainder of the probe is bulky and when used in two different sites *in vivo* have been separated by 2-3 mm[170]. Electrochemical probes for acetylcholine have 60 μm by ~750 μm active surfaces but similarly, the rest of the probe is bulky and has not been used as an array[86]. The diameter of CNiFER implants range from ~20-200 μm and although they

extend to a depth of up to ~1 mm, they are imaged in a plane ~5 μm thick[171] (Figure 14). A typical distance between neighboring CNiFER sites is 100-200 μm, placing a current spatial limitation on array implementation. Initial implants were a mixture of M1- and control-CNiFERs, but due to resolution limits of *in vivo* two photon microscopy and small, yet ongoing movement artifacts, we were not able to separate the two signals satisfactorily. We therefore chose to make separate implant sites. Furthermore, we chose to average over the implant field of view as this increases signal over noise. Looking intra-columnwise at CNiFER response could possibly increase spatial resolution (*e.g.*, which side did the activation within the column occur from), but the results may be confounded by a pathological substrate for acetylcholine diffusion, as the extracellular space in the implant is likely less tortuous than the surrounding parenchyma[172] and does not contain acetylcholinesterase.

Sensitivity

M1-CNiFERs detect bath applied acetylcholine monotonically from 1 nM to 100 nM, the physiological range in rat as measured by microdialysis[74,76-78]. Because many confounds exist in quantitative estimates of microdialysis measurements (see Chapter I: Introduction-Microdialysis and Chromatography), *in vivo* acetylcholine levels may be very different, especially phasic peaks that microdialysis measurements necessarily average over during the standard 5-10 minute acquisition times. Nevertheless, M1-CNiFERs respond monotonically to varying amplitude of NBM stimulation, suggesting that the EC_{50} to acetylcholine

of the M1-CNiFER clonal line chosen for this study is appropriate for these urethane-anesthesia experiments. It could be that in awake, behaving experiments, acetylcholine levels may be much higher in which case a clonal line with a higher EC_{50} may be preferred (see Chapter IV: Discussion-Sensitivity).

Glial Scar

The glial scar formed in *ex vivo* gene therapy experiments at 1 week, but more intensely at 3 weeks[107], are not seen in our implantation sites at 2 days. Astrocyte immunostaining against GFAP reveals astrocytes in the tissue, but not concentrated near the implants. Systemic cyclosporine is used in our chronic experiments to reduce the possibility of host graft rejection and may have helped to reduce glial scar formation. An *ex vivo* gene therapy study had immunosuppressed rats with cyclosporine and found that at 2 months only a mild accumulation of GFAP stained astrocytes had formed around the implantation[111]. In our experiments, at least up to 2 days, M1-CNiFERs remained responsive to NBM-evoked acetylcholine release into cortex (Figure 22).

Possibly, the glial scar will appear after several weeks, as seen in previous studies. Although evidence suggests that secreted recombinant protein from engineered fibroblasts used in *ex vivo* gene therapy does diffuse into surrounding parenchyma[173], diffusion of small molecules into the graft could be impaired. It remains to be seen if this is true and if it will significantly impact the ability of CNiFERs to detect released neurotransmitters.

Volume Transmission

The kinetics of volume transmission of acetylcholine through brain tissue has not been as thoroughly described as it has been for dopamine, where diffusion distances are estimated at ~30-40 micrometers in prefrontal cortex before uptake by the dopamine transporter[160]. If acetylcholine diffusion distances are similar, then CNiFER implants should be able to detect released acetylcholine as they abut immediately adjacent to parenchyma (Figure 23). However, acetylcholinesterase is one of the fastest known enzymes and it is quite possible that the diffusion distance could be significantly smaller and preclude detection by implanted CNiFERs. Clearly, our *in vivo* experiments suggest this is not the case since CNiFERs *are* capable of detecting released acetylcholine. However, this does not rule out the possibility that surrounding parenchyma experiences very high levels (> μM) of acetylcholine and that only a fraction diffuses to the CNiFER site.

Finally, it is a concern that long diffusion times into the implant site could smear out the temporal kinetics of acetylcholine release. This is unlikely since the NBM-evoked CNiFER response initiates within 2 seconds as does the *in vitro* fast perfusion-evoked response (Figure 4 and Figure 16). This suggests the diffusion of acetylcholine to implanted CNiFERs is not rate-limiting. Furthermore, CNiFERs are capable of resolving NBM stimulations that are separated by ~5-10 seconds, the same temporal resolution limit of CNiFERs as described *in vitro* with fast perfusion experiments.

Figures

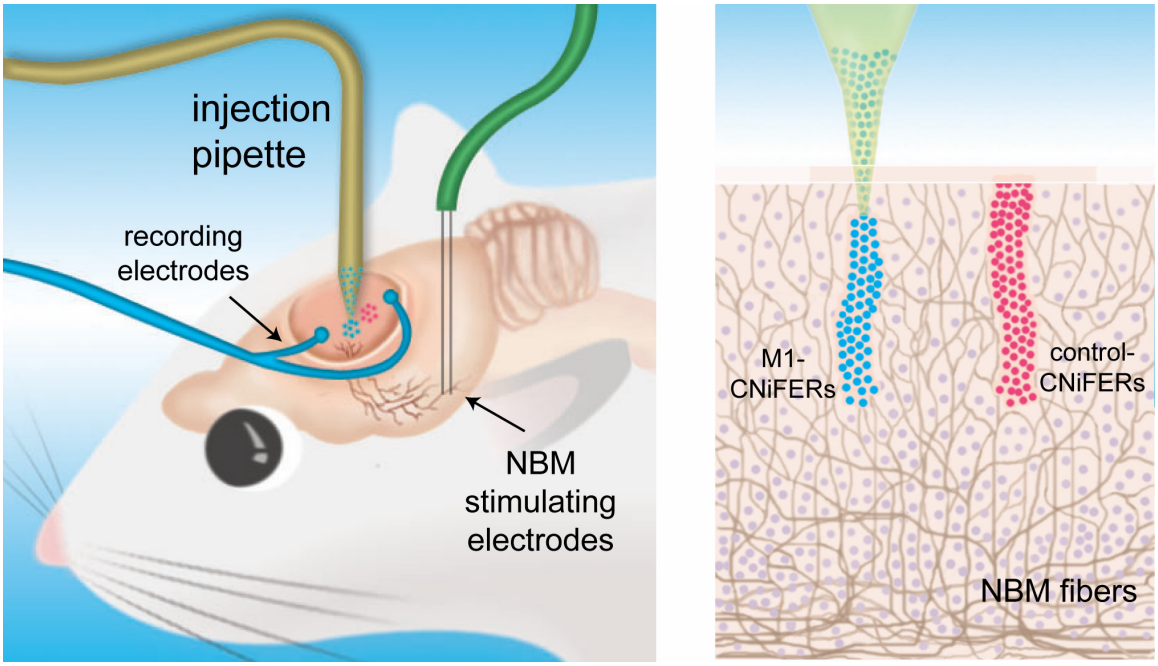

Figure 13 *In Vivo* Implantation of CNiFERs

CNiFERs are implanted into neocortex with a syringe pump and capillary pipette. Electrodes are placed in Nucleus Basalis Magnocellularis and electrocorticogram electrodes placed across the implant and across hemispheres. Imaging is obtained with two photon microscopy. Image on right

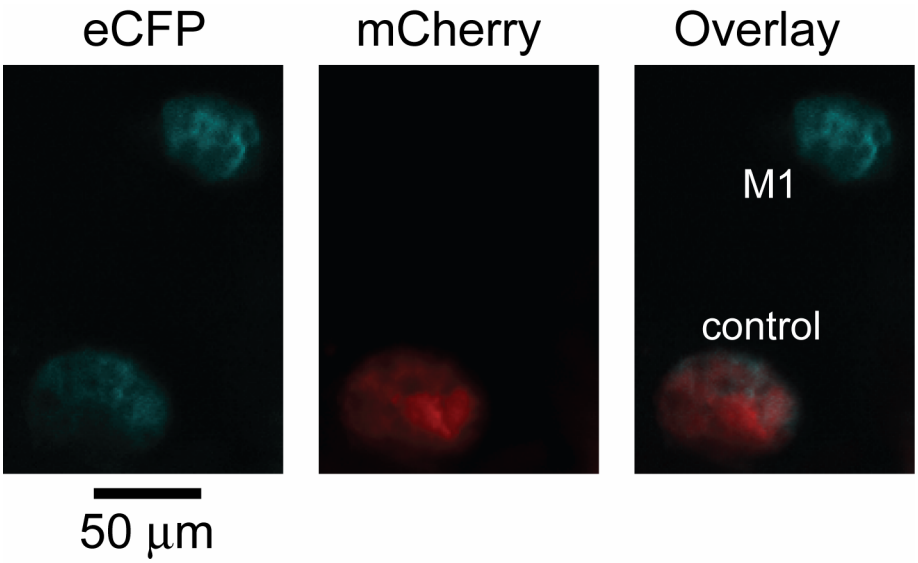

Figure 14 CNiFERs Implanted in Rat Motor Cortex

M1-CNiFERs (cyan) and control-CNiFERs (red) implanted in rat motor cortex in 25-50 μm diameter columns. Data is a Z-projection from 40-60 μm below the cortical surface. There are 10-20 CNiFER cells per site in this field of view.

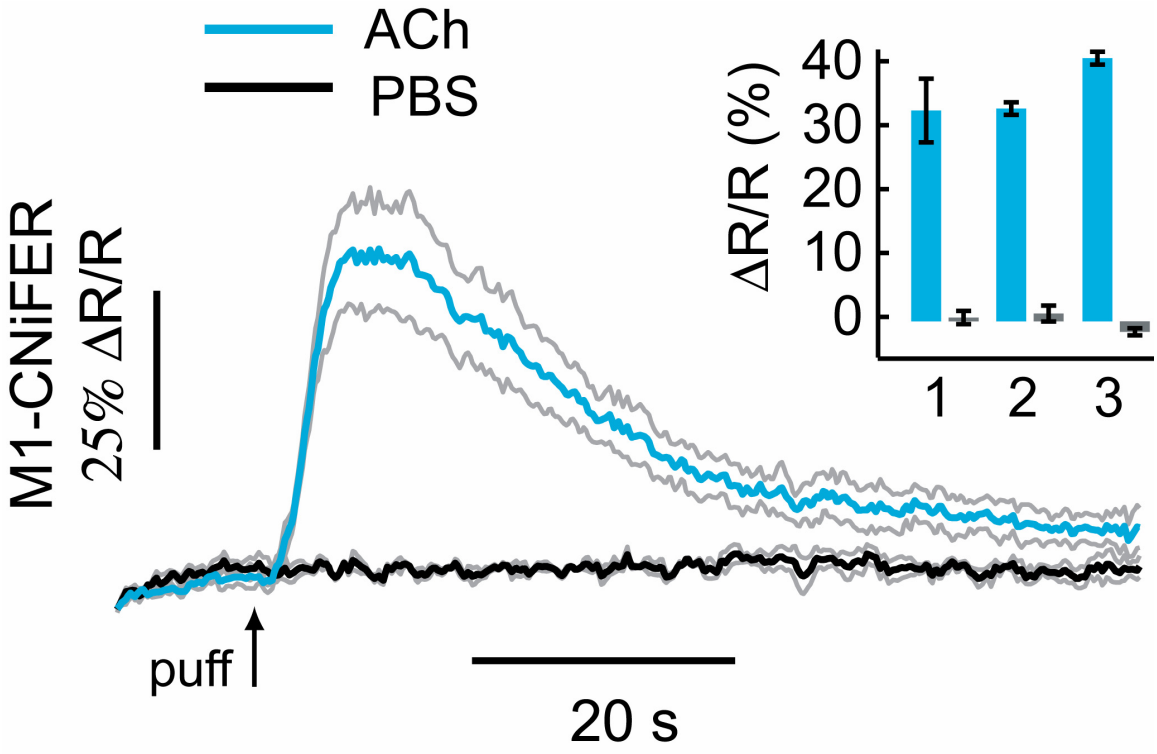

Figure 15 M1-CNiFERs Respond to a Puff of Acetylcholine *In Vivo*

M1-CNiFER response to acetylcholine is maintained after several hours of brain implantation. M1-CNiFERs respond to intracortical 27 nl puffs of 1 mM acetylcholine chloride (cyan) but not PBS (grey). Time trace shows average response and standard error for 3 injections, same animal. Inset shows the fractional change of 1/3 the area under the ΔR/R curve for 30 seconds after the stimulus as compared to that for 10 s before the stimulus, for either acetylcholine or PBS (3 animals, n = 3 trials each). Bars represent standard error.

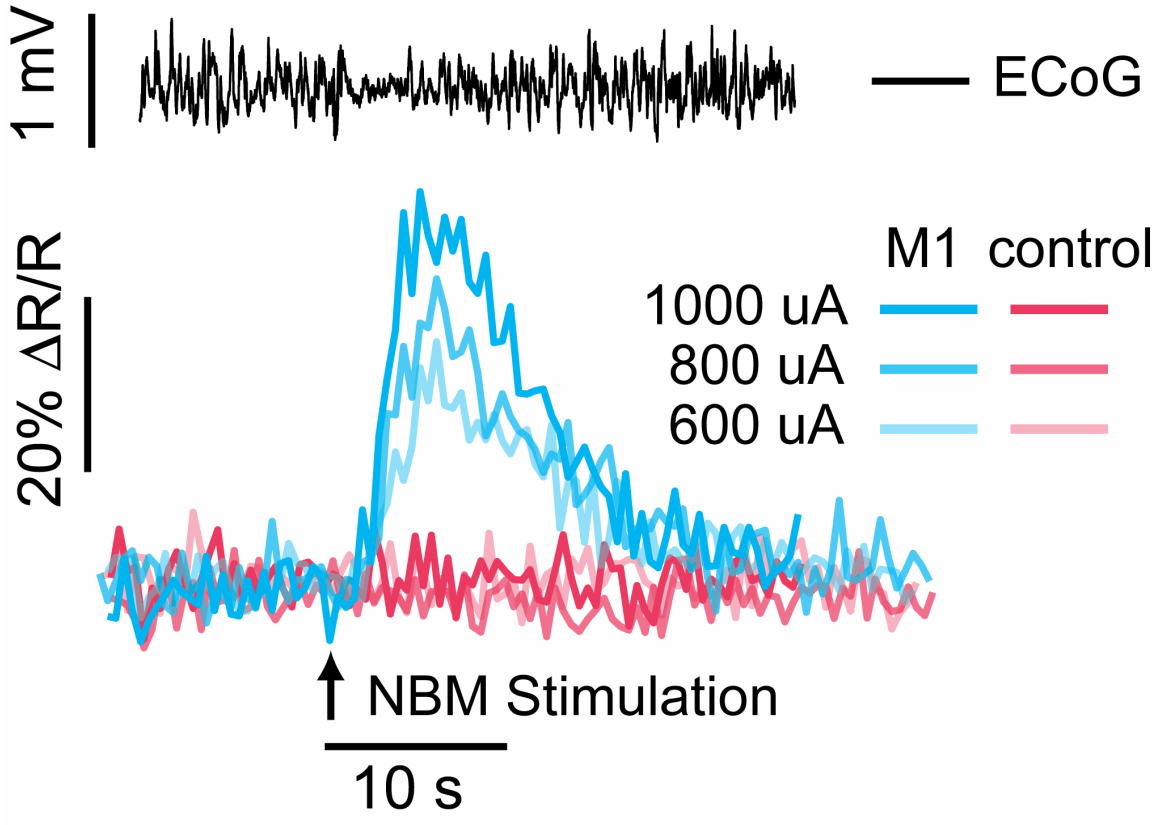

Figure 16 M1-CNiFERs Respond to Electrical Stimulation of NBM

M1-CNiFERs (cyan) but not control-CNiFERs (red) respond to varying intensities (1000 μA, 800 μA, 600 μA) of electrical NBM stimulation. Electrocorticogram shown for stimulation at 1000 μA. Note the shift from large to small amplitude electrical activity described as cortical activation.

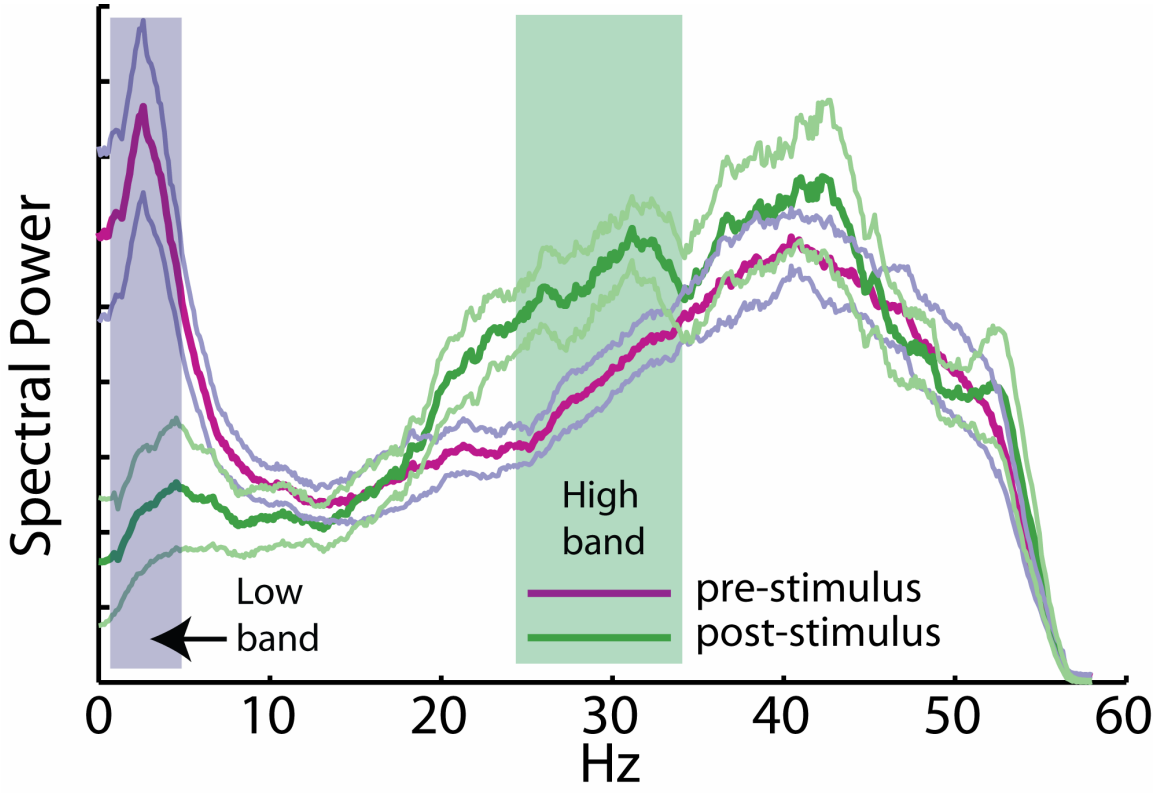

Figure 17 Modulation of Electrocorticogram Spectra by NBM Stimulation

ECoG spectra for 5 second intervals pre- and post-NBM electrical stimulation (purple and green, respectively. The pre-NBM spectra represent an average over 4 consecutive epochs. The low band only is used to calculate the ECoG Index of cortical activation (n = 24 stimulations; error bands represent standard error of the mean). For display, these spectra are prewhitened using an autoregressive model[174].

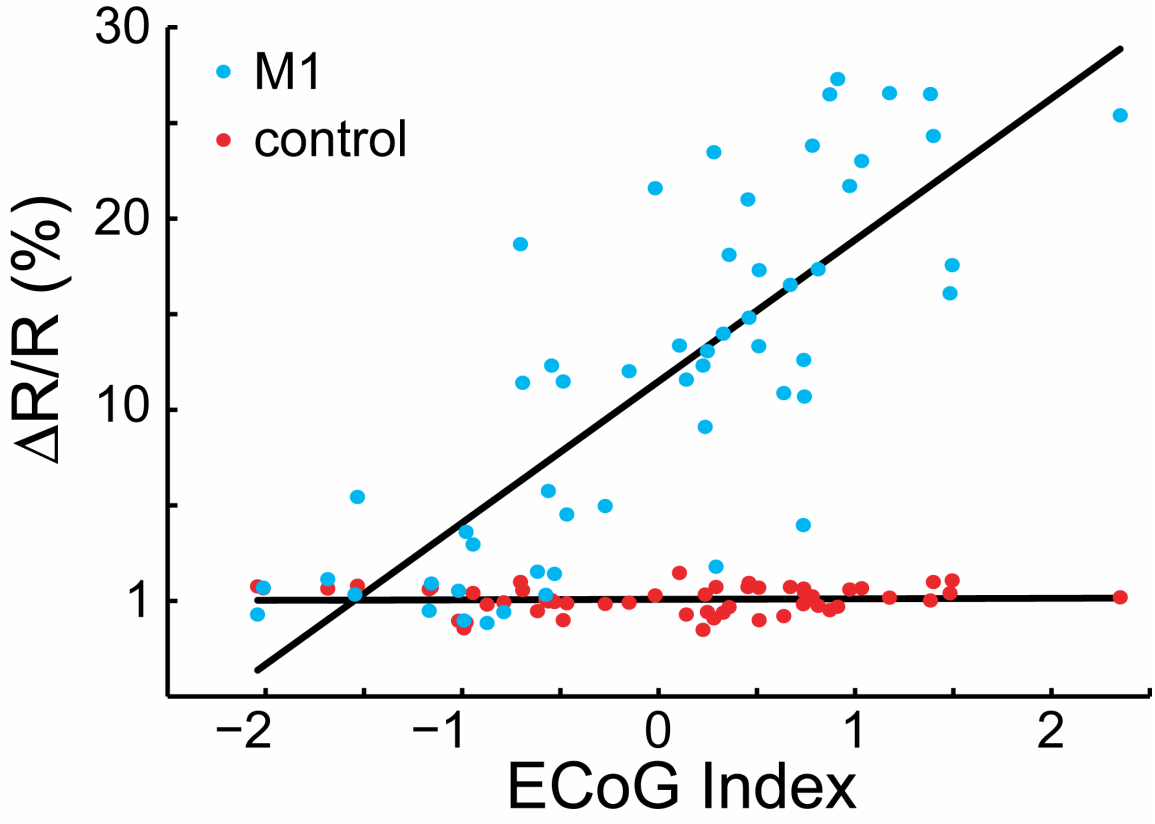

Figure 18 Scatterplot of CNiFER Response to ECoG Index of Cortical Activation

M1-CNiFER response to NBM stimulation is strongly correlated to loss of power in the electrocorticogram delta band. CNiFER responses are defined as the area under the curve of ΔR/R for 10 seconds after the stimulus normalized to that of 10 s before the stimulus. The ECoG Index is the logarithm of inverse power in the delta band, z-transformed within each experiment to equalize variance. Pearson correlations: rho = .8, $p < .001$ (M1-CNiFERs) and rho = .04, $p = .8$ (control-CNiFERs). Data collected from 4 animals, n=55 trials.

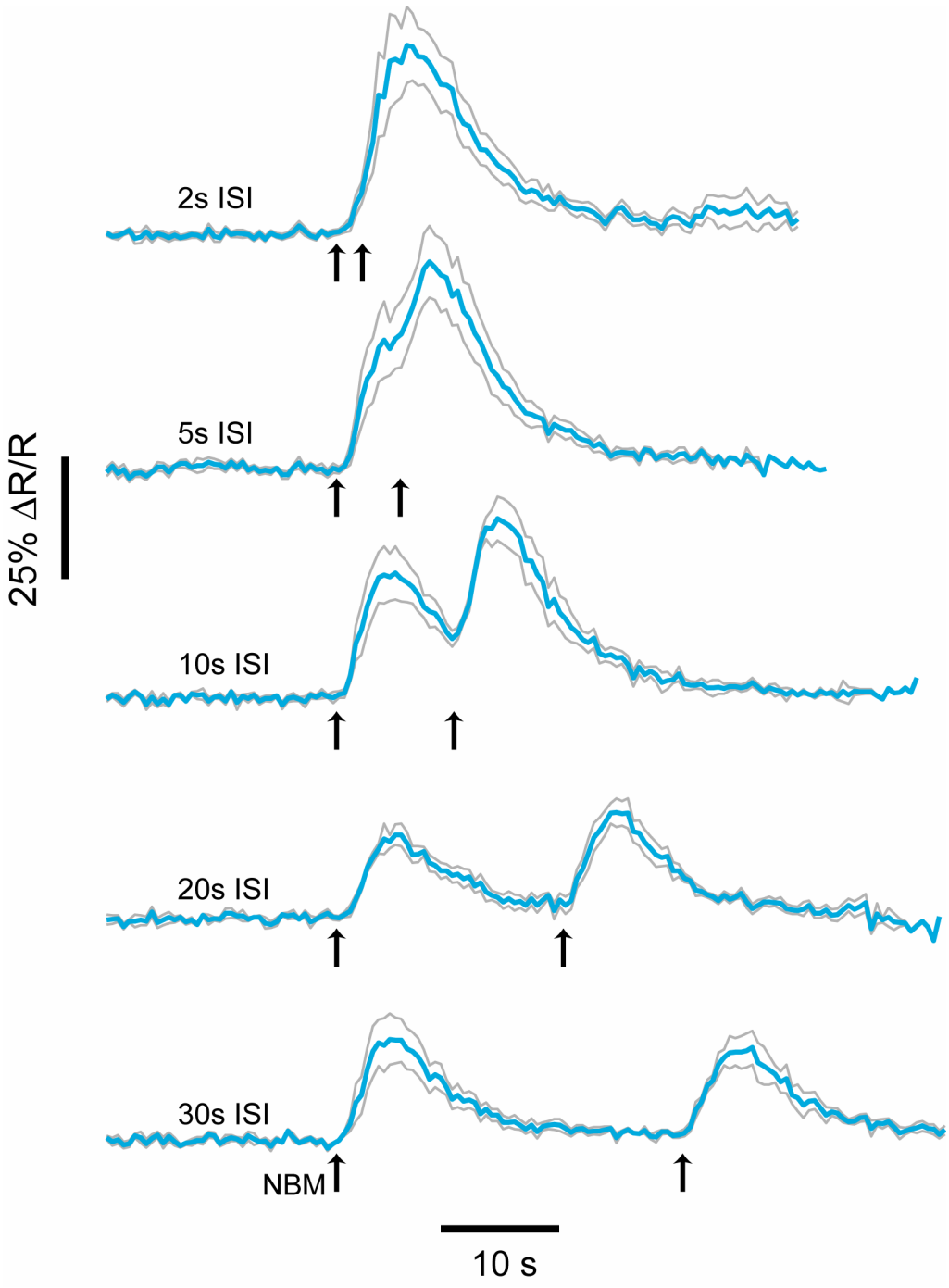

Figure 19 M1-CNiFER Temporal Resolution in Detection of NBM Stimulation

Each trace represents the mean response of M1-CNiFERs to consecutive stimulations of Nucleus Basalis Magnocellularis (arrows). Similar to *in vitro* fast perfusion experiments, the limit of detection is ~5-10 seconds between stimuli. Data collected over three animals, n = 5 for each trace. Gray traces represent standard error.

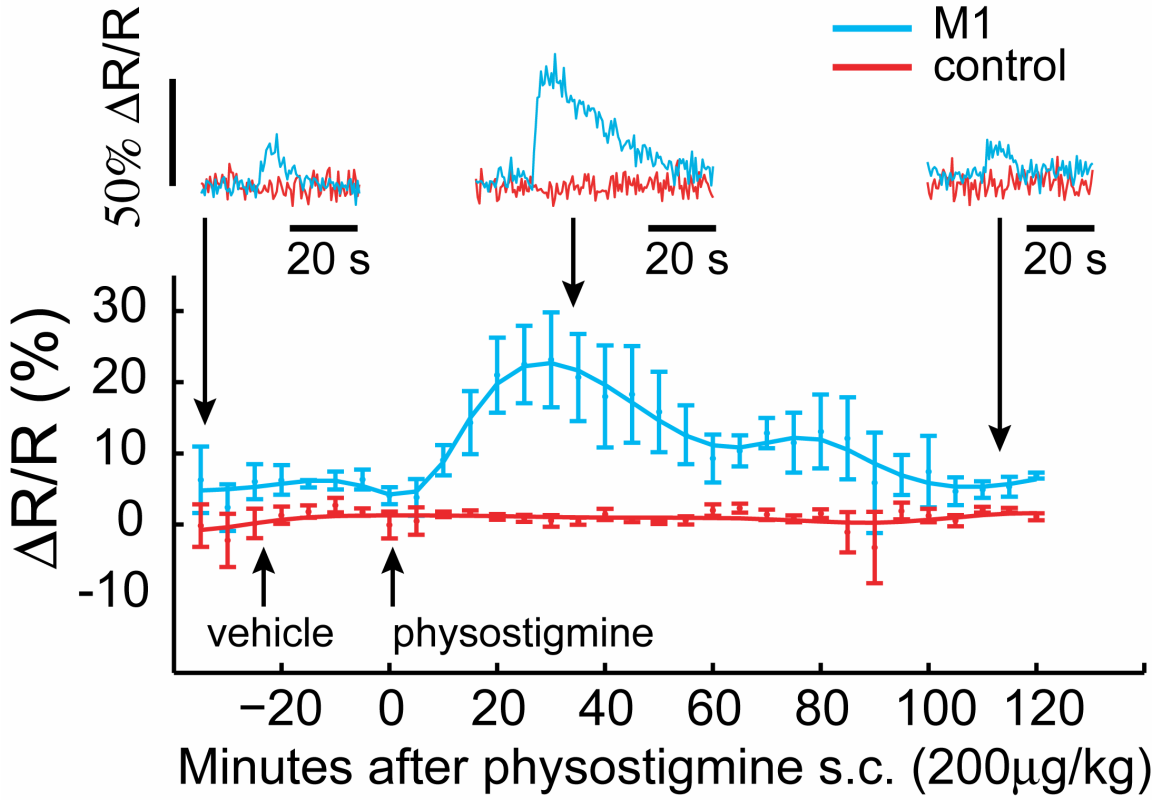

Figure 20 Physostigmine Enhances Transient Response of M1-CNiFERs to NBM-stimulation

Subcutaneous physostigmine salicylate (200 µg/kg) enhances the amplitude and duration of M1-CNiFER response to NBM stimulation and washes out by ~100 minutes. Data in bottom trace represents the percent change of 1/3 the area under the curve of ΔR/R for 30 seconds after the stimulus as compared to that of 10 s before the stimulus. Top traces are examples of raw data used to calculate bottom trace. NBM stimulation occurs every 5 minutes. Vehicle injection of PBS. Data collected over 3 animals, bars represent standard error.

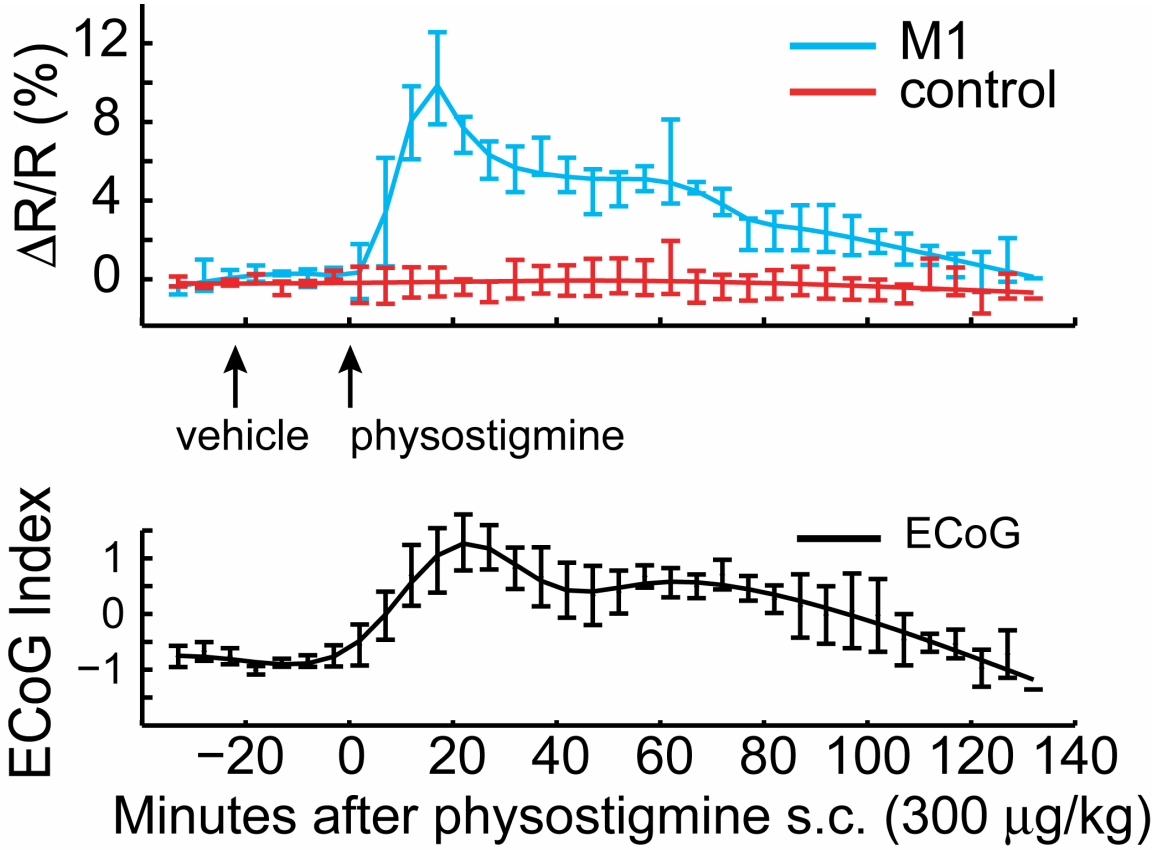

Figure 21 Physostigmine Enhances M1-CNiFER Tonic Response to Ambient Acetylcholine

Subcutaneous physostigmine salicylate (300 µg/kg) causes an increase in baseline M1-CNiFER FRET fluorescence over ~120 min, apparently due to modulation of background (not NBM-stimulated) cortical acetylcholine. M1-CNiFERs (cyan) and control-CNiFERs (red) measured as an average over 10 s every 5 minutes (top). All measurements are normalized to first 3 measurements before vehicle injection, and not to internal baselines, thus preserving the tonic response (see Chapter V: Methods). ECoG Index of spontaneous cortical activation calculated from 4 consecutive 5 s epochs, and plotted in black at each time point (bottom). Data collected over 4 animals.

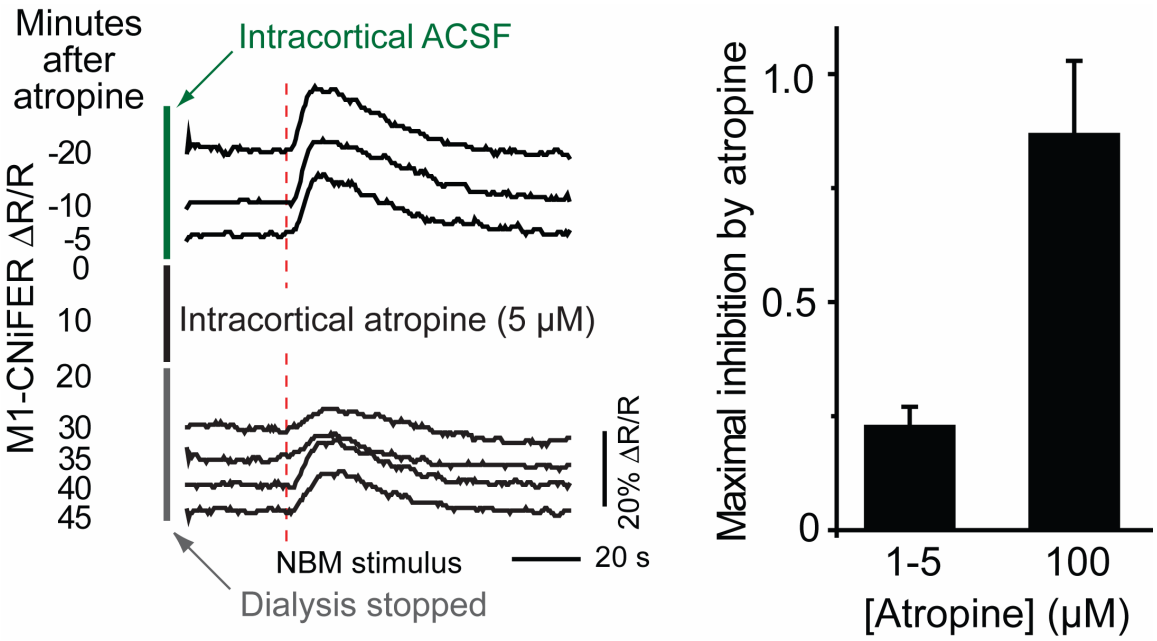

Figure 22 Atropine Antagonism of Chronically Implanted M1-CNiFERs

Left traces: M1-CNiFER responses to single-train NBM stimulation are inhibited by reverse dialysis of intracortical atropine sulfate. Bar graph: average peak inhibition of CNiFER response due to 1-5 μM atropine (23 ± 4%; n = 4 rats) or 100 μM atropine (87 ± 16%; n = 3 rats). Error bars represent standard errors.

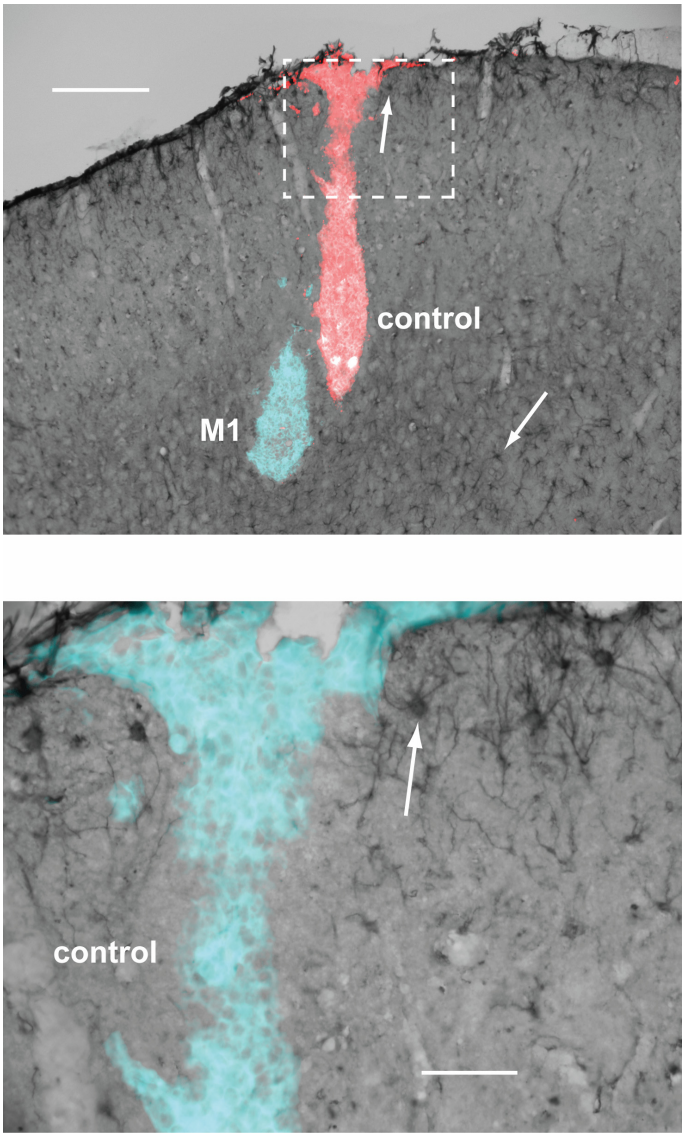

Figure 23 Immunostain Against Glial Acidic Fibrillary Protein (GFAP)

Immunostain against GFAP reveals no astrocytic scar around chronically implanted M1- and control-CNiFERs. In top image, mcherry and TN-XXL fluorescence are overlayed on a brightfield 3,3'-diaminobenzidine α-GFAP stain for astrocytes. Scale bar represents 200 μm. In bottom image, only TN-XXL fluorescence is overlayed to better visualize health of CNiFER cells. α-GFAP stain reveals cell bodies and long complex processes apparent in the glial limitans at the surface of the brain and in deeper layers at ~1 mm (see white arrows). There is no astrocytic concentration (glial scar) along the implantation site. Functional data with *in vivo* two photon microscopy is typically acquired at depths of 50-200 μm, where few astrocytes in this section are present. M1-CNiFER column extends to the cortical surface in neighboring section (data not shown). Scale bar represents 50 μm.

Chapter IV: Discussion

As described above, M1-CNiFERS enable *in vivo* measurements of acetylcholine release and *in situ* M1 muscarinic receptor activity. These measurements are provided at spatial and temporal resolutions competitive or better than traditional methods of *in vivo* neurotransmitter detection, namely microdialysis and electrochemistry. Still, CNiFER technology comes with several limitations and these are discussed in the following section.

Limitations of CNiFERs

As a Model of Endogenous Receptor Activity

CNiFERs might be viewed as a model system for endogenous extrasynaptic receptor activity. Specifically, M1-CNiFERs could be viewed as a model system for activation of the M1 muscarinic receptor, the primary post-synaptic muscarinic receptor in neocortex[175].

The extent of validity for such an assumption depends on two primary factors: the EC_{50} of the M1-CNiFER response to acetylcholine and the condition of volume transmission near the implantation site.

M1-CNiFER EC_{50}

M1-CNiFERs can act as models of endogenous extrasynaptic muscarinic receptors only to the extent that their acetylcholine-evoked muscarinic signaling resembles that of a particular cell class in the brain. The critical characteristic in this case is sensitivity or EC_{50}. Therefore, M1-CNiFERs may be a reasonable model for muscarinic activity in a cell class with a similar M1 muscarinic EC_{50} to

acetylcholine (*i.e.*, ~10 nM). Of course, the validity of the model would only pertain to extrasynaptic cholinergic activation by volume transmission.

Sensitivity is dependent in part upon receptor expression levels. Expression levels were not measured in CNiFERs, however levels have been measured in other systems and can provide context. Untransfected HEK293 tsA201 cells were found not to express detectable amounts of M1 as measured by cell homogenates of the membrane permeable radioligand [^{3}H]QNB (3-quinuclidinyl benzilate). After transfection with calcium phosphate, .39 pmoles/mg protein was detected on surface of intact transfected cells with the membrane impermeable [^{3}H]NMS (scopolamine methyl chloride). It was not stated if there was a correction for transfection efficiency of 10-20%, which would increase levels per cell by 5-10 times[152]. In another study, COS-7 cells were electroporated with the M1 receptor using the Biorad gene pulser. Approximately 1 pmole/mg protein was found in cell homogenates using [^{3}H]NMS[176]. Finally, M1 receptor was expressed by semliki forest virus in CHO cells and bound [^{3}H]QNB was .75 pmoles/mg[177]. This suggests that expression levels in heterologous systems of M1 muscarinic receptor may likely be ~1 pmole/mg of protein. Interestingly, measurements of M1 in the rodent brain are also ~1 pmole/mg protein[178 179]. In so far as receptor expression is concerned, and to first approximation, this suggests that M1-CNiFERs may act as reasonable models for extrasynaptic M1 muscarinic activity in the brain.

On the other hand, EC_{50} values for cholinergic stimulation in various *in vivo* and *ex vivo* preparations are typically higher than for M1-CNiFERs: ~250 nM

acetylcholine in hippocampal synaptosomes[180], 800 nM acetylcholine in hippocampal slice[181], and 1000 nM for striatal synaptosomes [182]. These values are significantly higher than our current line of M1-CNiFERs, which respond to acetylcholine with an EC_{50} ~10nM. By this measure, the current clone of M1-CNiFERs may not be appropriate models for many classes of cells *in vivo*. Choosing a clone with a lower expression of receptor and thus higher EC_{50} might be more suitable as such a model (see Sensitivity below).

Volume Transmission

Similarly, CNiFERs can act as models for endogenous extrasynaptic receptor activity only to the extent that endogenous properties of volume transmission are maintained near the implantation site. For example, diffusion of molecules in the brain follow different kinetics than through simple solutions. Additional factors must be taken into account: a tortuosity factor (λ) estimating the circuitous route the molecule must take to traverse the extrasynaptic space and a volume fraction (α) which is the ratio of extracellular volume to total volume. These factors modify the diffusion coefficient D as $\alpha D/\lambda^2$ [172]. Volume transmission near the implant site will mirror volume transmission in intact parenchyma to the extent that $\alpha D/\lambda^2$ is similar in both environments. This remains to be determined.

Quantification

A critical assumption if quantification of the CNiFER response is going to be attempted is that the CNiFERs are stable from experiment to experiment. In other words, receptor expression and the GCPR signaling pathway remains more or

less a constant. The M1-CNiFER dose-response curves to acetylcholine seem to stay relatively stable over time (*e.g.*, data for Figure 7 and Figure 9 were collected over many weeks) suggesting this assumption may be valid. However, before quantification would be attempted a more rigorous test of stability from passage to passage should be performed.

Tonic Response to Prolonged Acetylcholine Presentation

To date CNiFERs have only been used as qualitative reporters. Although the fractional tonic response to different concentrations of acetylcholine can be well-described *in vitro* where the baseline concentration of acetylcholine is controlled, once implanted in the brain, the baseline levels of acetylcholine are unknown. For this reason, looking at fractional changes from baseline is no longer a viable approach for quantification of acetylcholine levels. For example, baseline levels of acetylcholine levels in the brain may have already partially activated the M1-CNiFERs before the imaging session began. A 10% change from baseline levels during the experiment would then no longer represent the presence of 10 nM acetylcholine, as would be suggested from the *in vitro* calibration curves.

A way to circumvent this is to measure FRET efficiency directly, rather than look at fractional changes from baseline. FRET efficiency is a measure of how much FRET is occurring between two fluorophores: $(1 - (F_{DA}/F_D))$, where F_{DA} is the fluorescence intensity of the donor molecule in the presence of the acceptor, and F_D is the fluorescence intensity in the absence of the acceptor[183]. What makes the FRET efficiency measurement difficult is that there is typically excitation cross-talk and emission bleedthrough of the two fluorophores, such

that the contribution of collected light from fluorescence resonance energy transfer to the donor fluorophore is not known. FRET efficiency can be estimated in many different ways[184]. Typically, it involves multiple measurements using isolated fluorescent proteins (in the case of TN-XXL, Citrine and eCFP) to enable adjustments for excitation cross-talk and emission bleedthrough. Estimates of FRET efficiency for TN-XXL are simplified because it is a fusion protein and levels of Citrine and eCFP remain proportional. Once cross-talk and bleedthrough are accounted for, the FRET efficiency measurement is possible. In this way, implanted CNiFERs can be imaged and absolute FRET efficiency calculated and calibrated to *in vitro* FRET efficiency measurements. In this way, a quantitative *in vivo* measurement of tonic levels of acetylcholine *may* be possible. A potential confound is the differential absorption of light emitted from eCFP and Citrine as it travels through the implant site back to the objective. To control for this, an *in vitro* model of the implant site (*i.e.*, several layers of CNiFERs stacked together) would have to be employed.

Transient Response to Pulses of Acetylcholine

Quantification of the CNiFER transient responses, on the other hand, has an additional problem. M1-CNiFERs respond to concentration *and* duration of exposure. For example, Figure 3 shows a short 100 nM bolus of acetylcholine causes a transient peak of ~30%. However, Figure 7 shows a prolonged presentation of 100 nM acetylcholine results in a peak of ~110%. Currently, duration and concentration of exposure are not distinguishable in our system. It is possible, however, that ligand concentration is correlated to the rise time of the

CNiFER response. If so, this would provide a potential method of quantifying acetylcholine concentration. However, these experiments have yet to be performed.

Linearity

The log(dose)-response of M1-CNiFERs to acetylcholine follows a sigmoid curve as is generally seen for receptor-agonist binding. This is expected for G protein-coupled receptor cascades as they are driven by receptor-agonist binding and each additional step in the cascade follows the law of mass action[185]. *In vitro*, the M1-CNiFER phasic response to bath application is linear roughly from 5-20 nM acetylcholine while the tonic response is linear roughly from 6-13 nM acetylcholine. Although in the physiological range as measured by microdialysis[74,76-78], these ranges are probably too small to be of value. In other words, implanted M1-CNiFERs are not likely to be experiencing acetylcholine limited to their linear range. It is possible that choosing a clone with a higher EC_{50} would extend the linear range to more suitable levels, though this would obviously come at the expense of sensitivity.

Stationarity

M1-CNiFERs respond to short pulses of acetylcholine with a single peak, but this peak adapts to repetitive stimulation and stabilizes to a reduced level (Figure 5). Furthermore, Figure 6 shows M1-CNiFERs respond to prolonged acetylcholine presentation with a phasic peak followed by a sustained tonic plateau. These behaviors must be carefully accounted for when interpreting M1-

CNiFER responses. In the case of repetitive stimuli, the experiment should be performed after adaptation has occurred and the system is at equilibrium. In the case of prolonged acetylcholine exposure, assessment for the occurrence of a phasic/tonic response must be made. For example, Figure 21 demonstrates a tonic M1-CNiFER response to relatively prolonged levels of ambient acetylcholine caused by acetylcholinesterase inhibition. Qualitatively, the shape of the response to physostigmine is similar to the phasic/tonic response to constant levels of acetylcholine as seen in Figure 6. This may be interpreted then as physostigmine causing a rise of acetylcholine to a higher but constant level and that the peak M1-CNiFER response to physostigmine is merely reflecting non-stationarity of the sensor. However, a closer look suggests otherwise. First, the M1-CNiFER phasic response to prolonged bath-applied acetylcholine is relatively short, about 2-3 minutes, whereas the peak in Figure 21 is almost 10 minutes. Second, microdialysis measurements of acetylcholine after i.m. physostigmine injection show a peak at 15-30 minutes followed by somewhat of a plateau[166], similar to the M1-CNiFER response profile in Figure 21. Nevertheless, when experimenting over the scale of minutes, one must carefully consider this phasic-tonic non-stationarity of M1-CNiFER cells to prolonged acetylcholine exposure.

Interferents

An ideal CNiFER would respond only to ligands for the chosen expressed receptor. This, however, is not the case, though the response to acetylcholine is

~5 times the response to the most active interferents (Figure 11). A more detailed discussion of this can be found in Chapter II: Design and *In Vitro* Characterization of CNiFER Cells-Interferents. Briefly, control-CNiFERs are used expressly to deal with this problem. control-CNiFERs express the mCherry fluorescent protein instead of a receptor. Figure 11 shows that control-CNiFERs also respond to the same set of interferents, even if the magnitude is not identical. For a final verification that an M1-CNiFER response is cholinergic and not due to an interferent, atropine and physostigmine are used pharmacologically to either abolish or enhance the response, respectively (Figure 20, Figure 21, Figure 22).

Improving CNiFERs

Genetically Encoded Calcium Indicators

First generation CNiFERs were loaded with Oregon Green BAPTA and then implanted in the brain. Organic dyes offer many advantages: Ca^{2+}-dependent fluorescence increase of >100-fold, high specificity for Ca^{2+} over other divalent cations, tuned affinity by chlorination or fluorination, fast kinetics, varied excitation and emission spectra, and fluorescent ratiometric readouts of intensity or wavelength[186]. Organic dyes did work with CNiFERs (data not shown) but required loading cells with dye for each experiment and precluded chronic experiments in which dye fluorescence decreases over time[122]. Genetically encoded calcium indicators (GECIs) allow for chronic experiments and do not require loading before each implantation. There are numerous GECIs currently

available.[123-125,186]. When CNiFERs are used *in vivo*, it is useful to use a FRET-based (emission ratiometric) GECI to control for motion artifacts. Excitation ratiometric GECIs (*e.g.*, ratiometric pericam), although controlling for motion artifact, are not easily excited at two wavelengths in two photon microscopy, although epifluorescence systems are available and in continued development[187]. Of the FRET-based sensors, TN-XXL and D3cpv are viable options. D3cpv has a slightly larger dynamic range (5x ratio vs. 4x ratio) but TN-XXL has faster kinetics (~430ms rise time and ~240 decay time)[89,127]. We therefore chose TN-XXL for its FRET-based reporting, relatively large dynamic range and fast kinetics.

Adaptation

Adaptation of the M1-CNiFER response does occur. As seen in sustained acetylcholine perfusion, there is an initial phasic response followed by a reduced but stable plateau (Figure 6), while repetitive presentations of short acetylcholine pulses leads to a reduced but stable response (Figure 5). This in part may be due to a shift of calcium influx from internal to external stores (Figure 8). Or, it could reflect desensitization of the GPCR pathway (see Chapter II: Design and *In Vitro* Characterization of CNiFER Cells-Adaptation). To the extent that adaptation is due to GPCR desensitization and internalization, genetic manipulation of this pathway may diminish it. For example, mutation of the muscarinic receptor can inhibit its interactions with β-arrestins and thus reduce desensitization[188]. Another possible target is dynamin. Dynamin is a protein required for internalization of the

M1 muscarinic receptor in clathrin-coated vesicles. Dominant negative mutants of dynamin suppress this sequestration almost completely, suggesting a possible genetic approach to reduce internalization[152].

Improving Kinetics of CNiFERs

In their current form, CNiFER cells must have a surface receptor expressed that in some way increases cytosolic calcium levels. This can be achieved in multiple ways, but G protein coupled receptors and ligand-gated ion channels are two options. GPCRs provide two key advantages in CNiFER cells. First, they often have a strong affinity for their endogenous ligand[11,105]. Second, there are GPCRs specific for ~60 endogenous signaling molecules[105]. A drawback, however, is that the GPCR calcium cascade is relatively slow, and in our system provides a temporal resolution of ~6 seconds.

On the other hand, ligand-gated ion channels should provide much faster kinetics as the calcium influx is direct via the ion channel, not requiring a secondary messenger cascade. Unfortunately, there are only a few calcium permeable ligand gated ion channels, including nicotinic acetylcholine receptors, $5Ht_{3a}$ serotonin receptors, and NMDA glutamate receptors (see Ligand Gated Ion Channels below).

Sensitivity

The sensitivity of CNiFERs will depend on receptor concentration and different clonal lines will express different concentrations of receptor. Two clonal lines of M1-CNiFERs were tested by bath application of 20 second boluses of

acetylcholine (Figure 24). This variation between clonal lines (EC_{50} = 14 nM vs. 21 nM) can be used strategically. For instance, ambient levels of acetylcholine are much lower during anesthesia than during wakefulness. It is possible that a very sensitive clonal line may be suitable for experiments under anesthesia but might saturate in the awake state, when a less sensitive line may be more appropriate. The dissociation constant K_i for acetylcholine at the M1 muscarinic receptor is ~10 μM[105]. The EC_{50} for the phasic response of the current clone of M1-CNiFERs is ~8-14 nM acetylcholine, depending on the duration of presentation and system used for imaging (Figure 7, Figure 9, Figure 24). This represents a significant receptor reserve. Presumably, the EC_{50} range of M1-CNiFERs might be from as low as 10nM up to 10 μM-its dissociation constant with acetylcholine.

Cell Types

There are two primary reasons the choice of a cell line other than HEK293s may be desirable. First, autologous cell lines avoid concerns about host immune rejection of the implants for chronic studies. Of relevance to CNiFERs, *ex vivo* gene therapy studies identified several autologous cell lines appropriate for use: Schwann cells, endothelial cells, astrocytes, and skin fibroblasts. Fibroblasts emerged as the easiest to obtain and maintain[108]. Isogeneic grafts of fibroblasts from inbred strains (e.g., Fischer 344) allows for cells to be harvested from a single animal, transfected, then implanted into many animals with results similar to autologous grafts and survival of at least 24 months[107].

Second, some cell lines exhibit migration in the brain and will intercalate into the surrounding parenchyma. This would provide CNiFERs to be distributed throughout intact brain tissue in close proximity with axons and the extracellular space. Further, they will have moved away from the site of injection where tissue damage may impede volume transmission. Finally, spatial resolution should be commensurately increased as the cells move away from each other, though this would occur at the expense of spatial averaging over many cells. The following represents a sampling of potential cell lines for use as CNiFERs.

Isogeneic Fibroblasts

Ex vivo gene therapy studies have most fully characterized the use of primary fibroblasts for implantation and they exhibit favorable characteristics for our chronic sensor. These include viability measured on the order of a year, expression over a one month window, continued – albeit lower - expression up to one year thereafter, and contact inhibition[107,109]. Contact inhibition is important for chronic studies as HEK293s will continue to divide *in vivo* forming a tumor while primary fibroblasts will not[107].

Transduced fibroblasts have been found to survive and express proteins that can promote regeneration, rescue and recovery of damaged neural tissue[110,189-191]. Several early papers have noted a transgene shutdown in *ex vivo* fibroblast implants at ~ 30 days, with activity peaking at 5 or 13 days[192-194]. In other experiments, *in vivo* fibroblast expression continued for months[109,195,196]. CNiFERs are fluorescent and thus it is possible to assess transgene expression daily to delineate the optimal window for imaging. Should transgene shutdown

become problematic, the transgene could be coupled to a ‘housekeeping’ gene promoter, like dihydrofolate reductase, which has been shown not to shutdown after fibroblast implantation[193].

Migrating Cell Types

Glial Restricted Precursors (GRPs) have been used for *ex vivo* gene therapy implantations, expressing the mulitneurotrophin D15A[197]. These GRPs were harvested from day 14 spinal cord, retrovirally transduced and implanted. By 6 weeks, they had largely differentiated into oligodendrocytes, however, there may be a period of several weeks without differentiation when the cells could be imaged. It is also possible that differentiated cells would act as suitable reporters. Migration of transplanted GRPs at 6 weeks *in vivo* has been shown to be nearly 15 mm in spinal cord and 1 mm in gray matter with long processes and cell bodies extending into the surrounding parenchyma[198].

Glioma cell lines have been implanted in rodent brain to observe migration as this relates to metastasis. Glioma cell lines retrovirally expressing GFP were implanted into rodent brain. After 10 days, the brain was removed and 300μm sections were cut and followed with time lapse fluorescence microscopy. Glioma cells moved with a median migration of 5-10 microns per hour into the parenchyma[199].

Endogenous Response

HEK293 cells are often used in exogenous gene expression studies but they do express endogenous surface receptors. These include muscarinic, P2y

purogenic, somatostatin, AT1 angiotensin, β-adrenergic, A2b adenosine and prostaglandin E2 stimulated receptors[138,153,154]. In the case of endogenous muscarinic receptors, the expression levels are far lower than retrovirally expressed M1 as M1-CNiFERs have an EC_{50} of ~10 nM acetylcholine while control-CNiFERs have an EC_{50} of >10-100 μM acetylcholine (Figure 9).

One approach to correct for an endogenous response of CNiFERs to neurotransmitters released in the brain is to use control-CNiFERs that do not express the receptor of interest. For this approach to work, both the test and control CNiFER lines must express a similar profile of endogenous receptors and at relatively similar levels. The best way to approach this is to first transduce a calcium indicator into HEK293 cells and isolate multiple clonal lines. Then identify a clonal line with a desirable (probably short) profile of endogenous receptor expression as determined in Flexstation™ screening (see Figure 11). Finally, retrovirally transduce the receptor of interest into one population of this clonal line and mCherry into another population. Clonal lines can then be isolated from these transductions and rescreened with the Flexstation™ to assess similarity of receptor expression.

Another approach is to reduce expression of endogenous receptors. One possibility is to knock-down the expression of an endogenous receptor by using an antisense oligodeoxynucleotide strategy to suppress translation of mRNA transcripts[200,201]. A second possibility is to decouple the native G proteins from the native receptors using expression of carboxy-terminus blocking peptides that block the association of a given receptor with its Gα protein[202].

Expanding CNiFERs

CNiFERs for Other Neurotransmitters and Receptors

G Protein-Coupled Receptors

GPCRs form a large family of some 400 (non-olfactory) cell surface receptors that respond to roughly 60 endogenous signaling molecules[105,203]. GPCRs are characterized as having intermediate speed between fast millisecond ligand-gated ion channels to slow minutes to hours tyrosine kinase enzymatic receptors. The CNiFER technique can easily be adapted to detect neurotransmitters other than acetylcholine, by simply co-expressing TN-XXL with a different receptor coupled to G_q in HEK293 cells.

Designing CNiFERs for neurotransmitters that activate metabotropic receptors naturally coupled with G_s or G_i and the cAMP second messenger system will, however, require expression with another FRET reporter, such as the protein kinase A-sensitive AKAR[204] or cAMP-sensitive ICUE3 (Zhang, personal communication). Alternatively, coupling of these receptors with TN-XXL could be achieved either by using the promiscuous G protein Gα1629 or by co-expressing Ḍα chimeras that allow G_s and G_i protein-coupled receptors to link to G_q and the IP_3/Ca^{2+} pathway[120,205].

Ligand Gated Ion Channels

Another strategy involves expressing calcium permeable ionotropic receptors such as the 5-HT_{3A} serotonergic or α7 nicotinic receptor, allowing direct coupling of receptor opening with TN-XXL activation via direct extracellular calcium influx and possibly an enhanced temporal resolution (see Improving Kinetics of

CNiFERs above). These ion channels can have a lower affinity for ligand, e.g., α7 nicotinic receptors have a K_i of ~50-100 μM acetylcholine while many GPCRs have dissociation constants to endogenous neurotransmitters in the micromolar or nanomolar range[105]. Also, the α7 receptor strongly desensitizes to prolonged acetylcholine. A potential fallback would be to use a leucine 247 mutant of the α7 nicotinic receptor, which decreases the rate of desensitization while at the same time increases apparent affinity of the receptor for acetylcholine[206]. Finally, it may be that ligand-gated ion channel activation results in only small increases in concentrations of cytosolic calcium not detectable by TN-XXL. An option for signal amplification is the co-expression of voltage-sensitive Ca^{2+} channels[103,207]; a drawback is decreased specificity for our ligand, *i.e.*, any sufficient membrane potential change will be transduced to a Ca^{2+} signal, but as HEK293 are non-excitable cells this may not be a significant concern.

Tyrosine Kinase Receptors

Like GPCRs, some tyrosine kinases activate phospholipase C (PLC) and are therefore capable of increasing calcium flux into the cytoplasm of CNiFERs[94]. There are roughly 60 tyrosine kinase receptors grouped into 20 families. Tyrosine kinase receptors coupling to the SH2 domains of PLC include the growth factor EGF, FGF and PDGF receptors[208].

In Vivo Imaging

Head-Fixed Preparation

A drawback to using optical methods *in vivo* is stabilizing the optical field. One approach is to use a fixed-preparation where the animal is head-fixed and the light source is directed to a craniotomy or thinned-skull [209]. Although most head-fixed experiments are done on anesthetized animals, it is also possible to do so with a behaving animal [209-211]. With a fixed-preparation one can use epifluorescence imaging of the brain surface or two photon imaging to achieve some depth of penetration (~400 μm) [212,213]. Alternatively, a GRIN lens microendoscope can be used with either epifluorescence or two photon microscopy to image deep brain structures, though sacrificing numerical aperture and causing tissue damage[132,214-216].

Freely Moving Preparation

Another exciting possibility is to focus the light source to an unrestrained animal via fiber optic. The nature of fiber optical total-internal reflectance precludes transmitting anymore than a pixel of image. If only a pixel is required, a single fiber optic can be used. Alternatively, a bundle of fibers (up to 100,000) can be used to acquire pixilated images of brain surface and has been used in cat and mice [217,218]. Two photon microscopy has been achieved for the freely moving rat with a miniaturized scanning system mounted on the cranium [133,219]. In this study, the short, intense pulses required for two photon microscopy were severely degraded in regular fiber optics, but a hollow-core photonic crystal fiber

should reduce this effect [220]. This provides a few hundred micrometer field of view with ~250 micron depth penetration and optical sectioning, though intermittent motion artifact can be in issue.

Figures

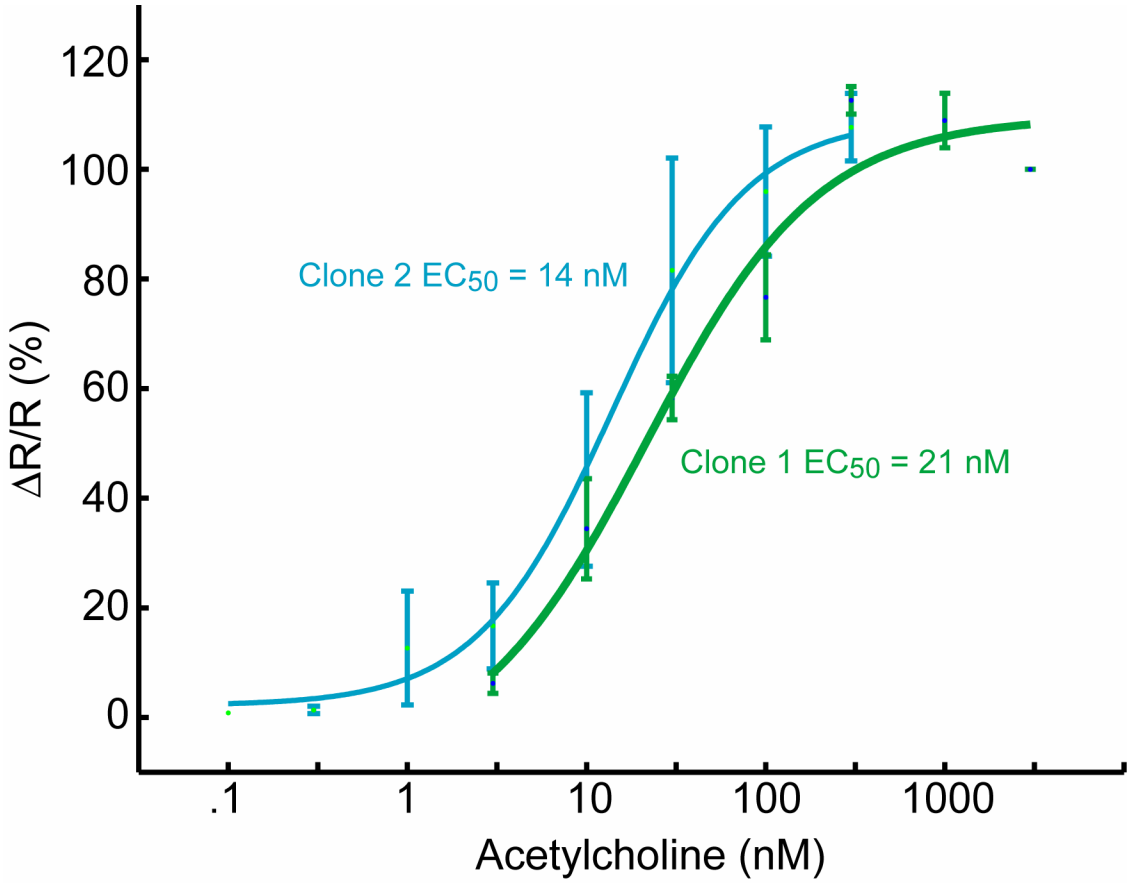

Figure 24 Dose Response of Two Clones of M1-CNiFERs

Two clonal lines of M1-CNiFERs demonstrate different sensitivities to acetylcholine. Acetylcholine was bath applied in 20 s boluses at each concentration. Bars represent standard errors, n = 3 experiments per clonal line with different passages of cells.

Chapter V: Methods

Tissue Culture

CNiFER cells were maintained humidified at 37°C and 10% CO_2 using a Fisher Scientific 10 and a Forma Scientific 3546 incubator(Thermo Scientific, MA). Upon confluence (approximately twice weekly), cells were trypsonized, triturated, and seeded into new, 500 ml flasks with .2 μm filtered caps, using Dulbecco's Modification of Eagle's Medium (DMEM Cellgro®; Mediatech, Inc, VA) with addition of Glutamax™-1 (Invitrogen, CA) and 10% (v/v) Fetalplex™ serum (Gemini Bio-Products, CA).

Molecular Biology

HEK293 cells were engineered to stably express proteins of interest using lentiviral transduction. cDNA for TN-XXL was contributed by Oliver Griesbeck (Max Planck Institute), mCherry by Roger Tsien (UCSD), and the human M1 muscarinic acetylcholine receptor by Paul Slesinger (Salk Institute). For TN-XXL and mCherry, the sequence encoding the complete protein was subcloned into lentiviral cloning vector pCDH1-MCS2 (System Biosciences, Mountain View, CA). The M1 muscarinic acetylcholine receptor was subcloned into pCDH1-MCS1-EF1-Puro, which provided puromycin resistance for selection. Lentivirus particle production and HEK293 transduction was performed by the UCSD Virus Facility. The Virus Facility is a centralized core component of the UCSD Gene Therapy Program, headed by Dr. Atsushi Miyanohara.

CNiFER Clone Selection

After the infectious period, transduced HEK293 cells were transferred to the Kleinfeld laboratory and stable lines were selected by serial dilution using fluorescence for TN-XXL and mCherry, and puromycin resistance for the M1 muscarinic acetylcholine receptor. Clones were screened for their response to acetylcholine by *in vitro* bath application using two photon laser scanning microscopy then divided into aliquots and frozen with 10% DMSO at T = -80°C. Additional aliquots were frozen approximately 1 year later. One clonal line was used in all experiments except Figure 24, with new aliquots thawed after 30-50 passages.

High-Throughput Screening of CNiFER Cells for Interferents

FRET responses of M1- and control-CNiFERs to acetylcholine and other neurotransmitters were measured *in vitro* using FlexStation™ 3(Molecular Devices, Sunnyvale, CA), a high-throughput fluorometric plate reader. M1- or control-CNiFERs were seeded into poly-D-lysine coated 96 well dishes at $.12*10^6$ cells per well the day before experimentation. DMEM media was replaced in each well with 100 µl artificial cerebral spinal fluid (ACSF; 125 mM NaCl, 5 mM KCl, 10 mM D-glucose, 10 mM HEPES, 3.1 mM $CaCl_2$, 1.3 mM $MgCl_2$, pH 7.4) and plates were loaded into the FlexStation™. Experiments were conducted at 37°C using a central spot of 435 nm laser illumination 1.5 mm across in each well. Light was collected at 485 nm (eCFP) and 527 nm (Citrine) bands every 3.8 s, and 50 µl of ligand diluted in ACSF was transferred to each well after a 40 s

baseline. The concentrations of ligand were such that after dilution in the well, the final concentrations displayed in Figure 9, Figure 10, and Figure 11 were obtained. In the case of atropine experiments (Figure 10), cells were pre-incubated in 100 µl of 100 nM atropine sulfate in ACSF. Then, 50 µl a combined solution of 300 nM acetylcholine and 100 nM atropine sulfate were transferred to each well after a 40 s baseline.

Two Photon Laser Scanning Microscopy

Besides high-throughput screening using the Flexstation™, *in vitro* and *in vivo* imaging experiments was performed on a two photon laser scanning microscope of local design based on standard techniques using a femtosecond laser (Verdi oscillator, pumped by a Mira green laser, Coherent, Mountain View, CA) [130,171]. Imaging of CNiFER cells for TN-XXL response was conducted at 800nm to minimize two photon excitation of Citrine while maintaining excitation of eCFP[171,221]. Imaging of mCherry labeling was conducted at 760nm, the location of an anomalous peak in the mCherry two photon excitation spectra[222,223]. 256x256 pixel images were acquired at 2 Hz, using a 40x or 20x objective. Three channels of data were collected using a 505 nm long pass dichroic with a 475df40 filter (eCFP channel) and 530df30 filter (Citrine and eCFP, hereafter referred to as the Citrine channel), and a 571 nm dichroic with a 580 nm long pass filter (mCherry channel). Data was collected using MPSCOPE[224].

Bath Application of Acetylcholine to CNiFER Cells

CNiFERs were seeded the night before onto fibronectin-coated glass coverslips, continuously ACSF-perfused by gravity-feed in a RC26 Warner Instruments laminar flow perfusion chamber (Warner Instruments, CT) at 32°C and imaged using two photon microscopy. In Figure 6, perfusion was switched to different concentrations of acetylcholine for 8 minutes, then returned again to ACSF. In Figure 24, acetylcholine was bath-applied at each concentration for 20 seconds then returned again to ACSF. Runs were separated by 5-15 minutes depending upon acetylcholine concentration in order to reduce possible CNiFER desensitization. Calcium-free media experiments were performed using media with calcium replaced by equimolar magnesium.

Fast-Perfusion of CNiFER Cells

The kinetics of the M1-CNiFER response were measured using a fast perfusion stepper (SF-77B, Warner Instruments, CT). CNiFERs were again seeded onto fibronectin-coated glass coverslips the night before, continuously ACSF-perfused by gravity-feed in a bath chamber (Warner Instruments) at 32°C and imaged using two photon microscopy. A glass pipette fastened to the perfusion stepper was positioned just outside the field of view, releasing acetylcholine in a laminar flow. The perfusion stepper was actuated by several hundred micrometers for short periods of time to directly perfuse the imaged cells. Alexa-594 was mixed into acetylcholine solutions to verify presence of acetylcholine and determine precise duration of exposure. Alexa-594 was diluted

to ensure no contamination occurred in the eCFP or Citrine channels. In Figure 5, no Alexa-594 was used and therefore the duration of exposure is unknown. Although the pipette tip was actuated for only 250 ms in that experiment, exposure probably occurred over a longer time period considering the large response amplitude. A discrepancy between actuation duration and Alexa-594 perfusion was seen in other experiments and is perhaps in part due to the water-immersion objective disrupting laminar flow.

Surgical Procedures

Anesthetics

Experiments were performed on male Sprague-Dawley rats (250-450g). Our whole animal imaging experiments required the use of an anesthetic to immobilize the animal in a calm and pain-free state. We used isoflurane for anesthetic induction and for injection of CNiFER cells then switched to urethane for the remainder of the experiment since it produces a reproducible electrophysiological response[225].

Animals were anesthetized with isoflurane at ~2% maximum alveolar concentration and mounting of the animal in a stereotaxic holder began only after the animal had reached an anesthetic plane, as assessed by the loss of pedal and corneal reflexes. After CNiFER injection, isoflurane was tapered off and i.p. urethane dose was incrementally increased so as to induce a surgical plane of anesthesia and slow, large amplitude electrocorticogram oscillations. Each animal received a prophylactic dose of atropine (0.1 mg s.c.), and was

supplemented with 5 % (w/v) glucose in saline (1-5 ml s.c. several times per experiment). The pulse, rate of breathing, and temperature of the animal were continually observed. The eyes were protected from dehydration by ophthalmic ointment.

Electrocorticogram

These consisted of a pair of 125 μm diameter Teflon coated silver wires (A-M Systems Inc., WA). We placed two such pairs to measure the electrocorticogram either across the imaging window or between the rostral and occipito-parietal cortices. Electrical signals were amplified using a DAM80 differential amplifier (World Precision Instruments, CT) set to a bandpass of .1-100 Hz, and gain of 1000. Data was collected at 400 Hz.

Imaging Window and CNiFER Implantation

A craniotomy was prepared above motor or parietal cortex and dura was removed. Harvesting and implantation of the cells roughly followed the procedures of Gage and co-workers[107]. The front-loaded capillary tip (~40 μm inner diameter, ~55 μm outer diameter) was lowered using a stereotaxic device to 500-1000 μm below the cortical surface, then retracted several hundred μm. We then injected ~10^3 cells in a volume of 10-100 nl ACSF (126 mM NaCl, 5 mM KCl, 2 mM $MgSO_4$, 26 mM $NaHCO_3$, 1.25 mM NaH_2PO_4, 2 mM $CaCl_2$, and 10 mM D-glucose) using a syringe pump, flow was stopped immediately after cells were seen to move down the pipette shaft. In an attempt to avoid damage to the parenchyma this is a far lower volume than used in previous *ex vivo* gene

therapy transplantation studies, which injected 10^5 cells in 3 µL of media[107,109]. After a pause of ~1-5 minutes to allow equilibration of pressure in the implantation site, the tip was slowly removed. The procedure was repeated several times for multiple M1- and control-CNiFER sites. The cortical surface was then filled with 1.5% (w/v) agarose in ACSF (see above) and a coverslip cemented over the craniotomy. Finally, a metal frame was fixed to the skull as a means of rigidly holding the head of the animal beneath the two photon microscope. In chronic experiments (Figure 22, Figure 23), cyclosporine was injected daily (Belford Laboratories; 20 µL/100 gm, i.p.) starting one day before implantation.

Nucleus Basalis Magnocellularis Electrode Placement

In each Nucleus Basalis Magnocellularis stimulation experiment, two .1 MΩ tungsten stimulating electrodes (Microprobes Inc., Maryland) spaced ~.5 mm apart were implanted at the coordinates (2.1 mm, -1.2 mm, -6.9 mm)[226]. Electrical stimulation consisted of 200 µs pulses of 100-1000 µA, at 100 Hz, for a duration of 200-500 ms. The depth of implantation and magnitude of current was adjusted to produce cortical activation as assayed by cessation of cortical large-amplitude irregular activity in the urethane-anesthetized animal[164,227]. This value was typically 200 µA.

In Vivo Experimental Procedures

Intracortical Acetylcholine Injection

Capillary pipettes with ~25 μm inner diameter were filled with phosphate buffered saline or 1mM acetylcholine chloride in phosphate buffered saline and affixed to an oocyte injector (Nanoject II, Drummond, PA). In these experiments, the coverslip over the imaging window was left open on the medial side. The capillary tip was maneuvered into the window using a micromanipulator (Sutter, CA) and positioned near the CNiFER implants. Experimental runs consisted of 10s baselines followed by 27 nl injections.

Nucleus Basalis Magnocellularis Stimulation

After a 30 second baseline, electrical stimulation of NBM consisted of 200 μs pulses of 100-1000 μA, at 100 Hz, for a duration of 200-500 ms.

Pharmacology

Physostigmine salicylate (Sigma-Aldrich, MO) was injected s.c. in the neck at 200 (Figure 20) or 300 μg/kg (Figure 21). ACSF or atropine sulfate was introduced intracortically with a reverse dialysis probe inserted into a chronically implanted cannula (CMA 11 probe, CMA Germany) (Figure 22).

Histological Procedure

Adult animals were perfused with phosphate buffered saline (PBS) then 4% (w/v) paraformaldehyde (PFA) in PBS. The typical perfusion volumes were 0.5 ml per gram animal and flow rates were 20 ml/min. The extracted brains were stored in 4 % PFA in PBS for post-fixation. α-GFAP rabbit antibodies (Zymed, CA) were

used to visualize astrocytes. Sections were quenched in 3% hydrogen peroxide for 15 minutes then incubated overnight in a 1:200 dilution of primary α-GFAP antibody in the diluent used throughout the histological process: PBS containing .25% Triton, 5% goat serum and .02% sodium azide. After washing for 1 hour, α-GFAP sections were incubated in a 1:500 dilution of biotinylated α-rabbit secondary antibody (Vector Laboratories, CA). This was followed by the avidin:biotinylated complex method (Vectastain ABC kit, Vector Laboratories, CA) and 3,3'-diaminobenzidine (DAB) visualization with nickel. Sections were mounted on slides and imaged on a Zeiss microscope with brightfield for DAB stains and epifluorescence for M1- and control-CNiFERs.

Animal Care

The University of California, San Diego is fully accredited by the American Association for Accreditation of Laboratory Animal Care, Int'l. (AAALAC) and holds an approved NIH Assurance and USDA License. Veterinary care was provided on a 24 hour basis, including weekends and holidays by a staff comprised of veterinarians and animal health technicians. Research support services included training classes and consultations for surgical protocols.

Euthanasia

The animals were euthanized by i.p. injection of a lethal overdose of pentobarbital (25 mg per 100 g rodent) which is a method consistent with the guideline provided by the Panel of Euthanasia of the American Veterinary Medical Association. Death was assayed by cessation of breathing and

heartbeat. For rats in which histology was performed, following anesthetic overdose and the loss of pedal and corneal blink reflexes, the chest cavity was opened to allow for transcardial perfusion of fixatives. The carcass of the animal was stored frozen at -4°C.

Data Analysis

All CNiFER responses and electrocorticogram data was analyzed in Matlab™ (Mathworks, MA).

CNiFER Cells

FRET-based imaging typically involves both excitation cross-talk, *i.e.* it is difficult to excite only eCFP (the donor) and not Citrine (the acceptor), and spectral bleedthrough, *i.e.*, the emission spectra of eCFP and Citrine overlap. Therefore, to determine the quantitative FRET efficiency, multiple filter sets must be used as well as normalization using samples containing isolated eCFP or Citrine. Since our experiments did not depend upon FRET efficiency *per se* but only relative changes in FRET signal, we chose to simply ratio the Citrine channel by the eCFP channel, a simple strategy that is reliable given a constant ratio of acceptor to donor molecules as is found in TN-XXL[184].

The general approach to calculating the two photon microscopic FRET-based signal change of TN-XXL included extraction of time series data using regions of interest, background subtraction at each time point from within the eCFP and Citrine channels, normalization of each trace to baseline, and division of Citrine/eCFP channels. For constructing dose-response curves, the peak

fractional response was measured from low-pass filtered data at .3 Hz. In measurements of phasic CNiFER cell response (*e.g.* to NBM stimulation) baseline was defined as the area under the curve of the FRET-based signal 10 seconds before the stimulus and the response was defined as that 30 seconds after the stimulus. The index of CNiFER response was the simple ratio of response/(3*baseline). In Figure 16, only 10 seconds of post-stimulus data was used instead of 30 seconds, and the index was the ratio response/baseline.

Tonic CNiFER responses to physostigmine were taken from experiments in which NBM was stimulated every 5 minutes, but the NBM-evoked response was not used. Instead, the 10 s period before each NBM stimulation was used in the analysis and normalization of each channel to its baseline was *not* performed. By retaining an absolute measure of the eCFP and Citrine channels, tonic FRET-based changes over consecutive runs within a session were preserved. During the experiment, care was taken not to disturb dichroic position between measurements so as not to artificially change the FRET-based signal. After region of interest time series extraction of a 10 s window and background subtraction at each time point, data was averaged and Citrine and eCFP readings were divided. These absolute measures at each 5 minute time point were then normalized to the first 3 measurements before vehicle injection.

In chronic experiments measuring atropine antagonism of the NBM-evoked M1-CNiFER response, inhibition was calculated as the fraction of the minimal NBM-evoked peak after atropine dialysis compared to that before atropine dialysis.

In the case of Flexstation™ 3 data, background from neighboring empty wells was subtracted from Citrine and eCFP time series, data normalized to baseline, and division of Citrine/eCFP performed. Peak response in each well was measured. Data in Figure 9 and Figure 11 presented as S/S_{M1}, where S/S_{M1} signifies the signal change as a fraction of the signal change of M1-CNiFERs to 100 nM acetylcholine.

Electrocorticogram

Baseline (Figure 17, Figure 21) and post-stimulus (Figure 17, Figure 18) electrocorticogram time series were Fourier transformed using the multi-taper algorithm in Chronux Analysis Software for Matlab (http://chronux.org). Post-stimulus time series consisted of a single 5 second epoch beginning 500 ms after the stimulus, while baseline consisted of 4 consecutive 5 second epochs directly preceding the stimulus. Each epoch was multi-taper transformed using 19 tapers. An index of ECoG activation was calculated by averaging the 1-6 Hz power band in the post-stimulus epoch (phasic response to NBM stimulation) or the baseline epochs (tonic response to physostigmine injection, Figure 21). These averages were then inverted and the logarithm taken to transform the data into a Gaussian-like distribution suitable to a subsequent z-transformation within experiments to equalize variance between animals.

References

[1] Lohse, Nikolaev, Hein, Hoffmann, Vilardaga & Bunemann. Optical techniques to analyze real-time activation and signaling of G-protein-coupled receptors *Trends Pharmacol Sci* 29, 159-65 (2008)

[2] Rasmusson. The role of acetylcholine in cortical synaptic plasticity *Behav Brain Res* 115, 205-18 (2000)

[3] Robbins & Everitt. in *The Cognitive Neurosciences* (ed. Gazzaniga, M. S.) 703-20 (MIT Press, Cambridge, 1995).

[4] Jones. Arousal systems *Front Biosci* 8, s438-51 (2003)

[5] Steriade. Acetylcholine systems and rhythmic activities during the waking--sleep cycle *Prog Brain Res* 145, 179-96 (2004)

[6] Kummer, Misgeld & Sanes. Assembly of the postsynaptic membrane at the neuromuscular junction: paradigm lost *Curr Opin Neurobiol* 16, 74-82 (2006)

[7] Tsien. Breeding molecules to spy on cells *Harvey Lect* 99, 77-93 (2003)

[8] Vilardaga, Bunemann, Krasel, Castro & Lohse. Measurement of the millisecond activation switch of G protein-coupled receptors in living cells *Nat Biotechnol* 21, 807-12 (2003)

[9] Okumoto, Looger, Micheva, Reimer, Smith & Frommer. Detection of glutamate release from neurons by genetically encoded surface-displayed FRET nanosensors *Proc Natl Acad Sci U S A* 102, 8740-5 (2005)

[10] Hires, Zhu & Tsien. Optical measurement of synaptic glutamate spillover and reuptake by linker optimized glutamate-sensitive fluorescent reporters *Proc Natl Acad Sci U S A* 105, 4411-6 (2008)

[11] Agnati, Zoli, Stromberg & Fuxe. Intercellular communication in the brain: wiring versus volume transmission *Neuroscience* 69, 711-26 (1995)

[12] Umbriaco, Watkins, Descarries, Cozzari & Hartman. Ultrastructural and morphometric features of the acetylcholine innervation in adult rat parietal cortex: an electron microscopic study in serial sections *J Comp Neurol* 348, 351-73 (1994)

[13] Mrzljak, Levey & Goldman-Rakic. Association of m1 and m2 muscarinic receptor proteins with asymmetric synapses in the primate cerebral cortex: morphological evidence for cholinergic modulation of excitatory neurotransmission *Proc Natl Acad Sci U S A* 90, 5194-8 (1993)

[14] Vizi & Lendvai. Modulatory role of presynaptic nicotinic receptors in synaptic and non-synaptic chemical communication in the central nervous system *Brain Res Brain Res Rev* 30, 219-35 (1999)

[15] Ellis. The state of GPCR research in 2004 *Nat Rev Drug Discov* 3, 575, 7-626 (2004)

[16] Volpicelli & Levey. Muscarinic acetylcholine receptor subtypes in cerebral cortex and hippocampus *Prog Brain Res* 145, 59-66 (2004)

[17] Bernard, Laribi, Levey & Bloch. Subcellular redistribution of m2 muscarinic acetylcholine receptors in striatal interneurons in vivo after acute cholinergic stimulation *J Neurosci* 18, 10207-18 (1998)

[18] Weisskopf, Zalutsky & Nicoll. The opioid peptide dynorphin mediates heterosynaptic depression of hippocampal mossy fibre synapses and modulates long-term potentiation *Nature* 362, 423-7 (1993)

[19] Moruzzi & Magoun. Brain stem reticular formation and activation of the electroencephalogram *Electroencephalogr. Clin. Neurophysiol*, 455-73 (1949)

[20] Celesia & Jasper. Acetylcholine released from cerebral cortex in relation to state of activation *Neurology* 16, 1053-63 (1966)

[21] Rovira, Ben-Ari & Cherubini. Dual cholinergic modulation of hippocampal somatic and dendritic field potentials by the septo-hippocampal pathway *Exp Brain Res* 49, 151-5 (1983)

[22] Alkondon, Pereira, Barbosa & Albuquerque. Neuronal nicotinic acetylcholine receptor activation modulates gamma-aminobutyric acid release from CA1 neurons of rat hippocampal slices *J Pharmacol Exp Ther* 283, 1396-411 (1997)

[23] Jones & Yakel. Functional nicotinic ACh receptors on interneurones in the rat hippocampus *J Physiol* 504 (Pt 3), 603-10 (1997)

[24] Adams, Brown & Constanti. Pharmacological inhibition of the M-current *J Physiol* 332, 223-62 (1982)

[25] Madison, Lancaster & Nicoll. Voltage clamp analysis of cholinergic action in the hippocampus *J Neurosci* 7, 733-41 (1987)

[26] Nakajima, Nakajima, Leonard & Yamaguchi. Acetylcholine raises excitability by inhibiting the fast transient potassium current in cultured hippocampal neurons *Proc Natl Acad Sci U S A* 83, 3022-6 (1986)

[27] Drachman. Memory and cognitive function in man: does the cholinergic system have a specific role? *Neurology* 27, 783-90 (1977)

[28] Warburton. in *Handbook of Psychopharmacology* (eds. Iversen, L. L., Iversen, S. D. & Snyder, S. H.) 385-431 (Plenum, New York, 1977).

[29] Drachman & Sahakian. in *Nutrition and the Brain* (eds. Barbeau, A., Growden, J. H. & Wurtman, R. J.) 351-66 (Raven, New York, 1979).

[30] Sillito & Kemp. Cholinergic modulation of the functional organization of the cat visual cortex *Brain Res* 289, 143-55 (1983)

[31] Sato, Hata, Masui & Tsumoto. A functional role of cholinergic innervation to neurons in the cat visual cortex *J Neurophysiol* 58, 765-80 (1987)

[32] Metherate, Tremblay & Dykes. The effects of acetylcholine on response properties of cat somatosensory cortical neurons *J Neurophysiol* 59, 1231-52 (1988)

[33] Metherate & Ashe. Basal forebrain stimulation modifies auditory cortex responsiveness by an action at muscarinic receptors *Brain Res* 559, 163-7 (1991)

[34] Hasselmo & Bower. Cholinergic suppression specific to intrinsic not afferent fiber synapses in rat piriform (olfactory) cortex *J Neurophysiol* 67, 1222-9 (1992)

[35] Hars, Maho, Edeline & Hennevin. Basal forebrain stimulation facilitates tone-evoked responses in the auditory cortex of awake rat *Neuroscience* 56, 61-74 (1993)

[36] Metherate & Ashe. Nucleus basalis stimulation facilitates thalamocortical synaptic transmission in the rat auditory cortex *Synapse* 14, 132-43 (1993)

[37] Hasselmo & Schnell. Laminar selectivity of the cholinergic suppression of synaptic transmission in rat hippocampal region CA1: computational modeling and brain slice physiology *J Neurosci* 14, 3898-914 (1994)

[38] Hsieh, Cruikshank & Metherate. Differential modulation of auditory thalamocortical and intracortical synaptic transmission by cholinergic agonist *Brain Res* 880, 51-64 (2000)

[39] Oldford & Castro-Alamancos. Input-specific effects of acetylcholine on sensory and intracortical evoked responses in the "barrel cortex" in vivo *Neuroscience* 117, 769-78 (2003)

[40] Woody, Swartz & Gruen. Effects of acetylcholine and cyclic GMP on input resistance of cortical neurons in awake cats *Brain Res* 158, 373-95 (1978)

[41] Rasmusson & Dykes. Long-term enhancement of evoked potentials in cat somatosensory cortex produced by co-activation of the basal forebrain and cutaneous receptors *Exp Brain Res* 70, 276-86 (1988)

[42] Metherate, Tremblay & Dykes. Acetylcholine permits long-term enhancement of neuronal responsiveness in cat primary somatosensory cortex *Neuroscience* 22, 75-81 (1987)

[43] Metherate & Weinberger. Acetylcholine produces stimulus-specific receptive field alterations in cat auditory cortex *Brain Res* 480, 372-7 (1989)

[44] Bakin & Weinberger. Induction of a physiological memory in the cerebral cortex by stimulation of the nucleus basalis *Proc Natl Acad Sci U S A* 93, 11219-24 (1996)

[45] Kilgard & Merzenich. Cortical map reorganization enabled by nucleus basalis activity *Science* 279, 1714-8 (1998)

[46] Baskerville, Schweitzer & Herron. Effects of cholinergic depletion on experience-dependent plasticity in the cortex of the rat *Neuroscience* 80, 1159-69 (1997)

[47] Delacour, Houcine & Costa. Evidence for a cholinergic mechanism of "learned" changes in the responses of barrel field neurons of the awake and undrugged rat *Neuroscience* 34, 1-8 (1990)

[48] Sachdev, Lu, Wiley & Ebner. Role of the basal forebrain cholinergic projection in somatosensory cortical plasticity *J Neurophysiol* 79, 3216-28 (1998)

[49] Conner, Culberson, Packowski, Chiba & Tuszynski. Lesions of the Basal forebrain cholinergic system impair task acquisition and abolish cortical plasticity associated with motor skill learning *Neuron* 38, 819-29 (2003)

[50] Conner, Chiba & Tuszynski. The Basal Forebrain Cholinergic System Is Essential for Cortical Plasticity and Functional Recovery Following Brain Injury in *Society for Neuroscience Annual Meeting* (San Diego, 2004).

[51] Parasuraman, Greenwood, Haxby & Grady. Visuospatial attention in dementia of the Alzheimer type *Brain* 115 (Pt 3), 711-33 (1992)

[52] Voytko, Olton, Richardson, Gorman, Tobin & Price. Basal forebrain lesions in monkeys disrupt attention but not learning and memory *J Neurosci* 14, 167-86 (1994)

[53] Baxter, Holland & Gallagher. Disruption of decrements in conditioned stimulus processing by selective removal of hippocampal cholinergic input *J Neurosci* 17, 5230-6 (1997)

[54] Sarter & Bruno. Cognitive functions of cortical acetylcholine: toward a unifying hypothesis *Brain Res Brain Res Rev* 23, 28-46 (1997)

[55] Bucci, Holland & Gallagher. Removal of cholinergic input to rat posterior parietal cortex disrupts incremental processing of conditioned stimuli *J Neurosci* 18, 8038-46 (1998)

[56] Baxter & Chiba. Cognitive functions of the basal forebrain *Curr Opin Neurobiol* 9, 178-83 (1999)

[57] Stewart, Burke & Marrocco. Cholinergic modulation of covert attention in the rat *Psychopharmacology (Berl)* 155, 210-8 (2001)

[58] McGaughy, Dalley, Morrison, Everitt & Robbins. Selective behavioral and neurochemical effects of cholinergic lesions produced by intrabasalis infusions of 192 IgG-saporin on attentional performance in a five-choice serial reaction time task *J Neurosci* 22, 1905-13 (2002)

[59] Robbins. The 5-choice serial reaction time task: behavioural pharmacology and functional neurochemistry *Psychopharmacology (Berl)* 163, 362-80 (2002)

[60] Beane & Marrocco. Norepinephrine and acetylcholine mediation of the components of reflexive attention: implications for attention deficit disorders *Progress in Neurobiology (Oxford)* 74, 167-81 (2004)

[61] Bentley, Husain & Dolan. Effects of cholinergic enhancement on visual stimulation, spatial attention, and spatial working memory *Neuron* 41, 969-82 (2004)

[62] Longo. Behavioral and electroencephalographic effects of atropine and related compounds *Pharmacol Rev* 18, 965-96 (1966)

[63] Perry, Tomlinson, Blessed, Bergmann, Gibson & Perry. Correlation of cholinergic abnormalities with senile plaques and mental test scores in senile dementia *Br Med J* 2, 1457-9 (1978)

[64] Dunnett, Everitt & Robbins. The basal forebrain-cortical cholinergic system: interpreting the functional consequences of excitotoxic lesions *Trends Neurosci* 14, 494-501 (1991)

[65] Everitt & Robbins. Central cholinergic systems and cognition *Annu Rev Psychol* 48, 649-84 (1997)

[66] Fine, Hoyle, Maclean, Levatte, Baker & Ridley. Learning impairments following injection of a selective cholinergic immunotoxin, ME20.4 IgG-saporin, into the basal nucleus of Meynert in monkeys *Neuroscience* 81, 331-43 (1997)

[67] Chiba, Bucci, Holland & Gallagher. Basal forebrain cholinergic lesions disrupt increments but not decrements in conditioned stimulus processing *J Neurosci* 15, 7315-22 (1995)

[68] Ridley, Baker, Drewett & Johnson. Effects of ibotenic acid lesions of the basal forebrain on serial reversal learning in marmosets *Psychopharmacology (Berl)* 86, 438-43 (1985)

[69] Ridley, Barefoot, Maclean, Pugh & Baker. Different effects on learning ability after injection of the cholinergic immunotoxin ME20.4IgG-saporin into the diagonal band of Broca, basal nucleus of Meynert, or both in monkeys *Behav Neurosci* 113, 303-15 (1999)

[70] Basile, Fedorova, Zapata, Liu, Shippenberg, Duttaroy, Yamada & Wess. Deletion of the M5 muscarinic acetylcholine receptor attenuates morphine reinforcement and withdrawal but not morphine analgesia *Proc Natl Acad Sci U S A* 99, 11452-7 (2002)

[71] Siegal, Erickson, Varoqui, Ang, Kalasinsky, Peretti, Aiken, Wickham & Kish. Brain vesicular acetylcholine transporter in human users of drugs of abuse *Synapse* 52, 223-32 (2004)

[72] Hikida, Kitabatake, Pastan & Nakanishi. Acetylcholine enhancement in the nucleus accumbens prevents addictive behaviors of cocaine and morphine *Proc Natl Acad Sci U S A* 100, 6169-73 (2003)

[73] Maskos, Molles, Pons, Besson, Guiard, Guilloux, Evrard, Cazala, Cormier, Mameli-Engvall, Dufour, Cloez-Tayarani, Bemelmans, Mallet, Gardier, David, Faure, Granon & Changeux. Nicotine reinforcement and

cognition restored by targeted expression of nicotinic receptors *Nature* 436, 103-7 (2005)

[74] Day, Kornecook & Quirion. Application of in vivo microdialysis to the study of cholinergic systems *Methods* 23, 21-39 (2001)

[75] Lada, Vickroy & Kennedy. High temporal resolution monitoring of glutamate and aspartate in vivo using microdialysis on-line with capillary electrophoresis with laser-induced fluorescence detection *Anal Chem* 69, 4560-5 (1997)

[76] Rasmusson, Clow & Szerb. Frequency-dependent increase in cortical acetylcholine release evoked by stimulation of the nucleus basalis magnocellularis in the rat *Brain Res* 594, 150-4 (1992)

[77] Jimenez-Capdeville & Dykes. Changes in cortical acetylcholine release in the rat during day and night: differences between motor and sensory areas *Neuroscience* 71, 567-79 (1996)

[78] Himmelheber, Fadel, Sarter & Bruno. Effects of local cholinesterase inhibition on acetylcholine release assessed simultaneously in prefrontal and frontoparietal cortex *Neuroscience* 86, 949-57 (1998)

[79] Day, Kornecook & Quirion. Application of in vivo microdialysis to the study of cholinergic systems *Methods* 23, 21-39 (2001)

[80] Parrot, Sauvinet, Riban, Depaulis, Renaud & Denoroy. High temporal resolution for in vivo monitoring of neurotransmitters in awake epileptic rats using brain microdialysis and capillary electrophoresis with laser-induced fluorescence detection *J Neurosci Methods* 140, 29-38 (2004)

[81] Zhou, Zuo, Stobaugh, Lunte & Lunte. Continuous in vivo monitoring of amino acid neurotransmitters by microdialysis sampling with on-line derivatization and capillary electrophoresis separation *Anal Chem* 67, 594-9 (1995)

[82] Robinson, Venton, Heien & Wightman. Detecting subsecond dopamine release with fast-scan cyclic voltammetry in vivo *Clin Chem* 49, 1763-73 (2003)

[83] Wightman & Robinson. Transient changes in mesolimbic dopamine and their association with 'reward' *J Neurochem* 82, 721-35 (2002)

[84] Parikh, Kozak, Martinez & Sarter. Prefrontal acetylcholine release controls cue detection on multiple timescales *Neuron* 56, 141-54 (2007)

[85] Xin & Wightman. Enzyme modified amperometric sensors for choline and acetylcholine with tetrathiafulvalene tetracyanoquinodimethane as the electron-transfer mediator 341, 43-51 (1997)

[86] Burmeister, Pomerleau, Huettl, Gash, Werner, Bruno & Gerhardt. Ceramic-based multisite microelectrode arrays for simultaneous measures of choline and acetylcholine in CNS *Biosens Bioelectron* 23, 1382-9 (2008)

[87] Inoue, Kirchhoff & Hudson. Enhanced measurement stability and selectivity for choline and acetylcholine by capillary electrophoresis with electrochemical detection at a covalently linked enzyme-modified electrode *Anal Chem* 74, 5321-6 (2002)

[88] Xin & Wightman. Enzyme modified amperometric sensors for choline and acetylcholine with tetrathiafulvalene tetracyanoquinodimethane as the electron-transfer mediator *Analytica Chimica Acta* 341, 43-51 (1997)

[89] Mank, Santos, Direnberger, Mrsic-Flogel, Hofer, Stein, Hendel, Reiff, Levelt, Borst, Bonhoeffer, Hubener & Griesbeck. A genetically encoded calcium indicator for chronic in vivo two-photon imaging *Nat Methods* 5, 805-11 (2008)

[90] Tsien. in *Imaging in Neurosciences and Development A Laboratory Manual* (eds. Yuste, R. & Konnerth, A.) 549-56 (Cold Spring Harbor Laboratory Press, 2005).

[91] Lohse, Hein, Hoffmann, Nikolaev, Vilardaga & Bunemann. Kinetics of G-protein-coupled receptor signals in intact cells *Br J Pharmacol* 153 Suppl 1, S125-32 (2008)

[92] Palmer, Giacomello, Kortemme, Hires, Lev-Ram, Baker & Tsien. Ca2+ indicators based on computationally redesigned calmodulin-peptide pairs *Chem Biol* 13, 521-30 (2006)

[93] Freshney. (Wiley-Liss, 2005) Culture of Animal Cells: A Manual of Basic Technique.

[94] Clapham. Calcium signaling *Cell* 131, 1047-58 (2007)

[95] Palmer & Tsien. Measuring calcium signalling using genetically targetable fluorescent indicators *Nature Protocols* 1, 1057-65 (2006)

[96] Epps, Wolfe & Groppi. Characterization of the steady-state and dynamic fluorescence properties of the potential-sensitive dye bis-(1,3-dibutylbarbituric

acid)trimethine oxonol (Dibac4(3)) in model systems and cells *Chem Phys Lipids* 69, 137-50 (1994)

[97] Holevinsky, Fan, Frame, Makielski, Groppi & Nelson. ATP-sensitive K+ channel opener acts as a potent Cl- channel inhibitor in vascular smooth muscle cells *J Membr Biol* 137, 59-70 (1994)

[98] Schroeder & Neagle. FLIPR: A New Instrument for Accurate, High Throughput Optical Screening *Journal of Biomolecular Screening* 1, 75-80 (1996)

[99] Waggoner, Taylor, Seadler & Dunlay. Multiparameter fluorescence imaging microscopy: reagents and instruments *Hum Pathol* 27, 494-502 (1996)

[100] Gonzalez & Tsien. Improved indicators of cell membrane potential that use fluorescence resonance energy transfer *Chemistry & Biology* 4, 269-77 (1997)

[101] Cohen, Chang, Boyer & Helling. Construction of biologically functional bacterial plasmids in vitro *Proc Natl Acad Sci U S A* 70, 3240-4 (1973)

[102] Grynkiewicz, Poenie & Tsien. A new generation of Ca2+ indicators with greatly improved fluorescence properties *J Biol Chem* 260, 3440-50 (1985)

[103] Velicelebi, Stauderman, Varney, Akong, Hess & Johnson. Fluorescence techniques for measuring ion channel activity *Methods Enzymol* 294, 20-47 (1999)

[104] Walker, Jones, Tamm, Zhong, Smith, Gerald, Vaysse & Branchek. Use of Caenorhabditis elegans G{alpha}q chimeras to detect G-protein-coupled receptor signals *J Biomol Screen* 10, 127-36 (2005)

[105] Enna. International Union of Basic and Clinical Pharmacology (2009) www.iuphar.org

[106] Gage, Wolff, Rosenberg, Xu, Yee, Shults & Friedmann. Grafting genetically modified cells to the brain: possibilities for the future *Neuroscience* 23, 795-807 (1987)

[107] Kawaja & Gage. Morphological and neurochemical features of cultured primary skin fibroblasts of Fischer 344 rats following striatal implantation *J Comp Neurol* 317, 102-16 (1992)

[108] Snyder & Senut. The use of nonneuronal cells for gene delivery *Neurobiol Dis* 4, 69-102 (1997)

[109] Pizzo, Paban, Coufal, Gage & Thal. Long-term production of choline acetyltransferase in the CNS after transplantation of fibroblasts modified with a regulatable vector *Brain Res Mol Brain Res* 126, 1-13 (2004)

[110] Tuszynski, Thal, Pay, Salmon, U, Bakay, Patel, Blesch, Vahlsing, Ho, Tong, Potkin, Fallon, Hansen, Mufson, Kordower, Gall & Conner. A phase 1 clinical trial of nerve growth factor gene therapy for Alzheimer disease *Nat Med* 11, 551-5 (2005)

[111] Liu, Himes, Tryon, Moul, Chow, Jin, Murray, Tessler & Fischer. Intraspinal grafting of fibroblasts genetically modified by recombinant adenoviruses *Neuroreport* 9, 1075-9 (1998)

[112] Agnati & Fuxe. in *Molecular Mechanisms of Neuronal Communication* (eds. Fuxe, K. et al.) 251-77 (Pergamon, Oxford, 1996).

[113] Girod, Eder-Colli, Medilanski, Dunant, Tabti & Poo. Pulsatile release of acetylcholine by nerve terminals (synaptosomes) isolated from Torpedo electric organ *J Physiol* 450, 325-40 (1992)

[114] Duff Davis & Schmidt. In vivo spectrometric calcium flux recordings of intrinsic Caudate-Putamen cells and transplanted IMR-32 neuroblastoma cells using miniature fiber optrodes in anesthetized and awake rats and monkeys *J Neurosci Methods* 99, 9-23 (2000)

[115] Westerink & De Vries. A method to evaluate the diffusion rate of drugs from a microdialysis probe through brain tissue *J Neurosci Methods* 109, 53-8 (2001)

[116] Nakamura, Nakamura, Lasser-Ross, Barbara, Sandler & Ross. Inositol 1,4,5-trisphosphate (IP3)-mediated Ca2+ release evoked by metabotropic agonists and backpropagating action potentials in hippocampal CA1 pyramidal neurons *J Neurosci* 20, 8365-76 (2000)

[117] Mishra & Bhalla. Simulations of inositol phosphate metabolism and its interaction with InsP(3)-mediated calcium release *Biophys J* 83, 1298-316 (2002)

[118] Gilman. G proteins: transducers of receptor-generated signals *Annu Rev Biochem* 56, 615-49 (1987)

[119] Zhang & Allen. FRET-based biosensors for protein kinases: illuminating the kinome *Mol Biosyst* 3, 759-65 (2007)

[120] Conklin, Farfel, Lustig, Julius & Bourne. Substitution of three amino acids switches receptor specificity of Gq alpha to that of Gi alpha *Nature* 363, 274-6 (1993)

[121] Tsien. A non-disruptive technique for loading calcium buffers and indicators into cells *Nature* 290, 527-8 (1981)

[122] Di Virgilio, Steinberg, Swanson & Silverstein. Fura-2 secretion and sequestration in macrophages. A blocker of organic anion transport reveals that these processes occur via a membrane transport system for organic anions *J Immunol* 140, 915-20 (1988)

[123] Pologruto, Yasuda & Svoboda. Monitoring neural activity and [Ca2+] with genetically encoded Ca2+ indicators *J Neurosci* 24, 9572-9 (2004)

[124] Mank & Griesbeck. Genetically encoded calcium indicators *Chem Rev* 108, 1550-64 (2008)

[125] Kleinfeld & Griesbeck. From art to engineering? The rise of in vivo mammalian electrophysiology via genetically targeted labeling and nonlinear imaging *PLoS Biol* 3, e355 (2005)

[126] Heim & Griesbeck. Genetically encoded indicators of cellular calcium dynamics based on troponin C and green fluorescent protein *J Biol Chem* 279, 14280-6 (2004)

[127] Mank, Reiff, Heim, Friedrich, Borst & Griesbeck. A FRET-based calcium biosensor with fast signal kinetics and high fluorescence change *Biophys J* 90, 1790-6 (2006)

[128] Davis & Schmidt. In vivo spectrometric calcium flux recordings of intrinsic Caudate-Putamen cells and transplanted IMR-32 neuroblastoma cells using miniature fiber optrodes in anesthetized and awake rats and monkeys *J Neurosci Methods* 99, 9-23 (2000)

[129] Mehta, Jung, Flusberg & Schnitzer. Fiber optic in vivo imaging in the mammalian nervous system *Curr Opin Neurobiol* 14, 617-28 (2004)

[130] Helmchen & Denk. Deep tissue two-photon microscopy *Nat Methods* 2, 932-40 (2005)

[131] Fan, Fujisaki, Miyawaki, Tsay, Tsien & Ellisman. Video-rate scanning two-photon excitation fluorescence microscopy and ratio imaging with cameleons *Biophys J* 76, 2412-20 (1999)

[132] Jung & Schnitzer. Multiphoton endoscopy *Opt Lett* 28, 902-4 (2003)

[133] Helmchen, Fee, Tank & Denk. A miniature head-mounted two-photon microscope. high-resolution brain imaging in freely moving animals *Neuron* 31, 903-12 (2001)

[134] Mank, Santos, Direnberger, Mrsic-Flogel, Hofer, Stein, Hendel, Reiff, Levelt, Borst, Bonhoeffer, Hubener & Griesbeck. A genetically encoded calcium indicator for chronic in vivo two-photon imaging *Nat Methods* 5, 805-11 (2008)

[135] Shaner, Campbell, Steinbach, Giepmans, Palmer & Tsien. Improved monomeric red, orange and yellow fluorescent proteins derived from Discosoma sp. red fluorescent protein *Nat Biotechnol* 22, 1567-72 (2004)

[136] Denk, Strickler & Webb. Two-photon laser scanning fluorescence microscopy *Science* 248, 73-6 (1990)

[137] Luo, Broad, Bird & Putney. Signaling pathways underlying muscarinic receptor-induced [Ca2+]i oscillations in HEK293 cells *J Biol Chem* 276, 5613-21 (2001)

[138] Roos, DiGregorio, Yeromin, Ohlsen, Lioudyno, Zhang, Safrina, Kozak, Wagner, Cahalan, Velicelebi & Stauderman. STIM1, an essential and conserved component of store-operated Ca2+ channel function *J Cell Biol* 169, 435-45 (2005)

[139] Berridge. Inositol trisphosphate and calcium signaling *Ann N Y Acad Sci* 766, 31-43 (1995)

[140] Luik, Wang, Prakriya, Wu & Lewis. Oligomerization of STIM1 couples ER calcium depletion to CRAC channel activation *Nature* 454, 538-42 (2008)

[141] Hein, Frank, Hoffmann, Lohse & Bunemann. Dynamics of receptor/G protein coupling in living cells *Embo J* 24, 4106-14 (2005)

[142] Bunemann, Frank & Lohse. Gi protein activation in intact cells involves subunit rearrangement rather than dissociation *Proc Natl Acad Sci U S A* 100, 16077-82 (2003)

[143] Hein, Rochais, Hoffmann, Dorsch, Nikolaev, Engelhardt, Berlot, Lohse & Bunemann. Gs activation is time-limiting in initiating receptor-mediated signaling *J Biol Chem* 281, 33345-51 (2006)

[144] Willets, Mistry, Nahorski & Challiss. Specificity of g protein-coupled receptor kinase 6-mediated phosphorylation and regulation of single-cell m3 muscarinic acetylcholine receptor signaling *Mol Pharmacol* 64, 1059-68 (2003)

[145] Nash, Young, Willars, Challiss & Nahorski. Single-cell imaging of graded Ins(1,4,5)P3 production following G-protein-coupled-receptor activation *Biochem J* 356, 137-42 (2001)

[146] Willars & Nahorski. Quantitative comparisons of muscarinic and bradykinin receptor-mediated Ins (1,4,5)P3 accumulation and Ca2+ signalling in human neuroblastoma cells *Br J Pharmacol* 114, 1133-42 (1995)

[147] van Koppen & Kaiser. Regulation of muscarinic acetylcholine receptor signaling *Pharmacol Ther* 98, 197-220 (2003)

[148] Moore, Milano & Benovic. Regulation of receptor trafficking by GRKs and arrestins *Annu Rev Physiol* 69, 451-82 (2007)

[149] Krasel, Bunemann, Lorenz & Lohse. Beta-arrestin binding to the beta2-adrenergic receptor requires both receptor phosphorylation and receptor activation *J Biol Chem* 280, 9528-35 (2005)

[150] Krasel, Vilardaga, Bunemann & Lohse. Kinetics of G-protein-coupled receptor signalling and desensitization *Biochem Soc Trans* 32, 1029-31 (2004)

[151] Tobin, Lambert & Nahorski. Rapid desensitization of muscarinic m3 receptor-stimulated polyphosphoinositide responses *Mol Pharmacol* 42, 1042-8 (1992)

[152] Vogler, Bogatkewitsch, Wriske, Krummenerl, Jakobs & van Koppen. Receptor subtype-specific regulation of muscarinic acetylcholine receptor sequestration by dynamin. Distinct sequestration of m2 receptors *J Biol Chem* 273, 12155-60 (1998)

[153] Mundell & Benovic. Selective regulation of endogenous G protein-coupled receptors by arrestins in HEK293 cells *J Biol Chem* 275, 12900-8 (2000)

[154] Mundell, Loudon & Benovic. Characterization of G protein-coupled receptor regulation in antisense mRNA-expressing cells with reduced arrestin levels *Biochemistry* 38, 8723-32 (1999)

[155] Bartfai, Iverfeldt, Fisone & Serfozo. Regulation of the release of coexisting neurotransmitters *Annu Rev Pharmacol Toxicol* 28, 285-310 (1988)

[156] Fisone, Wu, Consolo, Nordstrom, Brynne, Bartfai, Melander & Hokfelt. Galanin inhibits acetylcholine release in the ventral hippocampus of the rat: histochemical, autoradiographic, in vivo, and in vitro studies *Proc Natl Acad Sci U S A* 84, 7339-43 (1987)

[157] Soreq & Seidman. Acetylcholinesterase--new roles for an old actor *Nat Rev Neurosci* 2, 294-302 (2001)

[158] Quinn. Acetylcholinesterase: enzyme structure, reaction dynamics, and virtual transition states *Chem Rev* 87, 955-79 (1987)

[159] Gonon. Prolonged and extrasynaptic excitatory action of dopamine mediated by D1 receptors in the rat striatum in vivo *J Neurosci* 17, 5972-8 (1997)

[160] Garris & Wightman. Different kinetics govern dopaminergic transmission in the amygdala, prefrontal cortex, and striatum: an in vivo voltammetric study *J Neurosci* 14, 442-50 (1994)

[161] Mechawar, Cozzari & Descarries. Cholinergic innervation in adult rat cerebral cortex: a quantitative immunocytochemical description *J Comp Neurol* 428, 305-18 (2000)

[162] Saper. Organization of cerebral cortical afferent systems in the rat. II. Magnocellular basal nucleus *J Comp Neurol* 222, 313-42 (1984)

[163] Metherate, Cox & Ashe. Cellular bases of neocortical activation: modulation of neural oscillations by the nucleus basalis and endogenous acetylcholine *J Neurosci* 12, 4701-11 (1992)

[164] Metherate & Ashe. Ionic flux contributions to neocortical slow waves and nucleus basalis-mediated activation: whole-cell recordings in vivo *J Neurosci* 13, 5312-23 (1993)

[165] Rasmusson, Clow & Szerb. Modification of neocortical acetylcholine release and electroencephalogram desynchronization due to brainstem stimulation by drugs applied to the basal forebrain *Neuroscience* 60, 665-77 (1994)

[166] Messamore, Warpman, Ogane & Giacobini. Cholinesterase inhibitor effects on extracellular acetylcholine in rat cortex *Neuropharmacology* 32, 745-50 (1993)

[167] Henny & Jones. Projections from basal forebrain to prefrontal cortex comprise cholinergic, GABAergic and glutamatergic inputs to pyramidal cells or interneurons *Eur J Neurosci* 27, 654-70 (2008)

[168] Semba. Multiple output pathways of the basal forebrain: organization, chemical heterogeneity, and roles in vigilance *Behav Brain Res* 115, 117-41 (2000)

[169] Detari, Rasmusson & Semba. The role of basal forebrain neurons in tonic and phasic activation of the cerebral cortex *Prog Neurobiol* 58, 249-77 (1999)

[170] Jimenez-Capdeville, Dykes & Myasnikov. Differential control of cortical activity by the basal forebrain in rats: a role for both cholinergic and inhibitory influences *J Comp Neurol* 381, 53-67 (1997)

[171] Tsai, Nishimura, Yoder, Dolnick, White & Kleinfeld. in *In vivo optical imaging of brain function* (ed. Frostig, R. D.) 113-71 (CRC Press, Boca Raton, 2002).

[172] Nicholson. Interaction between diffusion and Michaelis-Menten uptake of dopamine after iontophoresis in striatum *Biophys J* 68, 1699-715 (1995)

[173] Conner, Darracq, Roberts & Tuszynski. Nontropic actions of neurotrophins: subcortical nerve growth factor gene delivery reverses age-related degeneration of primate cortical cholinergic innervation *Proc Natl Acad Sci U S A* 98, 1941-6 (2001)

[174] Percival. (Cambridge University Press, 1993) Spectral Analysis for Physical Applications.

[175] Levey, Kitt, Simonds, Price & Brann. Identification and localization of muscarinic acetylcholine receptor proteins in brain with subtype-specific antibodies *J Neurosci* 11, 3218-26 (1991)

[176] Lu, Curtis, Jones, Pavia & Hulme. The role of the aspartate-arginine-tyrosine triad in the m1 muscarinic receptor: mutations of aspartate 122 and tyrosine 124 decrease receptor expression but do not abolish signaling *Mol Pharmacol* 51, 234-41 (1997)

[177] Hassaine, Wagner, Kempf, Cherouati, Hassaine, Prual, Andre, Reinhart, Pattus & Lundstrom. Semliki Forest virus vectors for overexpression of 101 G protein-coupled receptors in mammalian host cells *Protein Expr Purif* 45, 343-51 (2006)

[178] Heilbronn & Bartfai. Muscarinic acetylcholine receptor *Prog Neurobiol* 11, 171-88 (1978)

[179] Cortes & Palacios. Muscarinic cholinergic receptor subtypes in the rat brain. I. Quantitative autoradiographic studies *Brain Res* 362, 227-38 (1986)

[180] Vickroy, Malphurs & Defiebre. Absence of receptor reserve at hippocampal muscarinic autoreceptors which inhibit stimulus-dependent acetylcholine release *J Pharmacol Exp Ther* 267, 1198-204 (1993)

[181] Wakamori, Hidaka & Akaike. Hyperpolarizing muscarinic responses of freshly dissociated rat hippocampal CA1 neurones *J Physiol* 463, 585-604 (1993)

[182] Raiteri, Marchi, Paudice & Pittaluga. Muscarinic receptors mediating inhibition of gamma-aminobutyric acid release in rat corpus striatum and their pharmacological characterization *J Pharmacol Exp Ther* 254, 496-501 (1990)

[183] Lakowicz. (Springer, 2006) Principles of Fluorescence Spectroscopy.

[184] Gordon, Berry, Liang, Levine & Herman. Quantitative fluorescence resonance energy transfer measurements using fluorescence microscopy *Biophys J* 74, 2702-13 (1998)

[185] Black & Leff. Operational models of pharmacological agonism *Proc R Soc Lond B Biol Sci* 220, 141-62 (1983)

[186] Hires, Tian & Looger. Reporting neural activity with genetically encoded calcium indicators *Brain Cell Biol* 36, 69-86 (2008)

[187] Fukano, Shimozono & Miyawaki. Development of microscopic systems for high-speed dual-excitation ratiometric Ca2+ imaging *Brain Cell Biol* 36, 43-52 (2008)

[188] Vilardaga, Krasel, Chauvin, Bambino, Lohse & Nissenson. Internalization determinants of the parathyroid hormone receptor differentially regulate beta-arrestin/receptor association *J Biol Chem* 277, 8121-9 (2002)

[189] Tuszynski, Peterson, Ray, Baird, Nakahara & Gage. Fibroblasts genetically modified to produce nerve growth factor induce robust neuritic ingrowth after grafting to the spinal cord *Exp Neurol* 126, 1-14 (1994)

[190] Grill, Murai, Blesch, Gage & Tuszynski. Cellular delivery of neurotrophin-3 promotes corticospinal axonal growth and partial functional recovery after spinal cord injury *J Neurosci* 17, 5560-72 (1997)

[191] Liu, Kim, Himes, Chow, Schallert, Murray, Tessler & Fischer. Transplants of fibroblasts genetically modified to express BDNF promote

regeneration of adult rat rubrospinal axons and recovery of forelimb function *J Neurosci* 19, 4370-87 (1999)

[192] Palmer, Rosman, Osborne & Miller. Genetically modified skin fibroblasts persist long after transplantation but gradually inactivate introduced genes *Proc Natl Acad Sci U S A* 88, 1330-4 (1991)

[193] Scharfmann, Axelrod & Verma. Long-term in vivo expression of retrovirus-mediated gene transfer in mouse fibroblast implants *Proc Natl Acad Sci U S A* 88, 4626-30 (1991)

[194] Shao, Huang, Wang, Zhang & Sun. Grafting of genetically modified human fetal fibroblasts to produce human butyrylcholinesterase in mice *Chem Biol Interact* 119-120, 361-9 (1999)

[195] Fisher, Jinnah, Kale, Higgins & Gage. Survival and function of intrastriatally grafted primary fibroblasts genetically modified to produce L-dopa *Neuron* 6, 371-80 (1991)

[196] Smith, Roberts, Gage & Tuszynski. Age-associated neuronal atrophy occurs in the primate brain and is reversible by growth factor gene therapy *Proc Natl Acad Sci U S A* 96, 10893-8 (1999)

[197] Cao, Xu, Devries, Enzmann, Ping, Tsoulfas, Wood, Bunge & Whittemore. Functional recovery in traumatic spinal cord injury after transplantation of multineurotrophin-expressing glial-restricted precursor cells *J Neurosci* 25, 6947-57 (2005)

[198] Han, Liu, Tyler-Polsz, Rao & Fischer. Transplantation of glial-restricted precursor cells into the adult spinal cord: survival, glial-specific differentiation, and preferential migration in white matter *Glia* 45, 1-16 (2004)

[199] Beadle, Assanah, Monzo, Vallee, Rosenfeld & Canoll. The role of myosin II in glioma invasion of the brain *Mol Biol Cell* 19, 3357-68 (2008)

[200] Zang, Florijn & Creese. Reduction in muscarinic receptors by antisense oligodeoxynucleotide *Biochem Pharmacol* 48, 225-8 (1994)

[201] Rohrer & Kobilka. G protein-coupled receptors: functional and mechanistic insights through altered gene expression *Physiol Rev* 78, 35-52 (1998)

[202] Gilchrist, Li & Hamm. Design and use of C-terminal minigene vectors for studying role of heterotrimeric G proteins *Methods Enzymol* 344, 58-69 (2002)

[203] Pierce, Premont & Lefkowitz. Seven-transmembrane receptors *Nat Rev Mol Cell Biol* 3, 639-50 (2002)

[204] Zhang, Hupfeld, Taylor, Olefsky & Tsien. Insulin disrupts beta-adrenergic signalling to protein kinase A in adipocytes *Nature* 437, 569-73 (2005)

[205] Coward, Chan, Wada, Humphries & Conklin. Chimeric G proteins allow a high-throughput signaling assay of Gi-coupled receptors *Anal Biochem* 270, 242-8 (1999)

[206] Revah, Bertrand, Galzi, Devillers-Thiery, Mulle, Hussy, Bertrand, Ballivet & Changeux. Mutations in the channel domain alter desensitization of a neuronal nicotinic receptor *Nature* 353, 846-9 (1991)

[207] Stetzer, Ebbinghaus, Storch, Poteur, Schrattenholz, Kramer, Methfessel & Maelicke. Stable expression in HEK-293 cells of the rat alpha3/beta4 subtype of neuronal nicotinic acetylcholine receptor *FEBS Lett* 397, 39-44 (1996)

[208] Schlessinger. Cell signaling by receptor tyrosine kinases *Cell* 103, 211-25 (2000)

[209] Yoder & Kleinfeld. Cortical imaging through the intact mouse skull using two-photon excitation laser scanning microscopy *Microsc Res Tech* 56, 304-5 (2002)

[210] Kleinfeld, Sachdev, Merchant, Jarvis & Ebner. Adaptive filtering of vibrissa input in motor cortex of rat *Neuron* 34, 1021-34 (2002)

[211] Shtoyerman, Arieli, Slovin, Vanzetta & Grinvald. Long-term optical imaging and spectroscopy reveal mechanisms underlying the intrinsic signal and stability of cortical maps in V1 of behaving monkeys *J Neurosci* 20, 8111-21 (2000)

[212] Kleinfeld & Delaney. Distributed representation of vibrissa movement in the upper layers of somatosensory cortex revealed with voltage-sensitive dyes *J Comp Neurol* 375, 89-108 (1996)

[213] Kleinfeld, Mitra, Helmchen & Denk. Fluctuations and stimulus-induced changes in blood flow observed in individual capillaries in layers 2 through 4 of rat neocortex *Proc Natl Acad Sci U S A* 95, 15741-6 (1998)

[214] Jung, Mehta, Aksay, Stepnoski & Schnitzer. In vivo mammalian brain imaging using one- and two-photon fluorescence microendoscopy *J Neurophysiol* 92, 3121-33 (2004)

[215] Levene, Dombeck, Kasischke, Molloy & Webb. In vivo multiphoton microscopy of deep brain tissue *J Neurophysiol* 91, 1908-12 (2004)

[216] Knittel, Schneider, Buess, Messerschmidt & Possner. Endoscope-compatible confocal microscope using a gradient-index lens system *Optics Communications*, 267-73 (2001)

[217] Ferezou, Bolea & Petersen. Visualizing the cortical representation of touch: voltage-sensitive dye imaging of barrel cortex spatiotemporal dynamics in freely moving mice in *Cold Spring Harbor: Imaging Neurons and Neural Activity* (2005).

[218] Rector, Poe & Harper. Imaging of hippocampal and neocortical neural activity following intravenous cocaine administration in freely behaving cats *Neuroscience* 54, 633-41 (1993)

[219] Nimmerjahn, Denk & Helmchen. Two - photon fiberscope imaging of cellular networks in the neocortex in vivo in *Society for Neuroscience Annual Meeting* (New Orleans, 2003).

[220] Gobel, Nimmerjahn & Helmchen. Distortion-free delivery of nanojoule femtosecond pulses from a Ti:sapphire laser through a hollow-core photonic crystal fiber *Opt Lett* 29, 1285-7 (2004)

[221] Zipfel, Williams & Webb. Nonlinear magic: multiphoton microscopy in the biosciences *Nat Biotechnol* 21, 1369-77 (2003)

[222] Nifosi & Luo. Origin of the anomalous two-photon absorption in fluorescent protein DsRed 111, 505-7 (2007)

[223] Drobizhev, Makarov, Hughes & Rebane. Resonance enhancement of two-photon absorption in fluorescent proteins *J Phys Chem B* 111, 14051-4 (2007)

[224] Nguyen, Tsai & Kleinfeld. MPScope: a versatile software suite for multiphoton microscopy *J Neurosci Methods* 156, 351-9 (2006)

[225] Armstrong-James, Fox & Das-Gupta. Flow of excitability within barrel cortex on striking a single vibrissa *Journal of Neurophysiology* 68, 1345-58 (1992)

[226] Berg, Friedman, Schroeder & Kleinfeld. Activation of nucleus basalis facilitates cortical control of a brain stem motor program *J Neurophysiol* 94, 699-711 (2005)

[227] Rasmusson, Szerb & Jordan. Differential effects of alpha-amino-3-hydroxy-5-methyl-4-isoxazole propionic acid and N-methyl-D-aspartate receptor antagonists applied to the basal forebrain on cortical acetylcholine release and electroencephalogram desynchronization *Neuroscience* 72, 419-27 (1996)